Molecular dynamics for fermions

Hans Feldmeier

Gesellschaft für Schwerionenforschung mbH, D-64220 Darmstadt, Germany

Jürgen Schnack

Universität Osnabrück, Fachbereich Physik, D-49069 Osnabrück, Germany

The time-dependent variational principle for many-body trial states is used to discuss the relation between the approaches of different molecular-dynamics models that describe indistinguishable fermions. Early attempts to include effects of the Pauli principle by means of nonlocal potentials, as well as more recent models that work with antisymmetrized many-body states, are reviewed under these premises.

CONTENTS

I. INTRODUCTION

When correlations and fluctuations become important in the dynamical evolution of a many-body system and mean-field approximations are not sufficient, molecular-dynamics methods are frequently invoked. Molecular dynamics means that the constituents (molecules) of the many-body system are represented by a few classical degrees of freedom (center-of-mass position and momentum, angle of rotation, etc.) and interact through potentials. The equations of motion (Newtonian or Hamiltonian) are solved numerically. The interactions that are used range from purely phenomenological to sophisticated *ab initio* quantal potentials. The major advantage of molecular-dynamics simulations is that they do not rely on quasiparticle approximations but include both mean-field effects and many-body correlations. Therefore they can provide insight into complex systems with correlations on different scales.

During the past decade, an increasing interest has developed in the dynamics of many-fermion systems in which correlations are important. In nuclear as well as in atomic physics, collisions of composite fermion systems like nuclei or atomic clusters demand many-body models that can account for a large variety of phenomena. Depending on the energy, one may observe fusion,

dissipative reactions, fragmentation and even multifragmentation, vaporization or evaporation, and ionization. Moreover, phase transitions in small systems are of current interest.

Classical molecular dynamics is applicable if the de Broglie wavelength of the molecules is small compared to the length scale of typical variations of the interaction; otherwise, the quantal uncertainty relation becomes important. If the molecules are identical fermions or bosons, the de Broglie wavelength should also be small compared to the mean interparticle distance in phase space; otherwise, the Pauli or Bose principle is violated and the model will have the wrong statistical properties.

For nucleons in a nucleus, for example, both conditions necessary for classical mechanics are not fulfilled. The same holds for electrons in bound states or at high densities and low temperatures. Nevertheless, one would like to utilize the merits of a molecular-dynamics model for indistinguishable particles in the quantum regime.

This article reviews attempts to combine Fermi-Dirac statistics with a semiquantal trajectory picture from the viewpoint of the quantal time-dependent variational principle. The closest quantum analog to a point in single-particle phase space representing a classical particle is a wave packet well localized in phase space. The analog to a point in many-body phase space representing several classical particles is a many-body state which is a product of localized single-particle packets. If the particles are identical fermions, this product state has to be antisymmetrized; in the case of bosons, it has to be symmetrized.

For models that are formulated in terms of trial states and a Hamilton operator, both static and dynamical properties can be obtained from appropriate quantum variational principles. Ground states can be determined with the help of the Ritz variational principle, and the equations of motion can be accessed through the time-dependent variational principle, which allows one to derive approximations of the time-dependent Schrödinger equation to different levels of accuracy.

In Sec. II we first discuss the time-dependent variational principle in general and then show how it works for various trial states and how classical mechanics can be obtained from quantum mechanics by an appropriate choice of dynamical variables.

Using wave packets automatically guarantees that the Heisenberg uncertainty principle is not violated by the model. That is actually a great problem in classical simulations of Coulomb systems, where, for instance, a hydrogen atom composed of a pointlike proton and electron remains infinitely bound.

Using antisymmetrized many-body trial states automatically guarantees that the Pauli exclusion principle is respected by the model. Phenomena like shell structure or Fermi-Dirac statistics emerge in a natural way, as discussed in Secs. III and V.

Although antisymmetrized product states of single-particle Gaussian wave packets already possess major relevant degrees of freedom, some processes like disintegration of wave packets, which can occur in coordinate space (by evaporation, capture, or tunneling) and in momentum space (by large momentum transfer due to collisions), are poorly described by the equations of motion. One therefore often represents the system with a mixture of trial states between which random transitions may occur. This branching procedure, which is employed in atomic as well as in nuclear physics, will be explained in Sec. II.C.2.

In Sec. IV, models used in nuclear and atomic physics are reviewed from the general point of view of Secs. II and III. When energetic collisions between heavy atomic nuclei became available, classical molecular-dynamics models were developed to describe the various phenomena observed. To simulate the effect of antisymmetrization on the classical trajectories many authors added to the Hamiltonian a two-body ''Pauli potential,'' which is supposed to keep fermions apart from each other in phase space.

Quantum molecular dynamics (QMD) attributes to each fermion a Gaussian wave packet with fixed width instead of a point, but still uses a simple product state for the many-body wave function and therefore obtains classical equations of motion with two-body forces acting on the centroids of the wave packets. These Newtonian forces are supplemented by random forces that simulate hard collisions. Pauli blocking is included in these collision terms. The statistical properties, however, are mainly those of distinguishable particles.

Antisymmetrized molecular dynamics (AMD) also uses Gaussian wave packets with fixed width, but antisymmetrizes the many-body state. As in QMD, a collision term is added to account in a phenomenological way for branching into other Slater determinants. In fermionic molecular dynamics (FMD), the width degree of freedom is also considered. This nonclassical degree of freedom is important for phenomena like evaporation, and it plays an important role in statistical properties of the model.

Section IV.C explains the different uses of the term ''quantum molecular dynamics'' in atomic and nuclear physics. It then refers to applications of trajectory calculations for individual electrons and ions where the density of the electrons is too large to neglect their fermionic character. Quantum branching in the atomic context is also briefly discussed.

Although designed for nonequilibrium simulations like collisions, molecular-dynamics models are also used to simulate systems in thermal equilibrium. In Sec. V their statistical properties are investigated by means of time averaging. As applications, the nuclear liquid-gas phase transition and the hydrogen plasma under extreme conditions are discussed.

In conclusion, this review shows that it is possible to extend the classical trajectory picture to identical fermions by means of localized wave packets. When the phase-space density increases, the classical notion of positions $\vec{r}_k$ and momenta $\vec{p}_k$ as mean values of narrow wave packets has to be reinterpreted as parameters that

identify an antisymmetrized many-body state $|Q\rangle = |\vec{r}_1,\vec{p}_1,\vec{r}_2,\vec{p}_2,\ldots\rangle$. When the individual packets overlap in phase space, $\vec{r}_k$ and $\vec{p}_k$ can no longer be identified with the classical variables. Calculating all observables with the many-body state $|Q\rangle$ as quantum expectation values, e.g., $\mathcal{H}(\vec{r}_1,\vec{p}_1,\vec{r}_2,\vec{p}_2,\ldots) = \langle Q|\hat{H}|Q\rangle/\langle Q|Q\rangle$, and not misinterpreting them as classical expressions, naturally and correctly includes the Pauli exclusion principle and Heisenberg's uncertainty principle. In the equations of motion, the exclusion principle causes a complicated metric in the N-particle parameter space in the sense that canonical pairs of variables can only be defined locally.

The antisymmetrization of localized wave packets, which brings together the Pauli exclusion principle, Heisenberg's uncertainty relation, and the classical trajectory picture, leads to many, sometimes unexpected, quantal features. Nevertheless one has to be aware that one is still dealing with a very simplified trial state, and other degrees of freedom may be important. Especially when the interaction is not smooth across a wave packet, it may want to change its shape to one that is not in the allowed set; for example, it may split with certain probability amplitudes into different parts, which after some time evolve independently. Or more generally, branching into other trial states away from the one that follows the approximate time evolution of a pure state leads to a mixture of antisymmetrized wave packets. The consistent treatment of this aspect of quantum branching needs further attention in the literature.

Common to all models discussed is the anticorrelation between the degree of consistent derivation and the computational effort required.

II. TIME-DEPENDENT VARIATIONAL PRINCIPLE

A. General remarks

The time evolution of a state in quantum mechanics is given by the time-dependent Schrödinger equation[1]

$$i\frac{d}{dt}|\Psi(t)\rangle = \hat{H}|\Psi(t)\rangle, \tag{1}$$

where $\hat{H}$ is the Hamiltonian and $|\Psi(t)\rangle$ the many-body state that describes the physical system. This equation of motion can be obtained from the variation of the action (Kerman and Koonin, 1976; Kramer and Saraceno, 1981; Drożdż *et al.*, 1986; Broeckhove *et al.*, 1988),

$$\mathcal{A}' = \int_{t_1}^{t_2} dt\, \mathcal{L}'(\Psi(t)^*,\Psi(t),\dot{\Psi}(t)), \tag{2}$$

keeping the variations fixed at the end points: $\delta\Psi(t_1) = \delta\Psi(t_2) = \delta\Psi^*(t_1) = \delta\Psi^*(t_2) = 0$. The Lagrange function

$$\mathcal{L}'(\Psi(t)^*,\Psi(t),\dot{\Psi}(t)) = \langle\Psi(t)|i\frac{d}{dt}|\Psi(t)\rangle - \langle\Psi(t)|\hat{H}|\Psi(t)\rangle \tag{3}$$

is a function of the dynamical variables, denoted by the set $\Psi(t)$. Usually they are chosen to be complex so that $\Psi(t)$ and $\Psi^*(t)$ may be regarded as independent variables. If the mapping of $\Psi(t)$ on the many-body state $|\Psi(t)\rangle$ is analytic, $|\Psi(t)\rangle$ depends only on $\Psi(t)$, and the Hermitian adjoint state $\langle\Psi(t)|$ depends only on the complex-conjugate set $\Psi^*(t)$. The Lagrange function depends on the first time derivatives $\dot{\Psi}(t)$ through $d/dt\,|\Psi(t)\rangle$.

In general, the set $\Psi(t)$ contains infinitely many dynamical degrees of freedom, for example, the complex coefficients of an orthonormal basis or the values of an N-body wave function on a $3N$-dimensional grid in coordinate space.

The Lagrange function (3) is appropriate if the set of variables $\Psi(t),\Psi^*(t)$ contains a complex overall factor to $|\Psi(t)\rangle$ that takes care of norm and phase. If $|\Psi(t)\rangle$ cannot be normalized by means of the set $\Psi(t)$, the Lagrange function defined in Eq. (14) should be used. We shall employ both forms.

For linearly independent variables $\Psi(t)$ and $\Psi^*(t)$ the variation of $\Psi^*(t)$ yields for the extremal action

$$0 = \delta\mathcal{A}' = \int_{t_1}^{t_2} dt\langle\delta\Psi(t)|i\frac{d}{dt} - \hat{H}|\Psi(t)\rangle. \tag{4}$$

If $|\Psi(t)\rangle$ represents the most general state in Hilbert space, the variation $\langle\delta\Psi(t)|$ is unrestricted and Eq. (4) can only be fulfilled if

$$\left(i\frac{d}{dt} - \hat{H}\right)|\Psi(t)\rangle = 0, \tag{5}$$

which is just the Schrödinger equation (1).

The variation of $\Psi(t)$ yields

$$0 = \delta\mathcal{A}' = \int_{t_1}^{t_2} dt\langle\Psi(t)|i\frac{d}{dt} - \hat{H}|\delta\Psi(t)\rangle, \tag{6}$$

which after partial integration over t with fixed end points $|\delta\Psi(t_1)\rangle = |\delta\Psi(t_2)\rangle = 0$ results in the Hermitian adjoint of the Schrödinger equation:

$$\langle\Psi(t)|\left(-i\frac{\tilde{d}}{dt} - \hat{\tilde{H}}\right) = 0. \tag{7}$$

As $\Psi(t)$ is linearly independent of $\Psi^*(t)$, both have to be varied. Therefore the time integral that was missing in early attempts, used by Frenkel (1934) and others, is necessary.

The reason for the reformulation of a differential equation as a variational principle is of course the anticipation that a suitably chosen restriction in the dynamical variables will lead to a useful approximation of the full

[1]Throughout the article all operators are marked with a hat symbol, e.g., $\hat{H}$, and expectation values are denoted by calligraphic letters, e.g., $\mathcal{H}$. If not needed explicitly, $\hbar$ is taken to be one.

problem. For more general considerations on the construction of variational principles see Gerjuoy, Rau, and Spruch (1983), Balian and Veneroni (1988), and references therein.

1. Restricted set of variables

Let a restricted choice of variables be denoted by the complex set $Q'(t)=\{q_0(t),q_1(t),q_2(t),\ldots\}$ which specifies the many-body state $|Q'(t)\rangle$. It is presumed that $q_0(t)$ is always a complex overall factor in the sense

$$|Q'(t)\rangle = q_0(t)|Q(t)\rangle = q_0(t)|q_1(t),q_2(t),\ldots\rangle. \tag{8}$$

Furthermore, the time dependence of $|Q'(t)\rangle$ is supposed to be implicit only through the variables $Q'(t)$.

It should be noted that the manifold $|Q'(t)\rangle$ is in general only a subset of Hilbert space and need not form a subspace.

Variation of the action (2) with the Lagrange function (3) with respect to $Q'^*(t)$ leads to

$$0=\delta\mathcal{A}'=\int_{t_1}^{t_2} dt \sum_\nu \delta q_\nu^*(t) \times\left(\frac{\partial}{\partial q_\nu^*}\langle Q'(t)|\right)\left(i\frac{d}{dt}-\hat{H}\right)|Q'(t)\rangle. \tag{9}$$

As $\delta q_\nu^*(t)$ are arbitrary functions, the action is extremal if the following equations of motion are fulfilled:

$$\left(\frac{\partial}{\partial q_\nu^*}\langle Q'(t)|\right)\left(i\frac{d}{dt}-\hat{H}\right)|Q'(t)\rangle=0 \tag{10}$$

or

$$i\sum_\mu \mathcal{C}'_{\nu\mu}\dot{q}_\mu=\frac{\partial}{\partial q_\nu^*}\langle Q'(t)|\hat{H}|Q'(t)\rangle, \tag{11}$$

where

$$\mathcal{C}'_{\nu\mu}=\frac{\partial^2}{\partial q_\nu^*\partial q_\mu}\langle Q'(t)|Q'(t)\rangle. \tag{12}$$

In contrast to the case of the unrestricted variation, one obtains equations of motion for the complex parameters, which in turn define the time evolution of the trial state $|Q'(t)\rangle$ in Hilbert space.

Variation with respect to $Q'(t)$, with fixed end points $\delta q_\nu(t_1)=\delta q_\nu(t_2)=0$, results in equations of motion that are the complex conjugate of Eqs. (10)–(12).

In the following, for the sake of simplicity, the explicit indication of the time dependence is sometimes omitted.

The time evolution of q_0 can be expressed in terms of the other variables. For that the Lagrangian $\mathcal{L}'$ may be written as

$$\begin{aligned}\mathcal{L}' &= \langle Q'|i\frac{d}{dt}-\hat{H}|Q'\rangle \\ &= i\,q_0^*\dot{q}_0\langle Q|Q\rangle + q_0^*q_0\langle Q|Q\rangle\,\mathcal{L}(Q,Q^*,\dot{Q},\dot{Q}^*) \\ &\quad -\frac{i}{2}\frac{d}{dt}(q_0^*q_0\langle Q|Q\rangle),\end{aligned} \tag{13}$$

where the set Q no longer contains q_0 [see Eq. (8)] and a new Lagrangian $\mathcal{L}(Q^*,Q,\dot{Q}^*,\dot{Q})$ is defined by

$$\begin{aligned}\mathcal{L}(Q^*,Q,\dot{Q}^*,\dot{Q}) &= \frac{i}{2}\left(\frac{\langle Q|\dot{Q}\rangle-\langle\dot{Q}|Q\rangle}{\langle Q|Q\rangle}\right)-\frac{\langle Q|\hat{H}|Q\rangle}{\langle Q|Q\rangle} \\ &\equiv \mathcal{L}_0(Q^*,Q,\dot{Q}^*,\dot{Q})-\mathcal{H}(Q^*,Q)\end{aligned} \tag{14}$$

with

$$|\dot{Q}\rangle\equiv\frac{d}{dt}|Q\rangle=\sum_\nu \dot{q}_\nu\frac{\partial}{\partial q_\nu}|Q\rangle \quad\text{and}$$

$$\langle\dot{Q}|\equiv\frac{d}{dt}\langle Q|=\sum_\nu \dot{q}_\nu^*\frac{\partial}{\partial q_\nu^*}\langle Q|. \tag{15}$$

The new Lagrange function $\mathcal{L}$ contains the norm explicitly and is made real by subtracting the total time derivative. Here $\mathcal{H}(Q^*,Q)$ is the expectation value of the Hamiltonian $\hat{H}$ and will be called the Hamilton function.

It is easy to verify that the solution of the equation of motion (10) for q_0 is

$$q_0(t)=\frac{1}{\langle Q(t)|Q(t)\rangle^{1/2}}\exp\left\{i\int^t dt'\,\mathcal{L}(t')\right\} \tag{16}$$

and the analog for the complex conjugate $q_0^*(t)$. Thus the variational freedom of an overall factor $q_0(t)$ is used by the time-dependent variational principle to provide a state $|Q'(t)\rangle$ with a time-independent norm and an additional phase $\int^t dt'\,\mathcal{L}(t')$ (where $\mathcal{L}$ is real by construction). Furthermore, insertion of the solution (16) into $\mathcal{L}'$ shows that along the trajectory

$$\mathcal{L}'(Q'^*(t),Q'(t),\dot{Q}'(t))=0, \tag{17}$$

irrespective of the choice of the remaining degrees of freedom in $|Q\rangle$.

The equations of motion (10) and their complex conjugates can of course also be expressed as Euler-Lagrange equations:

$$\frac{d}{dt}\frac{\partial\mathcal{L}'}{\partial\dot{q}_\nu^*}-\frac{\partial\mathcal{L}'}{\partial q_\nu^*}=0 \quad\text{and}\quad \frac{d}{dt}\frac{\partial\mathcal{L}'}{\partial\dot{q}_\nu}-\frac{\partial\mathcal{L}'}{\partial q_\nu}=0. \tag{18}$$

For the remaining variables $\{q_\nu^*,q_\nu;\nu\neq0\}$ they can be written in terms of the new Lagrange function $\mathcal{L}$ as

$$\begin{aligned}\frac{d}{dt}\frac{\partial\mathcal{L}'}{\partial\dot{q}_\nu^*}-\frac{\partial\mathcal{L}'}{\partial q_\nu^*} &= \left(\frac{d}{dt}\frac{\partial\mathcal{L}}{\partial\dot{q}_\nu^*}-\frac{\partial\mathcal{L}}{\partial q_\nu^*}\right)q_0^*q_0\langle Q|Q\rangle \\ &\quad+\frac{d}{dt}(q_0^*q_0\langle Q|Q\rangle)\frac{\partial\mathcal{L}}{\partial\dot{q}_\nu^*} \\ &\quad-(iq_0^*\dot{q}q_0+q_0^*q_0\mathcal{L})\frac{\partial\langle Q|Q\rangle}{\partial q_\nu^*} \\ &=0\end{aligned} \tag{19}$$

and the analogous complex conjugates. The last two terms vanish when the general solution (16) for q_0 is inserted. Hence for $\nu\neq0$ the Euler-Lagrange equations with $\mathcal{L}$ as given in Eq. (14) are equivalent to the equations with $\mathcal{L}'$.

Therefore the action

$$\mathcal{A}=\int_{t_1}^{t_2} dt\, \mathcal{L}(Q^*,Q,\dot{Q}^*,\dot{Q}), \tag{20}$$

which one also often finds as a starting point (Kerman and Koonin, 1976; Kramer and Saraceno, 1981; Drożdż *et al.*, 1986; Broeckhove *et al.*, 1988), is appropriate if the trial state $|Q\rangle$ is not normalized and the phase is disregarded.[2] This form will turn out to be more convenient when dealing with antisymmetrized states in Sec. III.

One should, however, keep in mind that the simple inclusion of q_0 automatically provides norm and phase.

The Euler-Lagrange equations, which result from variation of the action (20),

$$\frac{d}{dt}\frac{\partial \mathcal{L}}{\partial \dot{q}_\nu^*}=\frac{\partial \mathcal{L}}{\partial q_\nu^*} \quad \text{and} \quad \frac{d}{dt}\frac{\partial \mathcal{L}}{\partial \dot{q}_\nu}=\frac{\partial \mathcal{L}}{\partial q_\nu}, \tag{21}$$

can be written in terms of the Hamilton function $\mathcal{H}=\langle Q|\hat{H}|Q\rangle/\langle Q|Q\rangle$ as generalized Hamilton's equations:

$$i\sum_\nu \mathcal{C}_{\mu\nu}\dot{q}_\nu=\frac{\partial \mathcal{H}}{\partial q_\mu^*} \quad \text{and} \quad -i\sum_\nu \mathcal{C}_{\mu\nu}^*\dot{q}_\nu^*=\frac{\partial \mathcal{H}}{\partial q_\mu}. \tag{22}$$

The non-negative Hermitian matrix $\mathcal{C}$ depends in general on Q and is given by

$$\begin{aligned}\mathcal{C}_{\mu\nu}&=\frac{\frac{\partial}{\partial q_\mu^*}\frac{\partial}{\partial q_\nu}\langle Q|Q\rangle}{\langle Q|Q\rangle}-\frac{\frac{\partial}{\partial q_\mu^*}\langle Q|Q\rangle}{\langle Q|Q\rangle}\frac{\frac{\partial}{\partial q_\nu}\langle Q|Q\rangle}{\langle Q|Q\rangle}\\&=\frac{\partial}{\partial q_\mu^*}\frac{\partial}{\partial q_\nu}\ln\langle Q|Q\rangle.\end{aligned} \tag{23}$$

It plays the role of a metric on the manifold of dynamical variables Q.

There is no need to assume that the set Q contains only complex variables, but as will be seen later in the context of classical mechanics, the real and imaginary parts of q_ν play the role of canonical pairs of variables. On the other hand, for quantum mechanics it is only natural to work with complex variables because the quantum state $|Q\rangle$ is necessarily complex. The assumption of an analytic mapping of Q onto the trial state $|Q\rangle$ is also not compulsory, but usually makes the equations more transparent.

2. Deviation from the exact solution

The static analog to the time-dependent variational principle is the Rayleigh-Ritz variational principle for the energy. Here one can show that the overlap between the true ground state of the Hamiltonian and the trial state $|Q'\rangle$ is increasing when the energy $\langle Q'|\hat{H}|Q'\rangle$ is decreasing. Since any additional degree of freedom lowers the energy, more degrees of freedom always imply an improved description. General statements like that cannot be made for the time-dependent variational principle, although one would think that more degrees of freedom would result in a time evolution closer to that of the Schrödinger equation.

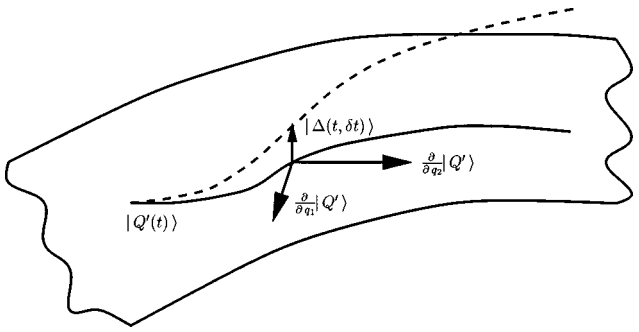

FIG. 1. Sketch of the manifold of trial states: solid line, the approximate time evolution; dashed line, the solution of the Schrödinger equation. The error $|\Delta(t,\delta t)\rangle$ is orthogonal to all tangent states $\partial/\partial q_\nu|Q'\rangle$.

In order to understand better the sense in which the time-dependent variational principle optimizes the evolution of the trial state, we consider the deviation of the approximate solution from the exact one, which develops during a short time δt,

$$\begin{aligned}|\Delta(t,\delta t)\rangle&=|\Psi_{exact}(t+\delta t)\rangle-|Q'(t+\delta t)\rangle\\&=\exp(-i\hat{H}\delta t)|Q'(t)\rangle-|Q'(t+\delta t)\rangle\\&=-i\left(\hat{H}-i\sum_\nu \dot{q}_\nu\frac{\partial}{\partial q_\nu}\right)|Q'(t)\rangle\delta t\\&\quad+\text{order}(\delta t^2).\end{aligned} \tag{24}$$

The equations of motion (10) which result from the time-dependent variational principle demand that

$$\left(\frac{\partial}{\partial q_\nu^*}\langle Q'(t)|\right)|\Delta(t,\delta t)\rangle=0, \tag{25}$$

which means that the deviation is orthogonal to all tangent states $\partial/\partial q_\nu|Q'\rangle$ (see Fig. 1). In other words, the approximate equations of motion evolve $Q'(t)$ to that point $Q'(t+\delta t)$ in the manifold where any small change in all possible directions increases the distance $\langle\Delta(t,\delta t)|\Delta(t,\delta t)\rangle$ between the true $|\Psi_{exact}(t+\delta t)\rangle$ and approximate solutions $|Q'(t+\delta t)\rangle$. The minimum condition

$$\begin{aligned}0&=\frac{\partial}{\partial q_\nu^*(t+\delta t)}\langle\Delta(t,\delta t)|\Delta(t,\delta t)\rangle\\&=-\left(\frac{\partial}{\partial q_\nu^*(t+\delta t)}\langle Q'(t+\delta t)|\right)|\Delta(t,\delta t)\rangle\\&=-\left(\frac{\partial}{\partial q_\nu^*(t)}\langle Q'(t)|\right)|\Delta(t,\delta t)\rangle+\text{order}(\delta t^3)\end{aligned} \tag{26}$$

is fulfilled because of Eq. (25). For variations with respect to q_ν, the complex conjugates of Eqs. (25) and

[2] $\mathcal{L}$ may also be written with normalized trial states $|Q\rangle/\sqrt{\langle Q|Q\rangle}$. The only difference is a total time derivative emerging from $\mathcal{L}_0$ so that the Lagrange functions are equivalent.

(26) have to be used. Of course, after many time steps δt, the deviation may become large.

3. Poisson brackets and canonical variables

With the help of the Hermitian matrix $\mathcal{C}$ it is possible to introduce Poisson brackets. Using the equations of motion (22), one can write the time derivative of the expectation value of a time-independent observable $\hat{B}$ as

$$\begin{aligned}\dot{\mathcal{B}} &= \frac{d}{dt}\frac{\langle Q|\hat{B}|Q\rangle}{\langle Q|Q\rangle} = \sum_\nu \left(\dot{q}^*_\nu \frac{\partial \mathcal{B}}{\partial q^*_\nu} + \dot{q}_\nu \frac{\partial \mathcal{B}}{\partial q_\nu} \right) \\ &= i \sum_{\mu,\nu} \left(\frac{\partial \mathcal{H}}{\partial q_\mu} \mathcal{C}^{-1}_{\mu\nu} \frac{\partial \mathcal{B}}{\partial q^*_\nu} - \frac{\partial \mathcal{B}}{\partial q_\mu} \mathcal{C}^{-1}_{\mu\nu} \frac{\partial \mathcal{H}}{\partial q^*_\nu} \right) \\ &=: \{\mathcal{H},\mathcal{B}\}. \end{aligned} \tag{27}$$

The real and imaginary parts of q_ν form pairs of canonical variables if $\mathcal{C}$ is the unit matrix. In Sec. II.B two examples will be given for this case, the Schrödinger equation and Hamilton's equation of motion.

In the general case, in which $\mathcal{C}_{\mu\nu}$ is not diagonal and depends on Q, pairs of canonical variables exist locally according to Darboux's theorem (Arnol'd, 1989). One possible transformation is given by

$$\mathrm{d}r_\mu = \sum_\nu \mathcal{C}^{1/2}_{\mu\nu}(Q^*,Q)\,\mathrm{d}q_\nu \qquad \text{and}$$

$$\mathrm{d}r^*_\mu = \sum_\nu \mathrm{d}q^*_\nu \mathcal{C}^{1/2}_{\mu\nu}(Q^*,Q). \tag{28}$$

Written with the new variables r_μ and r^*_μ, the Poisson bracket (27) takes the form

$$\{\mathcal{H},\mathcal{B}\} = i \sum_\mu \left(\frac{\partial \tilde{\mathcal{H}}}{\partial r_\mu}\frac{\partial \tilde{\mathcal{B}}}{\partial r^*_\mu} - \frac{\partial \tilde{\mathcal{B}}}{\partial r_\mu}\frac{\partial \tilde{\mathcal{H}}}{\partial r^*_\mu} \right), \tag{29}$$

so that (r_μ, r^*_μ) form pairs of canonical variables. The problem is, however, that in nontrivial cases the transformation (28) cannot be written in a global way as $R(Q)=\{r_0(q_0,q_1,\ldots),r_1(q_0,q_1,\ldots),\ldots\}$ and the Hamilton function $\mathcal{H}$ or the observable $\mathcal{B}$ cannot be expressed in the new variables

$$\tilde{\mathcal{H}}(R^*,R) = \mathcal{H}(Q^*,Q) \quad \text{and} \quad \tilde{\mathcal{B}}(R^*,R) = \mathcal{B}(Q^*,Q). \tag{30}$$

A set of canonical pairs, which are real, is given by

$$\rho_\mu = \frac{1}{\sqrt{2}}(r^*_\mu + r_\mu) \quad \text{and} \quad \pi_\mu = \frac{i}{\sqrt{2}}(r^*_\mu - r_\mu), \tag{31}$$

which yields the standard Poisson brackets

$$\{\mathcal{H},\mathcal{B}\} = \sum_\mu \left(\frac{\partial \tilde{\tilde{\mathcal{H}}}}{\partial \pi_\mu}\frac{\partial \tilde{\tilde{\mathcal{B}}}}{\partial \rho_\mu} - \frac{\partial \tilde{\tilde{\mathcal{B}}}}{\partial \pi_\mu}\frac{\partial \tilde{\tilde{\mathcal{H}}}}{\partial \rho_\mu} \right), \tag{32}$$

where $\tilde{\tilde{\mathcal{H}}}$ and $\tilde{\tilde{\mathcal{B}}}$ are now functions of ρ_μ and π_μ. Besides the trivial examples discussed in Sec. II.B, we give one nontrivial example in Sec. III.A.3.

The mere fact that, according to Darboux's theorem, canonical pairs (ρ_μ,π_μ) exist allows to guess or make an ansatz for the Hamilton function $\tilde{\tilde{\mathcal{H}}}(\rho_1,\rho_2,\ldots,\pi_1,\pi_2,\ldots)$ and use Hamilton's equations of motion. But with such a guess the connection to the trial state $|Q\rangle$ is lost and the physical meaning of ρ_μ and π_μ is obscured. This will become obvious when we discuss trial states for indistinguishable particles in Sec. III.

4. Conservation laws

An expectation value is conserved if (Broeckhove *et al.*, 1989)

$$\dot{\mathcal{B}} = \{\mathcal{H},\mathcal{B}\} = i \sum_{\mu,\nu} \left(\frac{\partial \mathcal{H}}{\partial q_\mu} \mathcal{C}^{-1}_{\mu\nu} \frac{\partial \mathcal{B}}{\partial q^*_\nu} - \frac{\partial \mathcal{B}}{\partial q_\mu} \mathcal{C}^{-1}_{\mu\nu} \frac{\partial \mathcal{H}}{\partial q^*_\nu} \right) = 0. \tag{33}$$

Hence the energy $\mathcal{H}$ itself is always conserved by the equations of motion, provided they are derived from the variational principle. This is completely independent of the choice of the trial state.

In the following we show how to identify other constants of motion and how the trial state has to be chosen in order to ensure desired conservation laws. For that, we consider a unitary transformation with the Hermitian generator $\hat{G}$,

$$\hat{U} = \exp(i\varepsilon\hat{G}), \tag{34}$$

where ε is real. If $\hat{U}$ maps the set of trial states onto itself,

$$\hat{U}|Q'\rangle \in \{|Q'\rangle\}, \tag{35}$$

then the special infinitesimal variation $|Q'(t) + \delta Q'(t)\rangle = \exp\{i\delta\varepsilon(t)\hat{G}\}|Q'(t)\rangle$ of the action (2) yields

$$\begin{aligned} 0 &= \int_{t_1}^{t_2} \mathrm{d}t \langle Q'(t)| \exp\{-i\,\delta\varepsilon(t)\hat{G}\} \left(i\frac{d}{dt} - \hat{H} \right) \\ &\quad \times \exp\{i\,\delta\varepsilon(t)\hat{G}\}|Q'(t)\rangle \\ &= \int_{t_1}^{t_2} \mathrm{d}t\,\delta\varepsilon(t) \Big\{ \frac{d}{dt}\langle Q'(t)|\hat{G}|Q'(t)\rangle \\ &\quad - \langle Q'(t)|i[\hat{H},\hat{G}]|Q'(t)\rangle \Big\} \\ &\quad + \text{total time derivative} + \text{order}(\delta\varepsilon^2). \end{aligned} \tag{36}$$

As $\delta\varepsilon(t)$ is arbitrary and vanishes at the end points, one obtains

$$\begin{aligned} \frac{d}{dt}\mathcal{G} &= \frac{d}{dt}\langle Q'(t)|\hat{G}|Q'(t)\rangle \\ &= \{\mathcal{H},\mathcal{G}\} = \langle Q'(t)|i[\hat{H},\hat{G}]|Q'(t)\rangle. \end{aligned} \tag{37}$$

That means that for this class of generators the generalized Poisson bracket is just the expectation value of the commutator with $i\hat{H}$.

Equation (37) is very useful for two reasons. First, if $\hat{G}$ commutes with the Hamiltonian $\hat{H}$ and $\exp(i\varepsilon\hat{G})|Q'_1\rangle = |Q'_2\rangle$, then $\langle Q'(t)|\hat{G}|Q'(t)\rangle$ is automati-

cally a constant of motion. Second, this relation is an important guide for the choice of the trial state $|Q'\rangle$. If one wants the model to obey certain conservation laws, then the set of trial states should be invariant under unitary transformations generated by the constants of motion. For example, total momentum conservation implies that a translated trial state is again a valid trial state. Conservation of total spin $\hat{\vec{J}}=\hat{\vec{L}}+\hat{\vec{S}}$ is guaranteed when a rotation of the trial state in coordinate and spin space results again in a trial state.

Equation (37) also sheds some light on the quality of the variational principle. It says that under the premises that $\exp(i\varepsilon\hat{G})$ does not map out of the set of trial states, the expectation value $\mathcal{G}(t)$ of $\hat{G}$ develops for short times like the exact solution. From Eq. (37), it follows that along the trajectory $|Q'(t)\rangle$ the time derivative of $\mathcal{G}(t)$ equals the exact one.

B. From quantum to classical mechanics

This section demonstrates that the time-dependent variational principle, discussed in general in the previous section, represents a method for going smoothly from quantum physics to classical physics by appropriately choosing the dynamical degrees of freedom in the trial state. In contrast to Ehrenfest's theorem, this method also works for identical particles and in finite-dimensional spin spaces.

1. Quantum mechanics

As a first illustration let us represent the trial state in terms of an orthonormal basis $|n\rangle$ in many-body space. We may write a general state $|Q'\rangle$ as

$$|Q'\rangle=|\rho_1,\rho_2,\ldots,\pi_1,\pi_2,\ldots\rangle$$
$$=\sum_n \frac{1}{\sqrt{2}}(\rho_n+i\pi_n)|n\rangle\equiv\sum_n c_n|n\rangle, \tag{38}$$

where the complex amplitudes are written in terms of their real and imaginary parts ρ_n and π_n. It is easy to verify that the Lagrange function for normalizable states defined in Eq. (3) is given by

$$\mathcal{L}'=\sum_n \frac{1}{2}(\pi_n\dot{\rho}_n-\rho_n\dot{\pi}_n)+\frac{d}{dt}\sum_n \frac{i}{4}(\rho_n^2+\pi_n^2)$$
$$-\mathcal{H}(\rho_1,\rho_2,\ldots,\pi_1,\pi_2,\ldots). \tag{39}$$

The real Hamilton function, expressed with the real and imaginary parts of the matrix elements $H_{nk}\equiv\langle n|\hat{H}|k\rangle$, is bilinear in ρ and π:

$$\mathcal{H}(\rho_1,\rho_2,\ldots,\pi_1,\pi_2,\ldots)=\frac{1}{2}\sum_{k,n}[(\rho_k\rho_n+\pi_k\pi_n)\mathrm{Re}\,H_{kn}$$
$$+(\pi_k\rho_n-\rho_k\pi_n)\mathrm{Im}\,H_{kn}]. \tag{40}$$

The Euler-Lagrange equations

$$\frac{d}{dt}\frac{\partial\mathcal{L}'}{\partial\dot{\rho}_n}=\frac{\partial\mathcal{L}'}{\partial\rho_n}\quad\text{and}\quad\frac{d}{dt}\frac{\partial\mathcal{L}'}{\partial\dot{\pi}_n}=\frac{\partial\mathcal{L}'}{\partial\pi_n} \tag{41}$$

yield

$$\frac{d}{dt}\pi_n=-\frac{\partial\mathcal{H}}{\partial\rho_n}\quad\text{and}\quad\frac{d}{dt}\rho_n=\frac{\partial\mathcal{H}}{\partial\pi_n}. \tag{42}$$

There is a very important message to be learned from this little exercise: Eqs. (42) look exactly like Hamilton's equations of motion, in which (ρ_n,π_n) are pairs of canonical variables and $\mathcal{H}(\rho_1,\rho_2,\ldots,\pi_1,\pi_2,\ldots)$ is the Hamilton function, bilinear in the coordinates and momenta of the system. But these seemingly classical equations are just a representation of the Schrödinger equation, as can easily be seen by rewriting the two real Eqs. (42) in terms of the complex coefficients $c_n=(1/\sqrt{2})(\rho_n+i\pi_n)$ as one complex equation, namely,

$$i\frac{d}{dt}c_n=\frac{\partial\mathcal{H}}{\partial c_n^*}=\sum_k H_{nk}c_k\quad\text{or}\quad i\frac{d}{dt}|Q'\rangle=\hat{H}|Q'\rangle. \tag{43}$$

The mere fact that the equations of motion (42) appear in a classical form does not necessarily imply that the system is classical and, for example, violates the uncertainty relation or, in the case of indistinguishable fermions, Fermi-Dirac statistics. This will be discussed in detail in Sec. V.

The symplectic structure of Eqs. (42) is fundamental to all energy-conserving dynamical theories, classical, quantum, or quantum field theories (see Katz, 1965). Only the physical meaning of the dynamical variables ρ_n and π_n and of the Hamilton function $\mathcal{H}$ determines which kind of physical system one is dealing with.

In the example Eq. (38), ρ_n and π_n are not the $6N$ positions and momenta of N particles but infinitely many variables which specify the many-body state $|Q'\rangle$. A truncation to a finite number results in an approximation of the exact time evolution. The quality depends on how well the selected set of basis states, $\{|n\rangle\}$, can represent the portion of Hilbert space that is occupied by the physical system under consideration.

2. Classical mechanics

A second example (Heller, 1975) shows that one can obtain the classical Hamilton equations of motion for the $6N$ positions and momenta from the time-dependent variational principle by choosing the following dynamical variables. The normalized trial state $|Q\rangle$ is set up to describe N distinguishable particles that are localized in phase space,

$$|Q\rangle=|\vec{r}_1,\vec{p}_1\rangle\otimes|\vec{r}_2,\vec{p}_2\rangle\otimes\cdots\otimes|\vec{r}_N,\vec{p}_N\rangle. \tag{44}$$

The single-particle states $|\vec{r}_k,\vec{p}_k\rangle$ in the direct product are taken to be the closest quantum analog to classical particles, namely Gaussian wave packets of minimum uncertainty, i.e., coherent states (Klauder and Skagerstam, 1985):

$$\langle\vec{x}|\vec{r}_k,\vec{p}_k\rangle=\left(\frac{1}{\pi a_0}\right)^{3/4}\exp\left\{-\frac{(\vec{x}-\vec{r}_k)^2}{2a_0}+i\vec{p}_k\vec{x}\right\}, \tag{45}$$

$$\langle \vec{k}|\vec{r}_k,\vec{p}_k\rangle=\left(\frac{a_0}{\pi}\right)^{3/4}\exp\left\{-\frac{a_0(\vec{k}-\vec{p}_k)^2}{2}-i\vec{r}_k(\vec{k}-\vec{p}_k)\right\}. \tag{46}$$

The dynamical variables $\vec{r}_k$ and $\vec{p}_k$ are just the mean values of the position and momentum operators, respectively,

$$\vec{r}_k=\langle \vec{r}_k,\vec{p}_k|\hat{\vec{x}}|\vec{r}_k,\vec{p}_k\rangle,\quad \vec{p}_k=\langle \vec{r}_k,\vec{p}_k|\hat{\vec{k}}|\vec{r}_k,\vec{p}_k\rangle. \tag{47}$$

The width parameter a_0 is a real fixed number here. In later applications it will also be taken as a complex dynamical variable.

The evaluation of the Lagrange function (14) is again simple and yields

$$\mathcal{L}=-\sum_{k=1}^{N}\vec{r}_k\dot{\vec{p}}_k-\mathcal{H}, \tag{48}$$

where the Hamilton function $\mathcal{H}=\langle Q|\hat{H}|Q\rangle$,

$$\mathcal{H}=\sum_{k=1}^{N}\left(\frac{\vec{p}_k^{\,2}}{2m_k}+\frac{3}{4m_k a}\right)+\sum_{k<l=1}^{N}\langle \vec{r}_k,\vec{p}_k|\otimes\langle \vec{r}_l,\vec{p}_l|\hat{V}(1,2)|\vec{r}_k,\vec{p}_k\rangle\otimes|\vec{r}_l,\vec{p}_l\rangle, \tag{49}$$

is the expectation value of the Hamiltonian

$$\hat{H}=\sum_{l=1}^{N}\frac{\hat{\vec{k}}^2(l)}{2m_l}+\sum_{k<l=1}^{N}\hat{V}(k,l). \tag{50}$$

The Euler-Lagrange equations

$$\frac{d}{dt}\frac{\partial\mathcal{L}}{\partial\dot{\vec{r}}_k}=\frac{\partial\mathcal{L}}{\partial\vec{r}_k}\rightarrow 0=-\dot{\vec{p}}_k-\frac{\partial\mathcal{H}}{\partial\vec{r}_k} \tag{51}$$

$$\frac{d}{dt}\frac{\partial\mathcal{L}}{\partial\dot{\vec{p}}_k}=\frac{\partial\mathcal{L}}{\partial\vec{p}_k}\rightarrow-\dot{\vec{r}}_k=-\frac{\partial\mathcal{H}}{\partial\vec{p}_k}, \tag{52}$$

result in

$$\frac{d}{dt}\vec{p}_k=-\frac{\partial\mathcal{H}}{\partial\vec{r}_k}\quad\text{and}\quad\frac{d}{dt}\vec{r}_k=\frac{\partial\mathcal{H}}{\partial\vec{p}_k}. \tag{53}$$

In a situation where classical mechanics holds, i.e., the wave packets are narrow enough that one can approximate the expectation value

$$\langle Q|\hat{H}|Q\rangle=\mathcal{H}(\vec{r}_1,\vec{r}_2,\ldots,\vec{p}_1,\vec{p}_2,\ldots)\approx H(\vec{r}_1,\vec{r}_2,\ldots,\vec{p}_1,\vec{p}_2,\ldots) \tag{54}$$

by replacing the momentum and position operators in the Hamiltonian by the respective mean values of their wave packets, Eqs. (53) become the classical form of Hamilton's equations of motion.

Up to this point the time-dependent variational principle has led to the same results as Ehrenfest's theorem, which usually establishes the connection between quantum and classical systems. As will be demonstrated in Sec. III, the prescription to replace the operators in the Heisenberg equation by their mean values does not work for indistinguishable particles. But the time-dependent variational principle for an antisymmetrized trial state $|Q\rangle$ provides the molecular-dynamics equations for identical fermions. For bosons, one would of course use a symmetrized state.

The canonical pair $(\vec{r}_k,\vec{p}_k)$ of real position and momentum can be combined in a complex variable $z_k=\sqrt{1/2a_0}\vec{r}_k+i\sqrt{a_0/2}\vec{p}_k$. The Hamilton equations (53) written in terms of z_k and z_k^* take the form

$$i\frac{d}{dt}z_k=\frac{\partial}{\partial z_k^*}\mathcal{H}(z_1^*,z_2^*,\ldots,z_1,z_2,\ldots), \tag{55}$$

which formally looks like the Schrödinger equation (43).

This and the previous example show that one cannot decide from the form of the equations of motion alone whether the system they are describing is classical or quantal. Furthermore, the time-dependent variational principle can provide both classical and quantal many-body equations of motion, depending on how the trial state $|Q\rangle$ is chosen. In the following third example, an intermediate situation is sketched, in which some quantum effects are included.

3. Semiclassical, semiquantal

A third example that includes some quantum effects is a trial state in which the width parameter a is both a dynamical variable and complex: $a=a_R+ia_I$ (Tsue and Fujiwara, 1991). Take the N-body trial state to be a product state,

$$|Q\rangle=|q_1\rangle\otimes|q_2\rangle\otimes\cdots\otimes|q_N\rangle, \tag{56}$$

of single-particle states, which are Gaussians,

$$\langle\vec{x}|q_l\rangle=\langle\vec{x}|\vec{r}_l,\vec{p}_l,a_l\rangle=\left(2\pi\frac{a_l^*a_l}{a_l^*+a_l}\right)^{-3/4}\times\exp\left\{-\frac{(\vec{x}-\vec{r}_l)^2}{2a_l}+i\vec{p}_l\vec{x}+i\phi_l\right\}, \tag{57}$$

characterized by their mean positions $\vec{r}_l$, mean momenta $\vec{p}_l$, widths a_l, and phases ϕ_l.

For a single-particle Hamiltonian that contains, in addition to the kinetic energy, a harmonic oscillator potential

$$\hat{H}_{\mathrm{HO}}=\sum_{l=1}^{N}\hat{h}_{\mathrm{HO}}(l)=\sum_{l=1}^{N}\left(\frac{\hat{\vec{k}}^2(l)}{2m_l}+\frac{1}{2}m_l\omega^2\hat{\vec{x}}^2(l)\right), \tag{58}$$

the equations of motion are

$$\frac{d}{dt}\vec{r}_l=\frac{\vec{p}_l}{m_l},\quad\frac{d}{dt}\vec{p}_l=-m_l\omega^2\vec{r}_l \tag{59}$$

$$\frac{d}{dt}a_l=\frac{i}{m_l}-im_l\omega^2a_l^2,$$

$$\frac{d}{dt}\phi_l=-\frac{\vec{p}_l^{\,2}}{2m_l}-\frac{3a_{Rl}}{2m_l|a_l|^2}-\frac{m_l}{2}\omega^2\vec{r}_l^{\,2}. \tag{60}$$

These equations, although looking classical for $\vec{r}_l$ and $\vec{p}_l$, represent the exact solution of the Schrödinger equation, provided the wave function is a Gaussian wave packet at time zero. The centers of the wave packets as well as the mean momenta oscillate harmonically with the frequency ω. Due to the time dependence of the widths, the packets also breathe, but with twice the frequency. The solution is fully quantum mechanical, although described by only a few (classical-looking) parameters. Free motion without a potential ($\omega=0$) is of course also exact. For general potentials the trial state of Eq. (57) may serve as an approximation if locally, in the region where $\langle\vec{x}|q_l\rangle$ does not vanish, the potential is well represented by a harmonic oscillator.

In general, one can say that a trial state provides an exact solution of the Schrödinger equation if the action of the Hamilton operator $\hat{H}$ on the trial state can be expressed in terms of parameters and first derivatives with respect to the parameters, as in the following example:

$$\hat{\vec{k}}|q\rangle=\left(i\frac{\partial}{\partial\vec{r}}-i\vec{p}\frac{\partial}{\partial\phi}\right)|q\rangle \tag{61}$$

and

$$\hat{\vec{k}}^2|q\rangle=\left(2i\frac{\partial}{\partial a_I}+2i\vec{p}\cdot\frac{\partial}{\partial\vec{r}}-i\left[\vec{p}^{\,2}+3\frac{a_R}{a_R^2+a_I^2}\right]\frac{\partial}{\partial\phi}\right)|q\rangle. \tag{62}$$

For a harmonic oscillator, the Schrödinger equation takes the form (index l omitted)

$$\begin{aligned}i\frac{d}{dt}|q\rangle&=i\sum_\nu\dot{q}_\nu\frac{\partial}{\partial q_\nu}|q\rangle=\hat{h}_{\rm HO}|q\rangle\\&=\left\{i\left(\frac{\vec{p}}{m}\right)\frac{\partial}{\partial\vec{r}}-i(m\omega^2\vec{r})\frac{\partial}{\partial\vec{p}}+i\,(2m\omega^2a_Ra_I)\frac{\partial}{\partial a_R}\right.\\&\quad+i\left(\frac{1}{m}-m\omega^2(a_R^2-a_I^2)\right)\frac{\partial}{\partial a_I}\\&\quad\left.-i\left(\frac{\vec{p}^{\,2}}{2m}+\frac{3a_R}{2m|a|^2}-\frac{m}{2}\omega^2\vec{r}^{\,2}\right)\frac{\partial}{\partial\phi}\right\}|q\rangle.\end{aligned} \tag{63}$$

From Eq. (63) the equations of motion (59) and (60) follow at once. Because Gaussian wave packets are an exact solution of the Schrödinger equation for these one-body Hamiltonians, the respective product states are also an exact solution for the corresponding many-body problem. Moreover, since antisymmetrization and symmetrization commute with the exact time evolution, the equations of motion (59) remain the same for antisymmetric product states (identical fermions) and symmetric product states (identical bosons).

The time-dependent width parameter a, which describes the variances in coordinate and momentum space, provides the first nonclassical degree of freedom in the parameter manifold. It completes the classical Eqs. (59) to the full quantum solution for spherical harmonic-oscillator potentials as well as for free motion. In Sec. V it is shown that for thermodynamic considerations the inclusion of finite widths leads to quantum statistics.

C. Further remarks

In the previous section, several examples are presented to get us acquainted with the numerous aspects of the time-dependent variational principle and its function as a bridge between quantum and classical physics. We now add further remarks, which are again of general type and will be useful for understanding the different models referred to later.

1. Self-consistency and nonlinearity

The equations of motion (11) [or (22)] determine the time evolution of the parameters $q_\nu(t)$ in parameter space. But, even if these parameters have an intuitive physical meaning, they first of all determine the trial state $|Q'(t)\rangle$ from which all physical observables have to be calculated in a quantum fashion. Therefore we derive here the corresponding equation of motion for $|Q'(t)\rangle$ in Hilbert space.

The Hamilton operator $\hat{H}_0$, which evolves the trial state $|Q'(t)\rangle$ in time according to the equations of motion (11), has to fulfill the condition

$$\hat{H}_0|Q'\rangle=i|\dot{Q}'\rangle\equiv i\sum_\nu\dot{q}_\nu\frac{\partial}{\partial q_\nu}|Q'\rangle. \tag{64}$$

It is given by

$$\begin{aligned}\hat{H}_0&=i(|\dot{Q}'\rangle\langle Q'|-|Q'\rangle\langle\dot{Q}'|)\\&\quad+\frac{i}{2}|Q'\rangle(\langle\dot{Q}'|Q'\rangle-\langle Q'|\dot{Q}'\rangle)\langle Q'|,\end{aligned} \tag{65}$$

where $|\dot{Q}'\rangle$ stands for

$$|\dot{Q}'\rangle=\frac{d}{dt}|Q'\rangle=-i\sum_{\mu,\nu}\frac{\partial}{\partial q_\mu}|Q'\rangle\mathcal{C}'^{-1}_{\mu\nu}\frac{\partial\mathcal{H}}{\partial q_\nu^*}, \tag{66}$$

and analogously for $\langle\dot{Q}'|$. Thus $\hat{H}_0$ itself depends on Q'^* and Q'. Using the fact that $|Q'\rangle$ is always normalized, we can easily show that $\hat{H}_0$, defined in Eq. (65), is the generator of the approximate time evolution

$$i\frac{d}{dt}|Q'\rangle=\hat{H}_0(Q'^*,Q')|Q'\rangle. \tag{67}$$

The equation of motion (67) for the trial state in Hilbert space is the counterpart of the equation of motion (11) in parameter space,

$$i\dot{q}_\mu=\sum_\nu\mathcal{C}'^{-1}_{\mu\nu}(Q'^*,Q')\frac{\partial}{\partial q_\nu^*}\mathcal{H}(Q'^*,Q'). \tag{68}$$

Equation (67) is self-consistent in the sense that the Hamiltonian depends on the actual state $|Q'(t)\rangle$. For example, if $|Q'(t)\rangle$ is a single Slater determinant, but otherwise unrestricted, $\hat{H}_0(Q'^*,Q')$ is the Hartree-Fock Hamiltonian (Kerman and Koonin, 1976). Further-

more, the approximate Eq. (67) is usually not a linear equation like the exact Schrödinger equation and therefore violates the superposition principle of quantum mechanics.

Both self-consistency and nonlinearity are common in classical molecular dynamics, in which the classical Hamilton function $H(r_1(t),\ldots,p_1(t),\ldots)$ depends on the actual physical state. The nonlinearity of $H(r_1(t),\ldots,p_1(t),\ldots)$ plays an important role for statistical properties like equilibration and chaotic behavior (see Sec. V). In quantum mechanics, these properties can only be investigated by breaking the superposition principle by coarse graining or phase averaging.

2. Quantum branching

The time-dependent variational principle creates an approximate quantum dynamics in a manifold of trial states. Due to their severely restricted degrees of freedom, it is very likely that areas of the Hilbert space are not reachable by approximate equations of motion which would be visited by the solution of the Schrödinger equation. The idea for an improved model is to allow branching from one trajectory $|Q_i'(t)\rangle$ to another one $|Q_j'(t)\rangle$, i.e., to jump in the parameter manifold with a certain probability.

If the local deviation between the exact solution and the solution of the time-dependent variational principle (see Sec. II.A.2) is not so large, the operator

$$\Delta\hat{H}=\left(\hat{H}-i\sum_{\nu}\dot{q}_{\nu}\frac{\partial}{\partial q_{\nu}}\right)\equiv\hat{H}-\hat{H}_0, \tag{69}$$

which appears in Eq. (24) for the error, may be regarded as a perturbation that causes transitions between the trial states $|Q_i'(t)\rangle$, while each $|Q_i'(t)\rangle$ follows the approximate time evolution given in Eqs. (65) and (66) with its self-consistent Hamiltonian $\hat{H}_0(Q_i'^*,Q_i')$. As in standard perturbation theory, the transition $|Q_i'(t)\rangle \rightarrow |Q_j'(t)\rangle$ should be related to the amplitude $\langle Q_j'(t)|\Delta\hat{H}|Q_i'(t)\rangle$ (Tully, 1990; Topaler *et al.*, 1997; Lacroix, Chomaz, and Ayik, 1998, 1999). One would, however, like to work with probabilities instead of amplitudes. This should be possible if the physical system is in an energy regime with high level density where statistical arguments may be used.

In the literature, one often employs phenomenological arguments (see Sec. IV) for random jumps in parameter space. The above-sketched procedure, which refers to $\Delta\hat{H}$ has several advantages here. The most important is self-consistency; the transition depends on the actual situation and the choice of trial states $|Q_i'(t)\rangle$. If, for example, $|Q_i'(t)\rangle$ is already a solution of the Schrödinger equation, $\Delta\hat{H}|Q_i'(t)\rangle=0$, and no branching occurs.

Another important aspect of branching is the breaking of symmetries (Colonna and Chomaz, 1998). Whereas the exact quantum state can retain dynamically conserved symmetries by linear superpositions of states, the nonlinearity and self-consistency of the approximate Hamiltonian (65) usually does not permit that. Take, for example, the mirror symmetry of a molecule or a nucleus that breaks into pieces. Each measured final channel that corresponds to one $|Q_i'\rangle$ does not possess mirror symmetry, but the ensemble of all measured channels does. If the initial trial state $|Q'(t=0)\rangle$ has this symmetry and $\hat{H}$ does not break it explicitly, the symmetry will be kept in $|Q'(t)\rangle$. Here, quantum branching into a nonsymmetric trial state $|Q_j'\rangle$ and its mirrored counterpart $|-Q_j'\rangle$ with equal probabilities would resolve the problem of spurious cross-channel coupling observed in self-consistent approximations (Griffin *et al.*, 1980). The transitions may also allow quantum fluctuations to configurations that are close in Hilbert space but cannot be reached by the approximate time evolution, for example, tunneling.

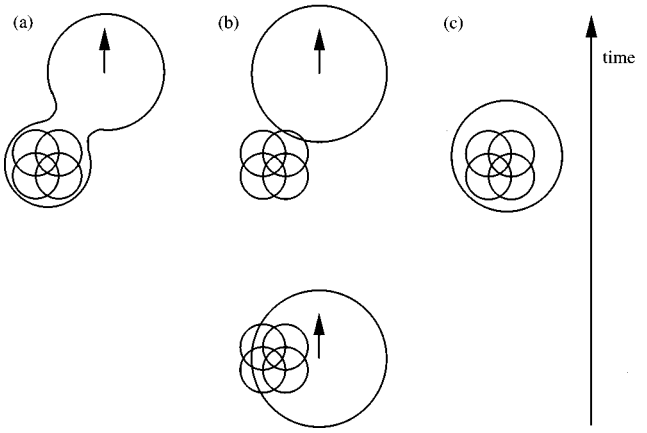

FIG. 2. Sketch of a four-particle cluster (small circles) and a passing wave packet (large circle). Circles indicate half-density contours. The molecular-dynamics equations of motion for the centroids and the widths of the packets can only influence the wave packet as a whole; either it passes by (b) or it is captured (c). The exact solution splits the packet into a captured and a proceeding part (a) (see text).

Another noteworthy example of quantum branching is displayed in Fig. 2, which shows four Gaussian wave packets $|q_l(t)\rangle$ [see Eq. (57)] forming a bound cluster and a wave packet (large circle) of an unbound particle that is passing by. The time-dependent width of this wave packet has spread in coordinate space because it has been moving freely for some time. Such situations occur frequently in simulations. In the exact case a piece of this wave packet would stick to the four-particle cluster, indicating that, with a certain probability, a five-particle cluster has been created. The remaining part of the wave packet would then move on. Because the Gaussian single-particle state does not permit this freedom, the wave packet can only be bound to the cluster in total or escape. However, in order for it to become bound its width has to shrink to the size of the cluster; otherwise, the matrix element of the interaction with the other wave packets is too weak. It is obvious that beyond a certain size of the passing packet, the overlap with the cluster will be too small to create a generalized

force on its width parameter sufficiently large to let it shrink. Therefore small capture probabilities cannot be described.

A branching procedure in the above given example would divide the time evolution into one branch of a five-particle cluster and another of a four-particle cluster and a freely moving wave packet with the respective probabilities. In general one can say that whenever the interaction varies strongly across the region of the wave packet, additional shape degrees of freedom should be considered. Otherwise, local actions are washed out and only mean-field properties survive.

But quantum branching also faces problems. In going from amplitudes to probabilities, one should not violate conservation laws. For instance, one should not alter the energy distribution of the system. The mean value and the variance of the energy of the ensemble of trial states that are populated during the branching should be the same as in the initial state. The same is true for other conserved quantities like total momentum or angular momentum. It is quite conceivable that variational principles with the appropriate constraints could be helpful (Balian and Veneroni, 1988; Lacroix, Chomaz, and Ayik, 1998, 1999).

3. Approximation or new dynamical model?

At this point a few remarks on the meaning of the results from the time-dependent variational principle seem to be in order. One could of course always claim that any restriction of the degrees of freedom in the trial state $|Q'\rangle$ leads to approximations of the Schrödinger equation—the more restraint in the trial state, the worse the approximation. But the simple examples in Sec. II.B and those for antisymmetric states in Sec. III demand a more subtle view.

Let us demonstrate this by restricting step by step the degrees of freedom in the general quantum state for a number of atoms. First we make a restricted ansatz for the trial state that contains only the coordinates and spins of nucleons and electrons, and we disregard completely the internal quark and gluon degrees of freedom for the nucleons and the quanta of the electromagnetic field. For low excitation energies this is certainly a good approximation.

The next step is to neglect the internal degrees of freedom of the nuclei, assuming that they are all in their ground states, and to retain only their center-of-mass coordinates and the electron variables. But this is still too complex to let us solve the Schrödinger equation. Therefore we describe the c.m. motion of the heavy nuclei with Gaussian packets, which leads to the classical equations of motion (53) for the nuclei with a Hamilton function $\mathcal{H}$ that couples to the quantal electrons. The state for the electrons may then be constrained to a single Slater determinant with no further restrictions on the single-particle states. Now we have arrived at the time-dependent Hartree-Fock model, which is a mean-field theory. The self-consistent Hamiltonian $\hat{H}_0$ is a one-body operator.

But we can of course go further and disregard the internal degrees of freedom of the atoms or the molecules altogether and treat only their center-of-mass motion by means of fixed-width Gaussians. At this point we obtain classical molecular dynamics with a Hamilton function $\mathcal{H}$ that contains two-body potentials between the molecules.

If the molecules are big, maybe chunks of crystals, maybe even stars held together by gravity, their center-of-mass coordinates may be adequate parameters for very narrow Gaussians. The time-dependent variational principle will now provide Newton's equations for macroscopic objects.

We do not believe that Newton's equations should be viewed as a bad approximation (bad because of the many constraints) of quantum chromodynamics where we started.[3] They should also not be regarded as an approximation of the time-dependent Hartree-Fock approach, which formally one could plead for because further constraints on the Slater determinant led there.

The question is, rather, which are the relevant degrees of freedom for a physical system? When these are identified, the time-dependent variational principle provides a dynamical model that is self-consistent and has all the properties of a Lagrange formalism, like the existence of canonical variables, Noether's theorem, etc.

Since the restriction of the trial state $|Q'\rangle$ can be made in finer or coarser steps, it is a matter of debate at which point one might want to speak of a new dynamical model or of an approximation.

III. ANTISYMMETRIZATION

The previous section demonstrated how to derive classical equations of motion from quantum mechanics by means of the time-dependent variational principle and localized single-particle states. It also showed that there is no clear boundary between quantum and classical mechanics. This will be even more the case in this Section, where we are dealing with indistinguishable fermions.

The natural generalization of the product state (44) (which led to classical molecular dynamics) to a trial state for identical fermions is the antisymmetrized product

$$|Q\rangle = \hat{A}|q_1\rangle\otimes|q_2\rangle\otimes\cdots\otimes|q_N\rangle = \frac{1}{N!}\sum_{all\ P}\ \mathrm{sgn}(P)|q_{P(1)}\rangle\otimes|q_{P(2)}\rangle\otimes\cdots\otimes|q_{P(N)}\rangle. \tag{70}$$

The sum runs over all permutations P, and $\mathrm{sgn}(P)$ is the sign of the permutation. The localized single-particle states $|q_l\rangle$ for spin-$\frac{1}{2}$ particles also contain two-component spinors $|\chi_l\rangle$,

[3]The time-dependent variational principle can also be formulated in quantum field theory, and it reduces to the nonrelativistic principle discussed here.

$$\langle \vec{x}|q_l\rangle = \exp\left\{-\frac{(\vec{x}-\vec{b}_l)^2}{2a_l}\right\}\otimes|\chi_l\rangle, \quad \vec{b}_l=\vec{r}_l+ia_l\vec{p}_l. \tag{71}$$

The spinor may, for example, be represented by the two complex parameters $\chi_l^{\uparrow}=\langle\uparrow|\chi_l\rangle$ and $\chi_l^{\downarrow}=\langle\downarrow|\chi_l\rangle$, where $|\uparrow\rangle$ and $|\downarrow\rangle$ are the eigenstates of the spin operator $\hat{s}_z$.

The general Lagrangian $\mathcal{L}$, as given in Eq. (14), calculated with the antisymmetrized trial state (70), provides through the Euler-Lagrange equations (21) or (22) the desired molecular-dynamics equations for fermions,

$$i\sum_{\nu}\mathcal{C}_{\mu\nu}(Q^*,Q)\dot{q}_{\nu}=\frac{\partial\mathcal{H}(Q^*,Q)}{\partial q_{\mu}^*}. \tag{72}$$

The Hermitian matrix $\mathcal{C}_{\mu\nu}(Q^*,Q)$, Eq. (23), is not as simple as in the classical case, where $\mathcal{C}_{\mu\nu}=\delta_{\mu\nu}$ [compare Eq. (55)], but depends on all parameters contained in Q.

Since the trial state is antisymmetric all consequences of the Pauli principle are incorporated in the equations of motion (72). Here, $\mathcal{C}_{\mu\nu}(Q^*,Q)$, which is the second logarithmic derivative of the determinant $\langle Q|Q\rangle = \det\{\langle q_k|q_l\rangle\}$, plays the role of a metric and will lead, for example, to large velocities $\dot{q}_{\nu}$ when the fermions get close to Pauli forbidden regions in phase space. In the energy $\mathcal{H}(Q^*,Q)=\langle Q|\hat{H}|Q\rangle/\langle Q|Q\rangle$, the Pauli principle causes exchange terms that induce, for example, additional momentum dependences. It should also be noted that the determinantal structure together with the nonorthogonality of the single-particle states result in an expression for the kinetic energy

$$\frac{\langle Q|\hat{T}|Q\rangle}{\langle Q|Q\rangle}=\sum_{k,l=1}^{N}\langle q_k|\hat{t}|q_l\rangle\mathcal{O}_{lk}, \tag{73}$$

which contains a twofold summation over all states (particles) compared to the single summation in classical molecular dynamics, Eq. (49). Here $\mathcal{O}_{lk}$ is the inverse of the overlap matrix,

$$(\mathcal{O}^{-1})_{kl}:=\langle q_k|q_l\rangle; \quad k,l=1,\ldots,N. \tag{74}$$

The expectation value of a two-body operator, like the interaction, is a fourfold sum,

$$\frac{\langle Q|\hat{V}|Q\rangle}{\langle Q|Q\rangle}=\frac{1}{2}\sum_{k,l,m,n=1}^{N}\langle q_kq_l|\hat{v}|q_mq_n\rangle \times(\mathcal{O}_{mk}\mathcal{O}_{nl}-\mathcal{O}_{ml}\mathcal{O}_{nk}). \tag{75}$$

The generalized forces $-(\partial/\partial q_{\mu})\mathcal{H}(Q^*,Q)$ are therefore rather involved expressions that reflect the fact that the antisymmetrization $\hat{A}$ is an N-body operation which correlates all N particles simultaneously.

The large numerical effort required has led different authors to propose approximations, which will be discussed in Sec. IV.

First we explain at some length the two-body case because many of the new features concerning antisymmetrization and indistinguishability can be understood in this simple study. Furthermore, attempts to approximate the effects of the Pauli principle in molecular dynamics by so-called Pauli potentials are based on considerations in two-body space.

The consequences of antisymmetrization in many-body space, which are discussed in Sec. III.B, are even more intricate. Depending on how much the single-particle states overlap, the antisymmetrization can change the properties of the trial state completely. There is, for example, Fermi motion even if the Gaussian single-particle states have no mean momentum.

A. Effects of antisymmetrization in two-body space

1. Static considerations

For two distinguishable particles the simplest trial state that leads in the proper limit to classical mechanics is the product of two Gaussians, $|q_1\rangle\otimes|q_2\rangle$. The corresponding state for indistinguishable fermions is the projection (70) onto the antisymmetric component

$$|Q\rangle=\hat{A}|q_1\rangle\otimes|q_2\rangle=\frac{1}{2!}\{|q_1\rangle\otimes|q_2\rangle-|q_2\rangle\otimes|q_1\rangle\}. \tag{76}$$

In order to simplify the following discussion, we do not use this Slater determinant but a trial state which separates center-of-mass and relative motion,

$$|Q\rangle=|q_{\text{c.m.}}\rangle\otimes|q\rangle. \tag{77}$$

The center-of-mass wave function is parametrized by $q_{\text{c.m.}}=\{A,\vec{B}\}$ as

$$\langle\vec{X}|q_{\text{c.m.}}(t)\rangle=\exp\left\{-\frac{[\vec{X}-\vec{B}(t)]^2}{2A(t)}\right\},$$
$$\vec{B}(t)=\vec{R}(t)+iA(t)\vec{P}(t), \tag{78}$$

where $\vec{X}=\frac{1}{2}(\vec{x}_1+\vec{x}_2)$ is the center-of-mass coordinate and the parameter set $q_{\text{c.m.}}=\{A,\vec{B}\}$ contains the mean c.m. position $\vec{R}$ and the mean c.m. momentum $\vec{P}$ combined in the complex parameter $\vec{B}$ and the complex width A.

The wave packet $|q\rangle$ for the relative motion also contains the spins, thus $q=\{a,\vec{b},\chi_1,\chi_2\}$. Its parametrized form in coordinate space reads

$$\langle\vec{x}|q(t)\rangle=\left[\exp\left\{-\frac{[\vec{x}-\vec{b}(t)]^2}{2a(t)}\right\}|\chi_1(t)\rangle\otimes|\chi_2(t)\rangle - \exp\left\{-\frac{[\vec{x}+\vec{b}(t)]^2}{2a(t)}\right\}|\chi_2(t)\rangle\otimes|\chi_1(t)\rangle\right], \tag{79}$$

where small letters denote the relative coordinates and parameters. In relative coordinate space the exchange of the two particles, $1\leftrightarrow2$, is equivalent to the parity operation $\vec{x}=\vec{x}_1-\vec{x}_2\leftrightarrow-\vec{x}=\vec{x}_2-\vec{x}_1$.

The two-body wave packet (77) is in general not a single Slater determinant because the center-of-mass motion for a Slater determinant does not separate if the single-particle packets have different width parameters. In this section we choose the widths $A(t)$ for the center-of-mass motion and $a(t)$ for the relative packet to be

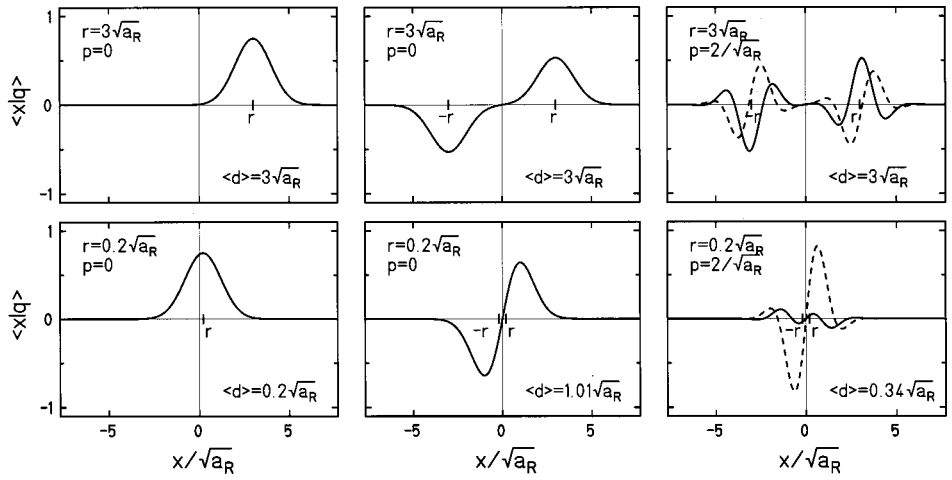

FIG. 3. The relative wave function for distinguishable particles (left column) and fermions (middle and right column) at different values of the parameters $\vec{r}=(r,0,0)$, $\vec{p}=(p,0,0)$, and $a=a_R$: solid line, real part; dashed line, imaginary part. $\langle d\rangle$ measures the distance between particles; see Eq. (88).

independent in order to decouple the center-of-mass degree of freedom. It should also be noted that trial state (79) is a linear combination of total spin $S=0$ and $S=1$.

The relation between $\vec{b}$ and the more intuitive quantities "distance" $\vec{r}$ and "relative momentum" $\vec{p}$ (time dependence is no longer indicated) is

$$\vec{b}_R=\vec{r}-a_I\vec{p} \quad \text{and} \quad \vec{b}_I=a_R\vec{p}, \tag{80}$$

$$\vec{r}=\frac{a^*\vec{b}+a\vec{b}^*}{a+a^*} \quad \text{and} \quad \vec{p}=\frac{1}{i}\frac{\vec{b}-\vec{b}^*}{a+a^*}. \tag{81}$$

Here and throughout this section the real and imaginary parts of complex numbers are denoted by the indices R and I, respectively.

It is important to realize that $\vec{r}$ and $\vec{p}$ retain their classical meaning only if the two particles are far apart in phase space. We illustrate this effect of antisymmetrization in Fig. 3, where on the left-hand side the relative wave function

$$\langle\vec{x}|q_d\rangle=\left(2\pi\frac{a^*a}{a^*+a}\right)^{-3/4}\exp\left\{-\frac{(\vec{x}-\vec{r})^2}{2a}+i\vec{p}\vec{x}\right\} \tag{82}$$

is plotted along the $\vec{r}$ direction. This trial state describes two distinguishable particles at relative distance $\vec{r}=\langle q_d|\hat{\vec{x}}|q_d\rangle$. For a single Gaussian the expectation value of $\hat{\vec{x}}=\hat{\vec{x}}(1)-\hat{\vec{x}}(2)$ is always equal to the parameter $\vec{r}$ independent of $\vec{p}$ and a_R.

This is a typical example where Ehrenfest's theorem can be used to derive the classical equations of motion from quantum mechanics. The method is to replace the expectation values of the Heisenberg equation,

$$\langle q_d|\frac{d}{dt}\hat{\vec{x}}|q_d\rangle=\langle q_d|i\left[\frac{1}{2\mu}\hat{\vec{k}}^2,\hat{\vec{x}}\right]|q_d\rangle=\frac{1}{\mu}\langle q_d|\hat{\vec{k}}|q_d\rangle, \tag{83}$$

for narrow wave packets by the mean values

$$\frac{d}{dt}\vec{r}=\frac{\vec{p}}{\mu}. \tag{84}$$

The analog for the relative momentum operator $\hat{\vec{k}}=\frac{1}{2}[\hat{\vec{k}}(1)-\hat{\vec{k}}(2)]$ is

$$\langle q_d|\frac{d}{dt}\hat{\vec{k}}|q_d\rangle=\langle q_d|i[V(\hat{\vec{x}}),\hat{\vec{k}}]|q_d\rangle$$

$$=-\langle q_d|\frac{\partial}{\partial\vec{x}}V(\hat{\vec{x}})|q_d\rangle \tag{85}$$

or

$$\frac{d}{dt}\vec{p}\approx\frac{\partial}{\partial\vec{r}}V(\vec{r}). \tag{86}$$

While Eq. (84) is exact for $|q_d\rangle$, Eq. (86) is only an approximate expression, which can be improved.

However, the antisymmetrized packet

$$\langle\vec{x}|q\rangle=\left[\exp\left\{-\frac{(\vec{x}-\vec{r})^2}{2a}+i\vec{p}\vec{x}\right\}-\exp\left\{-\frac{(\vec{x}+\vec{r})^2}{2a}-i\vec{p}\vec{x}\right\}\right], \tag{87}$$

displayed for two values of $\vec{r}$ and $\vec{p}$ in the middle and right columns of Fig. 3, leads to different results. First, for indistinguishable particles the operator $\hat{\vec{x}}=\hat{\vec{x}}(1)-\hat{\vec{x}}(2)$ is no longer an observable, because it is not symmetric with respect to particle exchange. Due to its negative parity, the expectation value $\langle q|\hat{\vec{x}}|q\rangle/\langle q|q\rangle$ is always zero even for particles that are far apart. The same holds true for the relative momentum: $\langle q|\hat{\vec{k}}|q\rangle/\langle q|q\rangle=0$. Therefore Ehrenfest's theorem is changed into a triviality because Eqs. (83) and (85) become meaningless ($0=0$). The conclusion is that Ehrenfest's theorem cannot be used to derive classical equations of motion for indistinguishable particles.

An observable that coincides with $|\vec{r}|$ at large distances is the root of the square radius minus the intrinsic width of the packet:

$$\langle d\rangle=\left(\frac{\langle q|\hat{\vec{x}}^2|q\rangle}{\langle q|q\rangle}-\frac{3|a|^2}{2a_R}\right)^{1/2}. \tag{88}$$

In the middle column of Fig. 3, which is for $\vec{p}=0$, it becomes evident that the observable distance $\langle d\rangle$ between two fermions with equal spin is larger than $|\vec{r}|$ and deviates most when $\vec{r}^2\ll a_R$. The right-hand side with

$|\vec{p}|=2/\sqrt{a_R}$ demonstrates that the distance $\langle d\rangle$ also depends on the relative momentum. For large relative momenta, $\vec{p}^2 a_R \gg 1$, the Pauli principle is again less effective, and $\langle d\rangle \approx |\vec{r}|$. The explicit expression for the mean-square radius in terms of parameters is

$$\frac{\langle q|\hat{\vec{x}}^2|q\rangle}{\langle q|q\rangle} = \vec{r}^2 + \frac{3|a|^2}{2a_R} + \frac{|a|^2}{a_R} f_{ex}(\xi, S_{12}), \tag{89}$$

where

$$f_{ex}(\xi, S_{12}) = \frac{\xi e^{-\xi} S_{12}}{1 - e^{-\xi} S_{12}} \quad \text{and}$$

$$\xi = \frac{|\vec{b}|^2}{a_R} = \frac{(\vec{r} - a_I \vec{p})^2}{a_R} + a_R \vec{p}^2. \tag{90}$$

The first two terms in Eq. (89) are the same as for distinguishable particles. The remaining part is the exchange term, which contains the quantity ξ and the spin overlap $S_{12}=|\langle\chi_1|\chi_2\rangle|^2$. From Eq. (90) it is evident that ξ may be regarded as a dimensionless measure for the distance in phase space where $\sqrt{a_R}$ is the length scale. For large $\xi \gtrsim 4$ the exchange vanishes and the Pauli principle is not active. For small ξ the distance between the fermions is always larger than $|\vec{r}|$ because the exchange term is positive definite. This effect is sometimes called "Pauli repulsion," but this is not a force between the particles.

The analogous expression for the distance in momentum space is

$$\langle\kappa\rangle = \left(\frac{\langle q|\hat{\vec{k}}^2|q\rangle}{\langle q|q\rangle} - \frac{3}{2a_R} \right)^{1/2}, \tag{91}$$

with the expectation value for the square momentum

$$\frac{\langle q|\hat{\vec{k}}^2|q\rangle}{\langle q|q\rangle} = \vec{p}^2 + \frac{3}{2a_R} + \frac{1}{a_R} f_{ex}(\xi, S_{12}). \tag{92}$$

Again a term proportional to $f_{ex}(\xi,S_{12})$ appears, so that there is complete analogy between coordinate and momentum space. The exchange term is again positive and causes a "Pauli repulsion" in relative momentum.

It is interesting to note that, for a mininum uncertainty state $|q\rangle$ with $a_I=0$ and equal spins ($S_{12}=1$), the sums of the observable distances in coordinate and momentum space fulfill

$$\langle d\rangle^2/a_R + \langle\kappa\rangle^2 a_R = \xi \frac{1+e^{-\xi}}{1-e^{-\xi}} \geqslant 2 \quad \text{for} \quad a_I = 0. \tag{93}$$

Unlike the measure ξ, the observable distance in phase space can never get smaller than 2; for details see Sec. III.A.4.

Equation (92) also states that the kinetic energy of relative motion

$$\mathcal{T} = \frac{1}{2\mu} \frac{\langle q|\hat{\vec{k}}^2|q\rangle}{\langle q|q\rangle} = \frac{\vec{p}^2}{2\mu} + \frac{3}{4\mu a_R} + \frac{1}{2\mu a_R} f_{ex}(\xi, S_{12}) \tag{94}$$

consists of a classical part $\vec{p}^2/(2\mu)$, a contribution from the uncertainty $3/(4\mu a_R)$, and an additional potential $f_{ex}(\xi,S_{12})/(2\mu a_R)$, which depends on $\vec{r}$, $\vec{p}$, a, and the spin overlap S_{12}.

An analogous expression can be obtained for a smooth spin-independent potential,

$$\mathcal{V} = \frac{\langle q|V(\hat{\vec{x}})|q\rangle}{\langle q|q\rangle} \approx V(\vec{r}) + \frac{1}{6}\Delta V(\vec{r}) \frac{3|a|^2}{2a_R} + \frac{1}{6} \frac{|a|^2}{a_R} \Delta V(\vec{r}=0) f_{ex}(\xi, S_{12}). \tag{95}$$

This expression is exact if $V(\hat{\vec{x}}) = V_0 + V_2 \hat{\vec{x}}^2$ and a good approximation if the Taylor expansion up to second order of $V(\hat{\vec{x}})$ around $\vec{x}=\vec{r}$ is adequate within the range of the wave packet. Please note that, due to rotational symmetry, $V(\hat{\vec{x}})$ depends only on $\hat{\vec{x}}^2$.

Combining Eqs. (94) and (95) yields a Hamilton function that splits into three parts,

$$\begin{aligned} \mathcal{H} &= \mathcal{T} + \mathcal{V} = \mathcal{H}_{classical} + \mathcal{V}_{uncertainty} + \mathcal{V}_{Pauli} \\ &= \left[\frac{\vec{p}^2}{2\mu} + V(\vec{r}) \right] + \left[\frac{3}{4\mu a_R} + \frac{|a|^2}{4a_R} \Delta V(\vec{r}) \right] \\ &\quad + \left[\frac{1}{2\mu a_R} + \frac{|a|^2}{6a_R} \Delta V(\vec{r}=0) \right] f_{ex}(\xi, S_{12}). \end{aligned} \tag{96}$$

Equation (96) is a basis for the approach used by several authors in nuclear physics[4] and atomic physics (Klakow *et al.*, 1994a, 1994b, Ebeling and Militzer, 1997) of incorporating the uncertainty principle and the Pauli principle into an extension of classical molecular dynamics. A two-body potential $\Sigma_{i<j}\mathcal{V}_{uncertainty}(\vec{r}_{ij},\vec{p}_{ij},a)$ is added to simulate the effects of the Heisenberg uncertainty principle, and $\Sigma_{i<j}\mathcal{V}_{Pauli}(\vec{r}_{ij},\vec{p}_{ij},a,S_{ij})$ is added to imitate the effects of the Pauli principle. The explicit form need not be the one given in Eq. (96); it is usually adapted to the specific use. The method is quite successful in calculating energies (Dorso *et al.*, 1987; Dorso and Randrup, 1987), but we advise caution in using the Hamilton function (96) naively in equations of motion like

$$\dot{\vec{r}}_i = \frac{\partial}{\partial \vec{p}_i}\mathcal{H} \quad \text{and} \quad \dot{\vec{p}}_i = -\frac{\partial}{\partial \vec{r}_i}\mathcal{H}. \tag{97}$$

The reason is that $\vec{r}_i$ and $\vec{p}_i$ are no longer canonical variables. As discussed earlier, although they still define the trial state $|Q\rangle$ uniquely, they lose their intuitive meaning when the particles are indistinguishable. The operator $\hat{\vec{x}}(i)$, "position of particle i," is meaningless and

[4]See, for example, Wilets *et al.*, 1977, 1978; Dorso *et al.*, 1987; Dorso and Randrup, 1987; Boal and Glosli, 1988; Peilert *et al.*, 1991; Maruyama, Toshiki, Ono, *et al.*, 1992; Niita *et al.*, 1995.

$\langle q|\hat{\vec{x}}(i)|q\rangle/\langle q|q\rangle$ is not $\vec{r}_i$! The analog statement holds for the momentum. Instead of postulating Eq. (97), we have to go back to the Lagrangian (14) and derive the equations of motion (72). It is evident that the matrix $\mathcal{C}$ will also be changed by the antisymmetrization.

2. Center-of-mass motion

Before discussing the relative motion in the antisymmetric case, we consider first the center-of-mass motion. The Lagrange function (14) for the center-of-mass wave packet, Eq. (78), is given by

$$\mathcal{L}_{\text{c.m.}}=\mathcal{L}_{0\ \text{c.m.}}-\mathcal{T}_{\text{c.m.}} \tag{98}$$

with

$$\begin{aligned}\mathcal{L}_{0\ \text{c.m.}}&=\frac{i}{2}\frac{\langle q_{\text{c.m.}}|\dot{q}_{\text{c.m.}}\rangle-\langle\dot{q}_{\text{c.m.}}|q_{\text{c.m.}}\rangle}{\langle q_{\text{c.m.}}|q_{\text{c.m.}}\rangle}\\&=\frac{i}{2}\frac{(\vec{B}^*-\vec{B})(\dot{\vec{B}}^*+\dot{\vec{B}})}{A^*+A}-\frac{i}{4}\left[\left(\frac{\vec{B}^*-\vec{B}}{A^*+A}\right)^2-\frac{3}{A^*+A}\right](\dot{A}^*-\dot{A})+\frac{3i}{4}\left(\frac{\dot{A}}{A}-\frac{\dot{A}^*}{A^*}\right)\\&=\vec{P}\cdot\dot{\vec{R}}+\frac{3}{4}\frac{\dot{A}_I}{A_R}+\text{total time derivative}\end{aligned} \tag{99}$$

and the kinetic energy

$$\begin{aligned}\mathcal{T}_{\text{c.m.}}&=\frac{\langle q_{\text{c.m.}}|\frac{1}{2M}\hat{\vec{K}}^2|q_{\text{c.m.}}\rangle}{\langle q_{\text{c.m.}}|q_{\text{c.m.}}\rangle}\\&=\frac{1}{2M}\frac{(\vec{B}^*-\vec{B})^2}{A^*+A}+\frac{3}{2M(A^*+A)}\\&=\frac{\vec{P}^2}{2M}+\frac{3}{4MA_R}.\end{aligned} \tag{100}$$

The Euler-Lagrange equations yield

$$\dot{\vec{B}}=0,\quad \dot{A}=\frac{i}{M}, \tag{101}$$

or if one transforms $\vec{B}$ and $\vec{B}^*$ into $\vec{R}$ and $\vec{P}$,

$$\dot{\vec{P}}=0,\quad \dot{\vec{R}}=\frac{\vec{P}}{M},\quad \dot{A}=\frac{i}{M}. \tag{102}$$

In the center-of-mass wave function $\vec{R}(t)$ and $\vec{P}(t)$ always have the classical meaning of the mean center-of-mass position and momentum, respectively. Nevertheless, when the width parameter A is included as a dynamical variable, the wave packet $|q_{\text{c.m.}}(t)\rangle=|A(t),\vec{B}(t)\rangle$ is the exact solution of the Schrödinger equation.

3. Relative motion

The Lagrange function for relative motion,

$$\begin{aligned}\mathcal{L}(q,q^*,\dot{q},\dot{q}^*)&=\frac{i}{2}\left(\frac{\langle q|\dot{q}\rangle-\langle\dot{q}|q\rangle}{\langle q|q\rangle}\right)-\frac{\langle q|\hat{\vec{k}}^2/2\mu|q\rangle}{\langle q|q\rangle}-\frac{\langle q|V(\hat{\vec{x}})|q\rangle}{\langle q|q\rangle}\\&\equiv\mathcal{L}_0-\mathcal{T}-\mathcal{V},\end{aligned} \tag{103}$$

features antisymmetrization not only in the kinetic and potential energy as seen in Eqs. (94) and (95), but also in the metric part $\mathcal{L}_0$.

For the sake of simplicity we treat in this subsection only equal, time-independent spins. In the general case the potential $V[\hat{\vec{x}},\hat{\vec{s}}(1),\hat{\vec{s}}(2)]$ may of course depend on the spin degrees of freedom. The parameters $\langle\uparrow,\downarrow|\chi_{1,2}(t)\rangle$ would then also appear in $\mathcal{L}_0$, $\mathcal{T}$, and $\mathcal{V}$, and one could get equations of motion for them. For time-independent equal spins, $\mathcal{L}_0$ is given by

$$\begin{aligned}\mathcal{L}_0&=\frac{i}{2}\frac{(\vec{b}^*-\vec{b})(\dot{\vec{b}}^*+\dot{\vec{b}})}{a^*+a}-\frac{i}{4}\left[\left(\frac{\vec{b}^*-\vec{b}}{a^*+a}\right)^2-\frac{3}{a^*+a}\right]\\&\quad\times(\dot{a}^*-\dot{a})+\frac{i}{2}\left[\frac{\dot{\vec{b}}\cdot\vec{b}^*-\vec{b}\cdot\dot{\vec{b}}^*}{\vec{b}^*\cdot\vec{b}}+\frac{\dot{a}^*-\dot{a}}{a^*+a}\right]f_{ex}(\xi,S_{12})\\&\quad+\text{total time derivative}\\&=\vec{p}\cdot\dot{\vec{r}}+\frac{3}{4}\frac{\dot{a}_I}{a_R}+\left[\frac{\vec{p}\cdot\dot{\vec{r}}-\vec{r}\cdot\dot{\vec{p}}}{\xi}+\frac{\vec{p}^2(\dot{a}_Ra_I-\dot{a}_Ia_R-\vec{r}\cdot\vec{p}\dot{a}_R)}{a_R}\right.\\&\quad\left.+\frac{\dot{a}_I}{a_R}\right]f_{ex}(\xi,S_{12})+\text{total time derivative}.\end{aligned} \tag{104}$$

As expected, $\mathcal{L}_0$ contains an exchange term, besides the terms for distinguishable particles; compare with $\mathcal{L}_{0\ \text{c.m.}}$ in Eq. (99). Although $\mathcal{L}_0$ looks very complicated, the Euler-Lagrange equations (72),

$$i\mathcal{C}\begin{pmatrix}\dot{a}\\ \dot{\vec{b}}\end{pmatrix}=\begin{pmatrix}\frac{\partial\mathcal{T}}{\partial a^*}\\ \frac{\partial\mathcal{T}}{\partial\vec{b}^*}\end{pmatrix}+\begin{pmatrix}\frac{\partial\mathcal{V}}{\partial a^*}\\ \frac{\partial\mathcal{V}}{\partial\vec{b}^*}\end{pmatrix}, \tag{105}$$

can be partially simplified because the free motion is, as for the c.m. state or the case of distinguishable particles, the exact solution of the Schrödinger equation,

$$\mathcal{C}^{-1}\begin{pmatrix}\frac{\partial\mathcal{T}}{\partial a^*}\\ \frac{\partial\mathcal{T}}{\partial\vec{b}^*}\end{pmatrix}=\begin{pmatrix}-\frac{1}{\mu}\\ 0\end{pmatrix} \tag{106}$$

hence

$$\begin{pmatrix} \dot{a} \\ \dot{\vec{b}} \end{pmatrix} = \begin{pmatrix} \dfrac{i}{\mu} \\ 0 \end{pmatrix} - i\mathcal{C}^{-1} \begin{pmatrix} \dfrac{\partial \mathcal{V}}{\partial a^*} \\ \dfrac{\partial \mathcal{V}}{\partial \vec{b}^*} \end{pmatrix}. \tag{107}$$

The complicated form of $\mathcal{C}^{-1}$ combines with the complicated derivatives ($\partial \mathcal{T}/\partial a^*$, $\partial \mathcal{T}/\partial \vec{b}^*$) of the kinetic energy such that the simple result of Eq. (106) is obtained. Although lengthy to calculate, it is easy to understand. The reason is that both states, $|a,\vec{b}\rangle$ and $|a,-\vec{b}\rangle$, are exact solutions of the Schrödinger equation; they differ only in the initial conditions. The antisymmetric state $|q\rangle = |a,\vec{b}\rangle - |a,-\vec{b}\rangle$, defined in Eq. (79), is therefore also an exact solution. The deeper reason is that both the time derivative and the Hamiltonian commute with the antisymmetrization operator $\hat{A}$ in Eq. (70):

$$\begin{aligned} 0 &= i\frac{d}{dt}\hat{A}|\Psi(t)\rangle - \hat{H}\hat{A}|\Psi(t)\rangle \\ &= \hat{A}\left(i\frac{d}{dt}|\Psi(t)\rangle - \hat{H}|\Psi(t)\rangle \right). \end{aligned} \tag{108}$$

Therefore, if $|\Psi(t)\rangle$ is the exact solution of the Schrödinger equation, so is $\hat{A}|\Psi(t)\rangle$. This general statement is not true if $|\Psi(t)\rangle$ is only an approximation.

In the special case of a harmonic interaction, $V(\hat{\vec{x}}) = V_0 + V_2\hat{\vec{x}}^2$, the contribution from the potential assumes a very simple form as well, because

$$\mathcal{C}^{-1} \begin{pmatrix} \dfrac{\partial \langle \hat{\vec{x}}^2 \rangle}{\partial a^*} \\ \dfrac{\partial \langle \hat{\vec{x}}^2 \rangle}{\partial \vec{b}^*} \end{pmatrix} = \begin{pmatrix} 2a^2 \\ 2a\dot{\vec{b}} \end{pmatrix} \tag{109}$$

The amazing result is that Eqs. (106) and (109) are the same for distinguishable particles and for indistinguishable particles, where $\mathcal{C}^{-1}$ is a complicated matrix depending on a^*, a and $\vec{b}^*, \vec{b}$. The exchange term in the expression for $\langle \hat{\vec{k}}^2 \rangle$, Eq. (92), and for $\langle \hat{\vec{x}}^2 \rangle$, Eq. (89), compensates for the different $\mathcal{C}$. It is also interesting to see that for a harmonic interaction the parameters $\vec{r}$ and $\vec{p}$ obey the classical equations of motion

$$\dot{\vec{r}} = \frac{\vec{p}}{\mu}, \quad \dot{\vec{p}} = -2V_2\vec{r}, \tag{110}$$

although the trial state $|q\rangle$ is antisymmetric and describes two identical fermions. This result, however, is only obtained if the width a is at the same time a dynamical variable with the equation of motion

$$\dot{a} = \frac{i}{\mu} - i2V_2a^2. \tag{111}$$

The case in which $a(t) = a_0$ is supposed to be a positive time-independent number leads to completely different results and is discussed in the following subsection.

4. Relative motion with a time-independent width parameter

This section investigates how the equations of motion change if the shape of the relative wave packet, Eq. (79), is restricted further by removing the width degree of freedom $a(t) = a_R(t) + ia_I(t)$ as a dynamical variable. For simplicity only parallel spins are considered, i.e., $S_{12} = 1$. By setting $a_R(t) = a_0$, $a_I(t) = 0$ and $\dot{a}(t) = 0$ in Eqs. (94) and (104) we obtain

$$\mathcal{L}_0 = \vec{p}\cdot\dot{\vec{r}} + (\vec{p}\cdot\dot{\vec{r}} - \vec{r}\cdot\dot{\vec{p}})\frac{e^{-\xi}}{1-e^{-\xi}} \tag{112}$$

$$\mathcal{T} = \frac{\vec{p}^2}{2\mu} + \frac{3}{4\mu a_0} + \frac{1}{2\mu a_0}\frac{\xi e^{-\xi}}{1-e^{-\xi}}, \tag{113}$$

where

$$\xi = \vec{r}^2/a_0 + \vec{p}^2 a_0 \quad \text{and} \quad \mathcal{L} = \mathcal{L}_0 - \mathcal{T} - \mathcal{V}. \tag{114}$$

The potential energy $\mathcal{V}$ is not given here explicitly and the spin dynamics is also not considered for simplicity. The equations of motion for $\vec{r}$ and $\vec{p}$ are

$$\begin{aligned} 0 &= \frac{d}{dt}\frac{\partial \mathcal{L}}{\partial \dot{\vec{p}}} - \frac{\partial \mathcal{L}}{\partial \vec{p}} \quad \text{or} \\ &-\dot{\vec{r}} - \frac{2e^{-\xi}}{1-e^{-\xi}}\left(\dot{\vec{r}} - \frac{\vec{r}(\vec{r}\dot{\vec{r}})/a_0 + \vec{p}(\vec{p}\dot{\vec{r}})a_0}{1-e^{-\xi}} \right) \\ &\quad + \frac{2e^{-\xi}a_0}{(1-e^{-\xi})^2}[\vec{r}(\vec{p}\dot{\vec{p}}) - \vec{p}(\vec{r}\dot{\vec{p}})] = -\frac{\partial}{\partial \vec{p}}\mathcal{H}(\vec{r},\vec{p}) \end{aligned} \tag{115}$$

and

$$\begin{aligned} 0 &= \frac{d}{dt}\frac{\partial \mathcal{L}}{\partial \dot{\vec{r}}} - \frac{\partial \mathcal{L}}{\partial \vec{r}} \quad \text{or} \\ &\dot{\vec{p}} + \frac{2e^{-\xi}}{1-e^{-\xi}}\left(\dot{\vec{p}} - \frac{\vec{r}(\vec{r}\dot{\vec{p}})/a_0 + \vec{p}(\vec{p}\dot{\vec{p}})a_0}{1-e^{-\xi}} \right) \\ &\quad + \frac{2e^{-\xi}}{(1-e^{-\xi})^2 a_0}[\vec{r}(\vec{p}\dot{\vec{r}}) - \vec{p}(\vec{r}\dot{\vec{r}})] \\ &\quad = -\frac{\partial}{\partial \vec{r}}\mathcal{H}(\vec{r},\vec{p}). \end{aligned} \tag{116}$$

For the reduced set of variables we are able to solve Eqs. (115) and (116) for $\dot{\vec{r}}$ and $\dot{\vec{p}}$. The result is

$$\begin{aligned} \dot{\vec{r}} &= \alpha_1(\xi)\frac{\partial \mathcal{H}}{\partial \vec{p}} + \alpha_2(\xi)\left\{ a_0\left(\vec{p}\frac{\partial \mathcal{H}}{\partial \vec{p}} + \vec{r}\frac{\partial \mathcal{H}}{\partial \vec{r}} \right)\vec{p} \right. \\ &\quad \left. + \left(\frac{\vec{r}}{a_0}\frac{\partial \mathcal{H}}{\partial \vec{p}} - a_0\vec{p}\frac{\partial \mathcal{H}}{\partial \vec{r}} \right)\vec{r} \right\} \end{aligned} \tag{117}$$

and

$$\dot{\vec{p}} = -\alpha_1(\xi)\frac{\partial \mathcal{H}}{\partial \vec{r}} + \alpha_2(\xi)\left\{\left(\frac{\vec{r}}{a_0}\frac{\partial \mathcal{H}}{\partial \vec{p}} - a_0\vec{p}\frac{\partial \mathcal{H}}{\partial \vec{r}}\right)\vec{p} - \left(\vec{r}\frac{\partial \mathcal{H}}{\partial \vec{r}} + \vec{p}\frac{\partial \mathcal{H}}{\partial \vec{p}}\right)\frac{\vec{r}}{a_0}\right\}, \tag{118}$$

where $\alpha_1(\xi)$ and $\alpha_2(\xi)$ are functions of $\xi = \vec{r}^2/a_0 + \vec{p}^2 a_0$ and are given by

$$\alpha_1(\xi) = \frac{1-e^{-\xi}}{1+e^{-\xi}} \tag{119}$$

and

$$\alpha_2(\xi) = \frac{2e^{-\xi}(1-e^{-\xi})}{(1+e^{-\xi})^2(1-e^{-\xi}) - 2\xi e^{-\xi}(1+e^{-\xi})}. \tag{120}$$

Since $\alpha_1(\xi \gg 1) = 1$ and $\alpha_2(\xi \gg 1) = 0$ one recognizes for $\xi \gg 1$ Hamilton's equations of motion. The condition $\xi \gg 1$ means that the two fermions are far from each other in phase space. In this limit the identical fermions behave like classical distinguishable particles, although their wave function is of course still antisymmetrized. When they get close in phase space (i.e., $\xi < 1$) $\alpha_1(\xi) \to \xi/2$ and $\alpha_2(\xi) \to 3/\xi^2$, which means that the Hamilton-like parts in Eqs. (117) and (118) vanish like $\xi/2$, but the remaining parts increase like $3/\xi^2$.

In this example one sees that for $\xi \lesssim 2$ the equations of motion, which result from the parametrization (79) with $a(t) \equiv a_0$, cannot be cast into Hamilton's form when $\vec{r}$ and $\vec{p}$ are regarded as canonical variables. To prove this statement let us suppose that a Hamilton function $\mathcal{H}_{Pauli}(\vec{r},\vec{p})$ exists such that Eqs. (117) and (118) can be written as

$$\dot{r}_i = \frac{\partial \mathcal{H}_{Pauli}}{\partial p_i} \quad \text{and} \quad \dot{p}_i = -\frac{\partial \mathcal{H}_{Pauli}}{\partial r_i}, \quad i = 1,2,3, \tag{121}$$

where i denotes the three spatial directions. Let us now disprove the existence of a function $\mathcal{H}_{Pauli}$ by calculating the mixed derivatives $\partial \dot{r}_i/\partial r_k$ and $\partial \dot{p}_k/\partial p_i$, which should add to zero if Eq. (121) is true. From the equations of motion (117) and (118) it is easy to verify that

$$\frac{\partial \dot{r}_i}{\partial r_k} + \frac{\partial \dot{p}_k}{\partial p_i} \neq 0. \tag{122}$$

This disproves the existence of a Hamiltonian $\mathcal{H}_{Pauli}(\vec{r},\vec{p})$ as a function of $\vec{r}$ and $\vec{p}$ that would describe the fermionic dynamics derived from the ansatz (79) with $a(t) \equiv a_0$ for the wave function.

It is, however, possible to find a pair of canonical variables $(\vec{\rho},\vec{\pi})$,

$$\vec{\rho} = \sqrt{\frac{1+e^{-\xi}}{1-e^{-\xi}}}\,\vec{r} \quad \text{and} \quad \vec{\pi} = \sqrt{\frac{1+e^{-\xi}}{1-e^{-\xi}}}\,\vec{p}, \tag{123}$$

that are nonlinear functions of the original variables $(\vec{r},\vec{p})$ (Saraceno *et al.*, 1983) such that $\mathcal{L}_0$ in Eq. (112) assumes the canonical form

$$\mathcal{L}_0 = \frac{1}{2}(\vec{\pi}\cdot\dot{\vec{\rho}} - \vec{\rho}\cdot\dot{\vec{\pi}}) + \frac{1}{2}\frac{d}{dt}(\vec{r}\vec{p}). \tag{124}$$

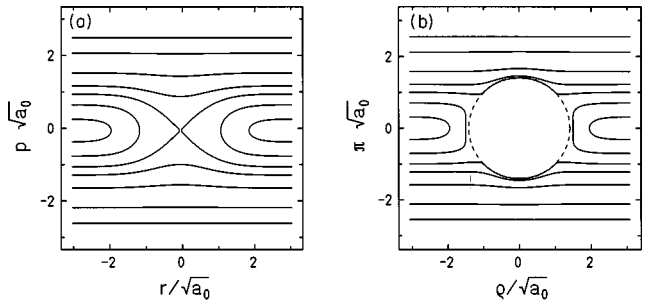

FIG. 4. Trajectories in phase space of one-dimensional free motion with fixed width: (a) variables r and p; (b) canonical variables ρ and π.

With these new variables, the equations of motion aquire the form of Eq. (121), where $\mathcal{H}_{Pauli}(\vec{\rho},\vec{\pi}) = \mathcal{H}(\vec{r},\vec{p})$ is the total energy expressed in the new canonical variables. However, $\mathcal{H}_{Pauli}(\vec{\rho},\vec{\pi})$ cannot be expressed in a closed form because Eqs. (123) cannot be solved for $\vec{r}(\vec{\rho},\vec{\pi})$ and $\vec{p}(\vec{\rho},\vec{\pi})$.

Equations (121) represent an approach often used in the literature to incorporate the effects of the Pauli principle by means of a two-body interaction. Different forms of momentum-dependent potentials have been added to the classical Hamiltonian or to the Lagrangian (Neumann and Fai, 1994). Here we see that this method differs in several aspects from fermionic dynamics. First, as discussed above, the dynamical behavior of $\vec{r}$ and $\vec{p}$ need not be of Hamilton's type. Second, one should not replace $\langle V(\hat{\vec{x}})\rangle$ simply by $V(\vec{r})$, because even for narrow wave packets there is an exchange term that is not small for $\xi < 1$; see Eq. (96).

The equations of motion simplify appreciably for a time-independent width parameter a_0, but the price to be paid is that free motion without interaction is no longer exact. For $\xi < 1$ the equations of motion differ essentially from the expected result $\dot{\vec{r}} = \vec{p}/\mu$ and $\dot{\vec{p}} = 0$ [see Eqs. (117) and (118)]. The shape of the wave packet is so restrained that the particles scatter even if there is no interaction.

There is, however, an appealing feature of the canonical variables $(\vec{\rho},\vec{\pi})$, namely, that they exhibit a geometrically forbidden region in phase space. From Eq. (123) it is evident that $\vec{\rho}^2/a_0 + \vec{\pi}^2 a_0 \geqslant 2$. This is demonstrated in Fig. 4, where in a one-dimensional example several trajectories of the relative motion are shown for two freely moving fermions. Figure 4(a) displays the trajectories, which are actually contours of constant kinetic energy, using r and p as dynamical variables, while the Fig. 4(b) shows the same trajectories, but using ρ and π. The empty area in the middle of Fig. 4(b) is the Pauli forbidden region of phase space. It corresponds to the single point at the origin ($r = 0$ and $p = 0$) in Fig. 4(a). The trajectories that cross there go around the circle in the canonical variables ρ and π.

Pauli potentials are usually chosen such that a pair of particles acquires a high energy in the forbidden region. One should, however, be aware that the kinetic energy at the boundary is finite, namely, $5/(4\mu a_0)$ in the three-

dimensional case; see Eq. (113). The deficiency that particles scatter even if there is no interaction is also present in all Pauli potentials. Inclusion of the complex width $a(t)$ as a dynamical variable cures this problem, as has been demonstrated.

At the end of this subsection, the reader should not be left with the impression that the Pauli principle is a two-body effect. In fact, antisymmetrization is a genuine N-body correlation, as will be discussed in Sec. III.

5. Resumé

(1) The intuitive idea of including the Pauli principle in a classical description by treating the exchange terms of the relative kinetic and potential energies of two identical fermions as an additional "Pauli potential" that supplements the classical equations of motion cannot be supported. It is not correct to regard the parameters $\vec{r}$ and $\vec{p}$ as canonical variables if

$$\vec{b}\cdot\vec{b}^{*}=|\vec{r}+ia\vec{p}|^{2}\lesssim 2|a^{*}+a| \tag{125}$$

and hence it is questionable whether the expectation value of the Hamiltonian can be used as the Hamilton function in Hamilton's equations of motion.

(2) Heisenberg's quantum uncertainty refers to the variances $(\langle\hat{\vec{x}}^{2}\rangle-\langle\hat{\vec{x}}\rangle^{2})$ and $(\langle\hat{\vec{k}}^{2}\rangle-\langle\hat{\vec{k}}\rangle^{2})$ of the wave packet which are given by the width parameter a and are not related to $\vec{r}^{2}$ or $\vec{p}^{2}$. It is therefore open to doubt whether inclusion of uncertainty in classical equations of motion can be achieved by using a potential that depends on $(\vec{r}_{ij}^{2}\cdot\vec{p}_{ij}^{2})$.

B. Effects of antisymmetrization in many-body space

1. Shell structure due to antisymmetrization

It is not immediately obvious that an antisymmetrized product state like Eq. (70) includes shell-model features, like the nodal structure of single-particle orbits, because the states are localized in coordinate and momentum space. But due to the invariance of a Slater determinant under linearly independent transformations among the occupied single-particle states, after antisymmetrization, any set of single-particle states that is complete in the occupied phase space is as good as any other. This applies also to nonorthogonal states. To illustrate this, we take four one-dimensional real Gaussians with the same real width parameter a_0 and zero mean momentum and displace them by $d=0.75\sqrt{a_0}$ (see left-hand side of Fig. 5). The one-body density can be written in terms of orthonormal states $|\psi_m\rangle$ as

$$\hat{\rho}^{(1)}=\sum_{k,l=1}^{N}|q_k\rangle\mathcal{O}_{kl}\langle q_l|=\sum_{m=1}^{N}|\psi_m\rangle\langle\psi_m|, \tag{126}$$

where the orthonormal eigenstates of $\hat{\rho}^{(1)}$, called natural orbits, are given by the following superposition of Gaussians:

$$|\psi_m\rangle=\sum_{k=1}^{N}|q_k\rangle(\mathcal{O}^{1/2})_{km}\,. \tag{127}$$

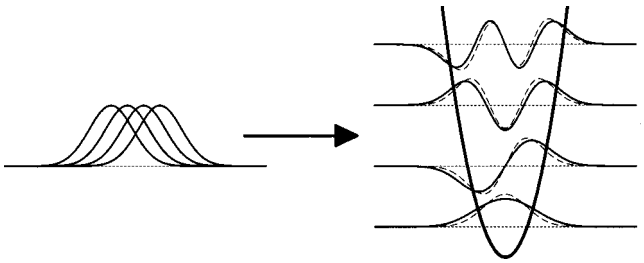

FIG. 5. Natural orbits. Antisymmetrization of four displaced Gaussians (left-hand side) leads to four occupied natural orbits (right-hand side), solid lines, which are almost harmonic-oscillator states (dashed lines).

Here $\mathcal{O}_{kl}$ is the inverse of the overlap matrix, $(\mathcal{O}^{-1})_{kl}=\langle q_k|q_l\rangle$. The occupied natural orbits are displayed on the right-hand side of Fig. 5 and compared to harmonic-oscillator eigenstates (dashed lines). One observes that the occupied single-particle states $|\psi_m\rangle$ consist of an s, p, d, and f state, all very close to harmonic-oscillator states. The difference between both sets can be made arbitrarily small by letting $d/\sqrt{a_0}$ approach zero. The f state, for example, is essentially the first Gaussian minus the second plus the third minus the fourth. All others are similar combinations. As already stressed for the two-body case in the previous section, when the wave packets overlap, r_l and p_l lose their classical meaning of position and momentum of particle l. In the limiting case $d\to 0$, all $r_l\to 0$, and all $p_l\to 0$, and the harmonic-oscillator shells emerge. The distributions in coordinate and momentum space are the quantum-mechanically correct ones of four spin-polarized fermions in a harmonic oscillator.

2. Fermi-Dirac distribution due to antisymmetrization

A second example is illustrated in Fig. 6, where we consider 100 equally spaced Gaussians in one dimension. Again all mean momenta are zero and the width a_0 is real. In Figs. 6(a) and (b), the width $\sqrt{a_0}$ is 0.2 of the mean distance d so that the wave packets are well separated. Therefore the spatial density $\rho_x=\langle x|\hat{\rho}^{(1)}|x\rangle$ and the momentum density $\rho_k=\langle k|\hat{\rho}^{(1)}|k\rangle$ are not changed by antisymmetrization. In Figs. 6(c) and (d), the width has been increased to $\sqrt{a_0}=d$. Without antisymmetrization (dot-dashed line), the spatial density is uniform and the momentum distribution is that of a single packet. After antisymmetrization (solid lines), one obtains typical shell-model oscillations in coordinate space and a Fermi distribution in momentum space. It is amazing to see how in Eq. (126) the superposition of Gaussians by means of the inverse overlap matrices can create a fully occupied momentum state; see, for example, in Fig. 6(d) the momentum distribution at $k=0.8k_F$, where the individual Gaussians give practically zero probability to measure this momentum. We also calculated the eigenstates of the kinetic energy in the occupied space and obtained perfect sinusoidal waves.

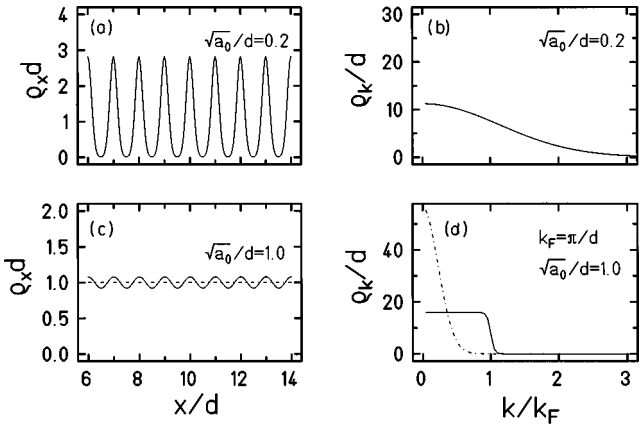

FIG. 6. Densities in coordinate and momentum space: solid line, with antisymmetrization; dot-dashed line, without. (a), (b) section with spatial density of 100 Gaussians (not overlapping in coordinate space) and the corresponding momentum distribution. Distributions with and without antisymmetrization are identical. (c), (d) same as above but for overlapping Gaussians. For details see text.

These two examples illustrate nicely that Slater determinants of localized single-particle states with zero mean momentum can describe the harmonic-oscillator shell model or even the Fermi motion of a gas of fermions in which plane waves are occupied up to the Fermi momentum. If one tries to simulate this effect by a ''Pauli potential,'' disregarding the momentum distribution in each wave packet, the resulting ground-state momentum distribution is unsatisfactory (Dorso *et al.*, 1987). The densities in coordinate and momentum space are just not given by the distributions of the r_l and p_l.

At this point we should like to remind the reader of the different meanings of the three ''momentum quantities'' used in this article:

(1) the momentum operator of particle l (not observable): $\hat{\vec{k}}(l)=\hat{\mathbb{1}}\otimes\cdots\otimes\hat{\vec{k}}\otimes\cdots\hat{\mathbb{1}}$,

(2) the momentum variable $\vec{k}$ as used in the momentum representation $\langle\vec{k}|q\rangle$, and

(3) the momentum parameter $\vec{p}_l$ which characterizes the state $|q_l\rangle=|\vec{r}_l,\vec{p}_l,a_l,\chi_l\rangle$.

3. Resumé

(1) The coordinate distribution $\rho_x(\vec{x})$ is given by the observable

$$\rho_x(\vec{x})=\frac{\langle Q|\Sigma_{l=1}^{N}\delta(\vec{x}-\hat{\vec{x}}(l))|Q\rangle}{\langle Q|Q\rangle} \tag{128}$$

and not by the (eventually time-averaged) distribution of the $\vec{r}_l$. Analogously the momentum distribution is given by

$$\rho_k(\vec{k})=\frac{\langle Q|\Sigma_{l=1}^{N}\delta(\vec{k}-\hat{\vec{k}}(l))|Q\rangle}{\langle Q|Q\rangle} \tag{129}$$

and not by the distribution of the $\vec{p}_l$. All $\vec{p}_l$ may be zero and there would still be Fermi motion.

(2) Fermi motion is not random motion in $\vec{r}_l$ and $\vec{p}_l$.

(3) The classical meaning of $\vec{r}_l$ and $\vec{p}_l$ is retained only when the system is so dilute in phase space that the Pauli principle has no consequences.

4. Dynamical considerations

The equations of motion for the simplest antisymmetric trial state (70) are [see Eq. (72)]

$$i\sum_{\nu}\mathcal{C}_{\mu\nu}(Q^*,Q)\dot{q}_\nu=\frac{\partial\mathcal{T}}{\partial q_\mu^*}+\frac{\partial\mathcal{V}}{\partial q_\mu^*}. \tag{130}$$

As in the two-body case, applying the inverse of $\mathcal{C}(Q^*,Q)$ to the derivatives of the kinetic energy yields the simple result

$$\begin{pmatrix}\dot{a}_1\\ \dot{\vec{b}}_1\\ \dot{\chi}_1\\ \dot{a}_2\\ \dot{\vec{b}}_2\\ \dot{\chi}_2\\ \vdots\end{pmatrix}=\begin{pmatrix}\frac{i}{m}\\ 0\\ 0\\ \frac{i}{m}\\ 0\\ 0\\ \vdots\end{pmatrix}-i\mathcal{C}^{-1}\begin{pmatrix}\frac{\partial\mathcal{V}}{\partial a_1^*}\\ \frac{\partial\mathcal{V}}{\partial\vec{b}_1^*}\\ \frac{\partial\mathcal{V}}{\partial\chi_1^*}\\ \frac{\partial\mathcal{V}}{\partial a_2^*}\\ \frac{\partial\mathcal{V}}{\partial\vec{b}_2^*}\\ \frac{\partial\mathcal{V}}{\partial\chi_2^*}\\ \vdots\end{pmatrix}. \tag{131}$$

Although in the case of free motion, $\vec{r}_l$ and $\vec{p}_l$ follow the classical path, this is once more the exact solution of the Schrödinger equation with $\dot{a}_l=i/m$ and $\dot{\vec{b}}_l$ and the spin parameters χ_l being constant. The reason is, of course, that the many-body time-evolution operator, which commutes with the antisymmetrization operator, is a product of single-particle time-evolution operators, and the free single-particle motion of Gaussians is exact.

The Pauli principle appears, as in the two-body case, in the interaction part in two ways. The interaction energy $\mathcal{V}(Q^*,Q)$ has exchange terms and the metric $\mathcal{C}^{-1}(Q^*,Q)$ couples all generalized forces $\partial\mathcal{V}/\partial q_\mu^*$ because it is in general not diagonal in the particle indices. Therefore the second term on the right-hand side of Eq. (131) acts like an N-body force.

Looking at the structure of Eq. (131), it seems more natural to replace the second term on the right-hand side with a two-body interaction than to consider the structure of the kinetic energy as was done in Sec. III.A. In nuclear physics, Wilets and co-workers (Wilets *et al.*, 1977, 1978) were the first to propose a space- and

momentum-dependent two-body ''Pauli core,'' which was later applied to atomic physics (Wilets and Cohen, 1998).

IV. MODELS IN NUCLEAR AND ATOMIC PHYSICS

In nuclear physics at nonrelativistic energies, nucleons cannot be treated as classical particles on trajectories. Their phase-space density is too large to ignore the Pauli principle. Therefore various molecular-dynamics models that incorporate the Pauli principle on different levels of sophistication are proposed in the literature. They will be discussed in more detail in the following subsections.

Molecular-dynamics calculations are also widespread in atomic physics to describe interacting atoms and molecules. But here the degrees of freedom are usually the classical c.m. positions and velocities of the nuclei. The quantal electrons which move in the electric field of the atoms and provide the attraction are often treated by mean-field methods. There are also applications in which each electron is treated as an individual entity localized in phase space. As for nucleons, if the density is high enough, electrons can become a degenerate Fermi gas for which a classical molecular-dynamics picture cannot be applied.

A. Antisymmetrized wave packets in nuclear physics

The time-dependent Hartree-Fock (TDHF) method (Davies *et al.*, 1985) was initially expected to be well suited to the description of colliding nuclei because stationary Hartree-Fock calculations successfully represent ground-state properties for all nuclei. The TDHF equations are obtained from the variational principle [Eq. (4)] when the single-particle states $|q\rangle$ that form the single Slater determinant $|Q\rangle$ are varied in an unrestricted way. However, it turned out that, even at low beam energies where the relative speed between the two colliding nuclei is small compared to the Fermi velocity and hence a mean field is always well established, the degree of fluctuation in the collective variables, like energy loss, scattering angle, or mass distribution, was much too small compared to the measured data (Davies *et al.*, 1985; Balian and Veneroni, 1992; Reinhard and Suraud, 1992; Lacroix, Chomaz, and Ayik, 1998, 1999). Moreover, the inclusion of collision terms in extended TDHF (see Goeke and Reinhard, 1982) did not improve the situation. The reason is that the TDHF equations contain a common mean field that does not allow fluctuations to grow. As discussed in Sec. II.C.2, quantum branching into other Slater determinants with different mean fields is missing. Even the collision integral, which induces fractional occupation of states and hence a mixing of Slater determinants, does not change that because one common mean field is again calculated from this mixture.

Calculations that treat the TDHF time evolution for each member of a thermal ensemble with its own specific mean field (Knoll and Strack, 1984; Knoll and Wu, 1988) can describe large fluctuations that develop during the expansion. The initial ensemble of Slater determinants, which could be envisaged as the result of quantum branching, was only assumed but not dynamically calculated.

The shortcomings of a common mean field apply also to models that solve the Vlasov equation augmented by a collision integral like VUU (Vlasov-Uehling-Uhlenbeck) or BUU (Boltzmann-Uehling-Uhlenbeck).[5] Although no explicit antisymmetrization like that in TDHF is present, Liouville's theorem and Pauli blocking in the collision term prevent an overoccupation of the single-particle phase space. The inherent lack of fluctations in these one-body descriptions led to molecular-dynamics models for fermions that will be discussed in the following subsections.

1. Time-dependent α-cluster model

The first molecular-dynamics model that uses antisymmetrized many-body states of localized constituents in nuclear physics is an extension of the α-cluster model, which successfully characterizes α-particle nuclei, to the time-dependent case. In the model, nuclei are represented as Slater determinants of wave packets for α particles. The width parameter of the Gaussian single-particle wave packets is chosen to be fixed (Caurier *et al.*, 1982; Saraceno *et al.*, 1983) as well as time dependent (Drożdż *et al.*, 1982). Even superpositions of two Slater determinants of wave packets for α particles with time-dependent width are investigated (Bauhoff *et al.*, 1985). Since these models are applicable only for nuclei with pronounced α substructure, new models were developed in the late 1980s, which address one wave packet for each single nucleon.

2. Fermionic molecular dynamics

The model of fermionic molecular dynamics (FMD) was suggested in 1990 (Feldmeier, 1990; Feldmeier *et al.*, 1995; Feldmeier and Schnack, 1997) in order to describe ground states of atomic nuclei and heavy-ion reactions in the energy regime below particle production. The many-body trial state of FMD is a Slater determinant $|Q(t)\rangle$ of single-particle Gaussian wave packets $|q_l(t)\rangle$, where $q_l(t)$ denotes the set of single-particle parameters $q_l(t)=\{\vec{b}_l(t),a_l(t),\chi_l(t),\xi_l\}$, $\vec{b}_l(t)=\vec{r}_l(t)+ia_l(t)\vec{p}_l(t)$, which contains mean position, mean momentum, and complex width. The spin degrees of freedom are represented by a spinor $|\chi_l(t)\rangle$ [see Eq. (71)]. The isospin part $|\xi_l\rangle$ is taken to be time independent and identifies either a proton or a neutron.

The equations of motion for all parameters are obtained from the variational principle as described in Sec. II [see Eq. (22)]. The Hamiltonian is an effective one, because the strong short-range repulsion in the nucleon-nucleon interaction causes correlations that cannot be

[5]See, for instance Aichelin and Bertsch (1985); Stöcker and Greiner (1986); Bertsch and Das Gupta (1988); Wolf *et al.* (1990); Gaitanos *et al.* (1999).

described by the trial state $|Q(t)\rangle$ (Feldmeier *et al.*, 1998). Moreover, the spin correlations caused by the strong tensor force are only poorly represented in a single Slater determinant.

In FMD, the ground state is defined by the deepest minimum of the energy $\mathcal{H}(Q^*,Q)=\langle Q|\hat{H}|Q\rangle$. Since all generalized forces $\partial\mathcal{H}/\partial q_l^*=0$ vanish in the minimum, this state is stationary, and all $\dot{q}_l=0$. There is no "Fermi motion" in the parameters $\vec{r}_l,\vec{p}_l,\ldots$. Ground-state properties like binding energies and rms radii can be reproduced equally well with a variety of effective nucleon-nucleon interactions, which differ mainly in their momentum dependence. But the intrinsic structure of the nuclei depends on the interaction. Superpositions of single-particle states as well as of Slater determinants can be used in order to obtain a more refined description of nuclear structure, e.g., for halo nuclei (Neff *et al.*, 1999).

Fermionic molecular dynamics is able to model a variety of heavy-ion reactions ranging from fusion to dissipative reactions and multifragmentation (Feldmeier and Schnack, 1997). Unlike the case of TDHF, fluctuations occur in these reactions, but the results also show that initial correlations given by the intrinsic structure of the ground states play a major role in the simulation of fragmentation reactions (Neff *et al.*, 1999).

The time-dependent width parameters are important nonclassical degrees of freedom (Feldmeier *et al.*, 1995), especially to allow for the evaporation of nucleons, a process that otherwise is strongly hindered, because each escaping wave packet takes away at least its zero-point energy. Inside a nucleus this zero-point energy is typically 10 MeV, but evaporated nucleons have a mean kinetic energy of only 2 MeV. Therefore the packet must spread during the evaporation process.

Thermodynamic equilibrium properties can be determined in FMD by means of time averaging; see Sec. V.C and Schnack and Feldmeier (1997).

As already explained in Sec. II.C.2, the restricted parametrization leads to barriers which would not exist for the exact solution. The splitting of wave packets is an especially important source of quantum branching. The lack of this dynamical freedom is a serious hindrance to forming clusters (Kiderlen and Danielewicz, 1996), which is also observed in antisymmetrized molecular dynamics and FMD investigations of the spinodal decomposition of nuclear matter. Without quantum branching possibly important reaction mechanisms in multifragmentation reactions are quenched (Colonna and Chomaz, 1998). Further study of this subject is needed.

3. Antisymmetrized molecular dynamics

Antisymmetrized molecular dynamics (AMD) is similar to FMD with respect to the choice of the trial state, but includes random branching between trial states. For details, the reader is referred to Ono *et al.*, 1992a, 1992b, 1993; Ono and Horiuchi, 1996a, 1996b. Antisymmetrized molecular dynamics describes the nuclear many-body system with a Slater determinant $|Q(t)\rangle$ of Gaussian wave packets characterized by the parameter set $q_l(t)=\{\vec{Z}_l(t),\chi_l,\xi_l\}$, In AMD notation the complex parameters $\vec{Z}_l=(1/\sqrt{2a_0})\vec{b}_l=(1/\sqrt{2a_0})\vec{r}_l+i\sqrt{a_0/2}\vec{p}_l$ denote the time-dependent centroids of the wave packets and χ_l,ξ_l the time-independent spin-isospin components, which can be either proton or neutron, spin up or down. The width parameter $\nu=1/2a_0$ is real and time independent and the same for all wave packets.

The time evolution of the $\vec{Z}_l(t)$ is determined by the time-dependent variational principle, Eq. (4), which leads to the equations of motion given in Eq. (22). The Hamilton function $\mathcal{H}$ used in AMD is the expectation value of a Hamiltonian $\hat{H}$ plus an additional term that removes the spurious zero-point energy of the center-of-mass wave packets for the different clusters. This c.m. energy, which is of the order of 10 MeV for all clusters, is an artifact of all product states.

The smooth variation of the $\vec{Z}_l(t)$ due to the generalized forces $\partial\mathcal{H}/\partial\vec{Z}_l^*$ is supplemented by different stochastic forces. These can be regarded as a phenomenological ansatz for quantum branching between different trial states $|Q_j(t)\rangle$ as discussed in Sec. II.C.2. One branching procedure takes care of deviations caused by the short-range repulsion between nucleons. For that, a collision term is introduced which randomly changes the relative canonical momenta of a pair of wave packets. In order to avoid entering Pauli-forbidden regions in phase space, approximate canonical variables are used which for two particles reduce to those discussed in Sec. III.A.4; compare to Fig. 4.

Another branching simulates the spreading and splitting of wave packets, which is an essential process for an adequate description of evaporation and absorption, but cannot be accomplished by the trial state (Ohnishi and Randrup, 1995 1997a, 1997b, Ono and Horiuchi, 1996a).

Antisymmetrized molecular dynamics is able to reproduce the essential properties of nuclear ground states [minima in $\mathcal{H}(Q^*,Q)$] and, when extended to trial states that use superpositions of single-particle states or Slater determinants, even the structure of halo nuclei (see, for example, Kanada-En'yo *et al.*, 1995).

Multifragmentation reactions are investigated for beam energies around the Fermi energy. Before comparison with experimental data from heavy-ion collisions, the result of a simulated collision is fed into a statistical decay program to account for long-time processes (Pülhofer, 1977; Ono, 1998).

Since the numerical effort of antisymmetrized molecular dynamics as well as of FMD grows with N^4, approximations are needed for the calculation of systems with more than $N=80$ nucleons. Recently the AMD group developed a "triple-loop approximation," which converts the fourfold sum of the potential energy [see Eq. (75)] into a threefold one, so that systems like Au+Au are now feasible (Ono, 1998).

B. Product states of wave packets—quantum molecular dynamics

Models that parametrize the many-fermion trial state by a simple product of Gaussian wave packets are called

quantum molecular dynamics (QMD) in nuclear physics. The first versions of QMD were invented in the eighties (Aichelin and Stöcker, 1986; Aichelin *et al.*, 1987; Aichelin 1991; Khoa *et al.*, 1992). They all employ a product state,

$$|Q(t)\rangle = |q_1(t)\rangle \otimes |q_2(t)\rangle \otimes \cdots \otimes |q_N(t)\rangle, \tag{132}$$

of single-particle states $|q_l(t)\rangle = |\vec{r}_l(t), \vec{p}_l(t)\rangle$ defined in Eq. (45), where only the mean positions $\vec{r}_l(t)$ and the mean momenta $\vec{p}_l(t)$ are time dependent. The width is fixed and the same for all wave packets.

The resulting equations of motion are the classical ones, given in Eq. (53). Moreover, the interpretation of $\vec{r}_l(t)$ and $\vec{p}_l(t)$ is purely classical and the particles are considered distinguishable. This simplifies the collision term, which acts as a random force, and at higher energies also simplifies the description of transitions from nucleons into resonances.

All QMD versions use a collision term with Pauli blocking in addition to classical dynamics. Some versions consider spin and isospin, others use nucleons with an average electric charge. Several QMD versions try to incorporate the Pauli principle by means of a Pauli potential that prevents nucleons of the same kind from coming too close in phase space; see Sec. III.A. Due to these simplifications, QMD has the advantage that numerical effort grows only with N^2, thus allowing the simulation of large systems. In addition, all QMD versions use a statistical decay program for the long-time dynamics.

1. Versions

Quantum molecular-dynamics models are widely used in nuclear physics and exist in many versions. We shall list some of them and apologize for not mentioning all others. A more thorough overview of QMD models is provided by Hartnack *et al.* (1998).

(1) From experience with VUU/BUU models (Aichelin and Bertsch, 1985), one of the first versions of QMD (Aichelin and Stöcker, 1986; Aichelin, 1991) was suggested. It exploited the trial state (132) only insofar as the interaction could get an effective range due to folding with the wave packets. In all other respects the model propagates point particles along classical trajectories. The zero-point energy originating from localization is omitted. Random distributions of mean coordinates and momenta are taken as initial states according to the experimental ground-state density profile and binding energy. This distribution, however, is not the ground state of the model Hamiltonian but an unstable excited state. The model ground state is highly overbound. This QMD model does not distinguish between protons and neutrons; all nucleons carry an average charge.

(2) The isospin QMD model treats the isospin explicitly but is the same in all other respects. This version was designed for the analysis of collective flow and pions (Hartnack *et al.*, 1989).

(3) Another branch of QMD evolution uses a Pauli potential and takes the trial state (132) more seriously (Peilert *et al.*, 1992; Konopka *et al.*, 1995) Since nucleons are kept apart in phase space by the Pauli potential (Peilert *et al.*, 1991), the minimum of the Hamiltonian determines the nuclear ground state. This is not only theoretically attractive, but is also very important if one wants to investigate the survival of initial ground-state correlations in the final products. An ensemble of random initial states is not able to answer such questions.

(4) The Japanese extended QMD model (Maruyama *et al.*, 1992; 1996; Niita *et al.*, 1995; Chiba *et al.*, 1996) is constructed in the same spirit. Moreover, the width parameter, which is time independent in all other versions, is chosen to be time dependent here. As in AMD, the c.m. zero-point energies are subtracted from the Hamiltonian, which is difficult because of the changing width. Some observations in extended QMD are similar to those in FMD. In particular, evaporation processes are described much better than with a fixed width. For fusion reactions the time-dependent width plays a major role because the fusion cross sections are too small with a fixed width.

(5) Another version of QMD was developed in Copenhagen and called nuclear molecular dynamics (Bondorf *et al.*, 1995).

(6) Many attempts have been undertaken to extend the applicability of QMD towards higher (relativistic) energies. These include a relativistic model (Sorge *et al.*, 1989; Lehmann *et al.*, 1995; Sorge, 1995) and an ultrarelativistic model (Bass *et al.*, 1998).

2. Decoupling of center-of-mass and relative motion

A prominent problem of many-body trial states expressed in terms of single-particle quantities, irrespective of whether they are antisymmetrized or not, is the center-of-mass motion that does not separate from the relative motion. One attempt to solve the problem is the construction of a trial state in which the single-particle width parameters are replaced by a width matrix $A_{kl}(t)$ (Kiderlen and Danielewicz, 1996),

$$\begin{aligned}\langle \vec{x}_1, \ldots, \vec{x}_N | Q(t) \rangle &= \exp\Bigg\{ -\sum_{k,l} (\vec{x}_k - \vec{r}_k(t)) A_{kl}(t) (\vec{x}_l - \vec{r}_l(t)) \\ &\quad + i \sum_k \vec{p}_k(t) \vec{x}_k \Bigg\} |\chi\rangle, \end{aligned} \tag{133}$$

where $|\chi\rangle$ is a normalized spin-isospin state. The dynamical freedom of the matrix elements $A_{kl}(t)$ allows this state to factorize into c.m. and intrinsic degrees of freedom for subgroups of particles. For two particles, the advantage of ansatz (133) can be seen immediately:

$$\begin{aligned}\langle \vec{x}_1, \vec{x}_2 | Q \rangle &= \exp\{ -A_{\text{c.m.}} (\vec{X} - \vec{R})^2 + i \vec{P} \vec{X} \} \\ &\quad \times \exp\{ -A_{rel} (\vec{x} - \vec{r})^2 + i \vec{p} \vec{x} \} |\chi\rangle. \end{aligned} \tag{134}$$

With the usual definitions of relative $(\vec{x},\vec{r},\vec{p})$ and c.m. $(\vec{X},\vec{R},\vec{P})$ coordinates, the width matrix elements are related by $A_{\text{c.m.}}=2(A_{11}+A_{12})$, $A_{rel}=(A_{11}-A_{12})/2$, and $A_{11}=A_{22}$. Independent of the relative motion, which can be in a bound state with width A_{rel}, the c.m. wave-packet width $A_{\text{c.m.}}(t)$ can spread according to free motion. For product states, the variance in the c.m. coordinate is always connected to that of the relative motion. For the product of two identical Gaussian wave packets, the relation is $A_{\text{c.m.}}(t)=4A_{rel}(t)$ (Kiderlen and Danielewicz, 1996).

The separation of internal and c.m. variables should enhance fragment production, which is otherwise suppressed due to the localization energy of the c.m. motion. Kiderlen and Danielewicz could demonstrate a significant improvement in the description of light fragments. Unfortunately, a way of extending the proposed ansatz to antisymmetrized states has not been found to date. The trial state (133) is also not flexible enough to describe the splitting of wave packets necessary to model particle capture, as discussed in connection with quantum branching in Sec. II.C.2.

3. Approximate canonical variables—Pauli potential

Historically the first models that tried to describe fragmentation reactions on the basis of single-particle motion were classical models; see, for instance, Bodmer and Panos, 1977; Bodmer *et al.*, 1980. Problems arising from the fact that classical particles obey neither the Heisenberg uncertainty relation nor the Pauli principle of identical fermions were addressed by introducing two-body interactions $\Sigma_{i<j}\mathcal{V}_{uncertainty}(\vec{r}_{ij},\vec{p}_{ij},a)$ (Wilets *et al.*, 1977, 1978) and $\Sigma_{i<j}\mathcal{V}_{Pauli}(\vec{r}_{ij},\vec{p}_{ij},a,S_{ij})$ (Wilets *et al.*, 1977, 1978; Dorso *et al.*, 1987; Dorso and Randrup, 1987; Boal and Glosli, 1988; Peilert *et al.*, 1991; Maruyama *et al.*, 1992; Niita *et al.*, 1995; Ebeling and Militzer, 1997), which imitate the two quantum effects; see Eq. (96).

This method is quite successful in calculating energies and reasonable single-particle occupations in momentum space for the free Fermi gas at finite temperatures (Dorso *et al.*, 1987; Dorso and Randrup, 1987), but as already mentioned in Sec. III.A, care should be taken in using these variables in Hamilton's equations of motion as if they were canonical. In addition, classical models cannot correctly describe quantum-statistical properties in general, like occupation numbers, mean energy, specific heat, etc.

Nevertheless, the idea of simulating the Heisenberg uncertainty and Pauli exclusion principles by means of two-body interactions is still being used nowadays in applications of classical dynamics to many-fermion problems (e.g., Latora *et al.*, 1994; Wilets and Cohen, 1998).

C. Atomic physics

In atomic physics, molecular-dynamics applications are widespread because the de Broglie wavelength of the atoms (molecules) is often much shorter than the variations in the intermolecular potential. Therefore a trial state for the center-of-mass coordinates, which is a product of well-localized Gaussians as discussed in Sec. II.B.2, is well suited to this task:

$$|Q'_{atom}\rangle=|\vec{B}_1\rangle\otimes\cdots\otimes|\vec{B}_N\rangle \quad \text{with} \quad \vec{B}_l=\vec{R}_l+iA_0\vec{P}_l. \tag{135}$$

Electrons are much lighter, so quantum effects like the Pauli principle and uncertainty are important. Their trial state may be thought of as an antisymmetrized many-body state $|Q'_{el};Q'_{atom}\rangle$ that depends on electronic degrees of freedom summarized in the set $Q'_{el}=\{q_0,q_1,q_2,\ldots\}$, e.g., characterizing different orbits. It also depends on the variables of the atoms $\{\vec{R}_l,\vec{P}_l\}$ that mark, for example, the phase-space centers of the orbits. The dependence on $\vec{P}_l$ is usually neglected because the velocities of electrons are much larger than those of atoms. The total trial state is the product

$$|Q'\rangle=|Q'_{atom}\rangle\otimes|Q'_{el};Q'_{atom}\rangle. \tag{136}$$

In contrast to the case of nuclear physics, here the Hamiltonian is known. It can be well approximated (when spin and other relativistic effects are neglected) by

$$\hat{H}=\sum_{l=1}^{N}\left[\frac{\hat{\vec{K}}^2(l)}{2M_l}-\sum_{i=1}^{N_{el}}\frac{Z_l e^2}{|\hat{\vec{X}}(l)-\hat{\vec{x}}(i)|}\right]+\sum_{l<k}^{N}\frac{Z_l Z_k e^2}{|\hat{\vec{X}}(l)-\hat{\vec{X}}(k)|}+\hat{H}_{el} \tag{137}$$

$$\hat{H}_{el}=\sum_{i=1}^{N_{el}}\frac{\hat{\vec{k}}^2(i)}{2m_{el}}+\sum_{i<j}^{N_{el}}\frac{e^2}{|\hat{\vec{x}}(i)-\hat{\vec{x}}(j)|}, \tag{138}$$

where capital and small letters denote atomic and electronic variables, respectively. From the Lagrange function $\mathcal{L}'$, Eq. (3), one obtains, with the appropriate approximations, the well-known quantum molecular-dynamics equations for atomic physics. The atomic variables $\vec{R}_l$, and $\vec{P}_l$ follow classical equations of motion (width A_0 small) under the influence of electron potentials given by

$$\mathcal{V}_{atom\text{-}el}=\langle Q'_{el};Q'_{atom}|\sum_{l=1}^{N}\left[-i\dot{\vec{B}}_l\frac{\partial}{\vec{B}_l}+\sum_{i=1}^{N_{el}}\frac{Z_l e^2}{|\vec{R}_l-\hat{\vec{x}}(i)|}\right]\times|Q'_{el};Q'_{atom}\rangle+\langle Q'_{el};Q'_{atom}|\hat{H}_{el}|Q'_{el};Q'_{atom}\rangle. \tag{139}$$

The coupled equations of motion for the electron degrees of freedom Q'_{el} are approximated at various levels of sophistication.

These quantum molecular-dynamics models are not the subject of this review because they do not treat the electrons (fermions) as being localized in phase space.

1. Product states of wave packets in atomic physics

For simple Coulomb systems (Suarez-Barnes *et al.*, 1993) and for hydrogen plasmas, models are proposed that employ trial states of the type

$$|Q'\rangle = |Q'_{atom}\rangle \otimes |Q'_{el}\rangle, \tag{140}$$

where the electronic state $|Q'_{el}\rangle$ consists of localized Gaussian wave packets [Eq. (45)]. These models are QMD models in the sense of Sec. IV.B, either with time-independent width but without the Pauli potential (Ebeling and Militzer, 1997), or with the Pauli potential (Ebeling and Schautz, 1997), or with time-dependent width and the Pauli potential (Klakow *et al.*, 1994a, 1994b). Only the electronic part is represented by a wave function; the protons of the hydrogen plasma move on classical trajectories.

An interesting application, which is referred to in Sec. V.C.2, is the study of a plasma under extreme conditions—high temperature or pressure—and phase transitions to the liquid and solid phases (Klakow *et al.*, 1994a, 1994b). Other investigations focus on the degree of ionization of a partially ionized plasma Ebeling *et al.*, 1996; Ebeling and Militzer, 1997).

2. Quantum branching

When the Born-Oppenheimer approximation is valid, adiabatic energy surfaces can be calculated as

$$\mathcal{V}_{ad}(Q'^{*}_{atom}, Q'_{atom}; \nu_{el}) = \langle \nu_{el}; Q'_{atom} | \sum_{l=1}^{N} \sum_{i=1}^{N_{el}} \frac{Z_l e^2}{|\vec{R}_l - \hat{\vec{x}}(i)|} + \hat{H}_{el} | \nu_{el}; Q'_{atom} \rangle, \tag{141}$$

where $\nu_{el}=0$ denotes the lowest energy state of the electrons under the influence of the charges Z_l of static ions positioned at $\vec{R}_l$. The excited eigenstates of the electronic system, for example vibrational modes or particle-hole excitations are numerated by $\nu_{el}=1,2,\ldots$. In principle one can set up an improved trial state as a linear combination,

$$|Q'\rangle = \sum_{\nu_{el}} q_{\nu_{el}} |Q'_{atom,\nu_{el}}\rangle \otimes |\nu_{el}; Q'_{atom,\nu_{el}}\rangle, \tag{142}$$

and then try to solve the coupled equations that result from the variational principle (9) for the complex amplitudes $q_{\nu_{el}}$ and the ion variables $Q'_{atom,\nu_{el}} = \{\vec{R}_l^{\,\nu_{el}}, \vec{P}_l^{\,\nu_{el}}; l = 1,\ldots,N; \nu_{el}=1,2,\ldots\}$. From energy, momentum, and angular momentum conservation it is obvious that one has to have as many different trajectories $\{\vec{R}_l^{\,\nu_{el}}, \vec{P}_l^{\,\nu_{el}}\}$ for the ions as there are excited states that can be populated, because an inelastic excitation $\nu_{el} \to \nu'_{el}$ will change the ion trajectories accordingly.

But these equations of motion are usually too complex to be solved numerically, and therefore one introduces quantum branching (as discussed in Sec. II.C.2) by what is called the quasiclassical trajectory surface-hopping method; see, for example, references in Topaler *et al.* (1997). Different approaches are tested against an accurate quantum-dynamics calculation of a realistic system by Topaler *et al.* (1997). They find fair agreement between the quantum branching methods and the results of quantum equations that result from a trial state of the type found in Eq. (142). This is to be expected if electronic coherence is not important on time scales of the ion motion so that hopping between the energy surfaces [Eq. (141)] acts as a random Langevin force on the ion trajectories.

V. STATISTICAL PROPERTIES

Molecular-dynamics models are used to simulate not only nonequilibrium but also equilibrium situations, especially when correlations require descriptions that go beyond mean-field approaches and quasiparticles. In the context of classical mechanics, a vast literature exists (Hoover, 1986), even for relativistic cases (Belkacem *et al.*, 1998), in which equilibrium properties are studied. So-called thermostated time evolutions (Nosé, 1984, 1991; Hoover, 1985; Kusnezov *et al.*, 1990), in which appropriate coupling to external degrees of freedom adjusts the temperature, are on firm ground in classical mechanics and have been used successfully for equilibrium situations, e.g., to investigate classical spin systems, as well as for nonequilibrium situations, e.g., to study glass transitions.

Classical procedures fail for quantum systems and especially for identical fermions when the phase-space density is no longer small and the effects of the Pauli principle become important. No analog to thermostated time evolutions exists as yet for quantum systems. There are a few attempts to infer thermodynamic properties from dynamical simulations in quantum mechanics.[6] Usually one performs time averages and relies on the ergodic assumption. The validity of this method, of course, crucially depends on the statistical and ergodic properties of the dynamical model. From the articles just cited, one realizes that the matter is still under debate.

Two issues are discussed in detail in the following sections. One is how to determine thermostatic properties in a molecular-dynamics model where thermostatic refers to the static thermal properties governed by the partition function $Z(T) = \mathrm{Tr}(\exp\{-\hat{H}/T\})$. Once the trace is evaluated within a given model, its thermostatic properties can be deduced by standard methods like partial derivatives of $\ln Z(T)$ with respect to temperature T or other parameters contained in the Hamilton operator $\hat{H}$.

The other and even more important issue, which is discussed in Sec. V.B, is the dynamical behavior of a molecular-dynamics model. For example, a dissipative system that is initially far from equilibrium is expected to equilibrate towards the canonical ensemble. The simulation of such a system within the model provides a crucial test of its thermodynamic properties. Often one

[6] Some examples are given by Kusnezov, 1993; Ohnishi and Randrup, 1993, 1997a, 1997b; Blaise *et al.*, 1994; Klakow *et al.*, 1994a, 1994b; Ono and Horiuchi, 1996b; Schnack and Feldmeier, 1996, 1997; Ebeling and Militzer, 1997; Schnack, 1998.

uses an ergodicity assumption, i.e., that time averages are equivalent to ensemble averages, which should be verified.

A. Thermostatics

The question of thermostatic properties can be reduced to the question of whether the set of model states $|Q\rangle$ is complete, i.e., able to span the many-particle Hilbert space. If that is the case, the unit operator in N-particle space can be written as

$$\hat{\mathbb{1}}^{(N)} = \int \mathrm{d}\mu(Q)\, \frac{|Q\rangle\langle Q|}{\langle Q|Q\rangle}, \tag{143}$$

where $\mathrm{d}\mu(Q)$ is a measure that depends on the parameter set Q because the trial states $|Q\rangle$ are in general nonorthogonal. For fermions and Gaussian wave packets, the measure is derived in the following subsection.

Once completeness is shown, the thermostatic relations have to be correct, provided the trace of the partition function

$$\begin{aligned} Z(T) &= \mathrm{Tr}(\exp\{-\hat{H}/T\}) \\ &= \int \mathrm{d}\mu(Q)\, \frac{\langle Q|\exp\{-\hat{H}/T\}|Q\rangle}{\langle Q|Q\rangle} \end{aligned} \tag{144}$$

is calculated with the trial states $|Q\rangle$ in quantum fashion.

In the case of fermionic molecular dynamics (FMD) and antisymmetrized molecular dynamics (AMD; Ono *et al.*, 1992a, 1992b; Schnack and Feldmeier, 1996), the antisymmetric many-body states form an overcomplete set and provide a full representation for the unit operator. Because the calculation of the trace does not depend on the representation, all thermostatic properties like the Fermi-Dirac distribution, specific heat, mean energy as a function of temperature, etc. ought to be correct and fully quantal using FMD or AMD trial states. The difficult task is to calculate $\langle Q|\exp\{-\hat{H}/T\}|Q\rangle$ or $\langle Q|\hat{B}\exp\{-\hat{H}/T\}|Q\rangle$, where $\hat{B}$ is an observable. The trace integral can be evaluated by Monte Carlo methods.

1. Completeness relation with coherent states

In the following it is shown that Slater determinants of coherent states span the whole Hilbert space for fermions.

Coherent states $|\vec{z}\rangle$ that are defined as the eigenstates of the harmonic-oscillator destruction operator $\hat{\vec{a}} = \sqrt{1/(2a_0)}\hat{\vec{x}} + i\sqrt{a_0/2}\hat{\vec{k}}$,

$$\hat{\vec{a}}\,|\vec{z}\rangle = \vec{z}\,|\vec{z}\rangle, \quad \hat{h}_{\mathrm{HO}} = \frac{1}{ma_0}\left(\hat{\vec{a}}^{+}\hat{\vec{a}} + \frac{3}{2}\right), \tag{145}$$

form an overcomplete set of states. They are the Gaussian states defined in Eq. (45) with $\vec{z} = \sqrt{1/(2a_0)}\vec{r} + i\sqrt{a_0/2}\vec{p} = \vec{b}/\sqrt{2a_0}$ for a real width parameter a_0. Their completeness relation reads in single-particle space

$$\begin{aligned} \hat{\mathbb{1}}^{(1)} &= \int \frac{\mathrm{d}^3\,\mathrm{Re}\, z\, \mathrm{d}^3\,\mathrm{Im}\, z}{\pi^3}\, \frac{|\vec{z}\rangle\langle\vec{z}|}{\langle\vec{z}|\vec{z}\rangle} \\ &= \int \frac{\mathrm{d}^3 r\, \mathrm{d}^3 p}{(2\pi)^3}\, \frac{|\vec{r},\vec{p}\rangle\langle\vec{r},\vec{p}|}{\langle\vec{r},\vec{p}|\vec{r},\vec{p}\rangle}, \end{aligned} \tag{146}$$

where $|\vec{z}\rangle$ labels the coherent states by their eigenvalue with respect to $\hat{\vec{a}}$, and the phase-space notation $|\vec{r},\vec{p}\rangle$ labels the states by the expectation values of their coordinate and momentum operators. Coherent states are extensively discussed by in Klauder and Skagerstam (1985).

Since we are dealing with fermions, the spin degree of freedom has to be considered and consequently the resolution of unity changes to

$$\hat{\mathbb{1}}^{(1)} = \int \frac{\mathrm{d}^3 r\, \mathrm{d}^3 p}{(2\pi)^3} \sum_m \frac{|q\rangle\langle q|}{\langle q|q\rangle}, \tag{147}$$

where the sum runs over the two magnetic quantum numbers $m = \pm\frac{1}{2}$ which are included in the set of parameters denoted by q [see Eq. (71)].

Proceeding one step further, the unit operator in the antisymmetric part of the two-particle Hilbert space is the antisymmetric product of two single-particle unit operators,

$$\begin{aligned} \hat{\mathbb{1}}^{(2)} &= \hat{A}^{(2)}\,(\hat{\mathbb{1}}^{(1)} \otimes \hat{\mathbb{1}}^{(1)})\,\hat{A}^{(2)} \\ &= \tfrac{1}{2}(\mathbb{1} - \hat{P}_{12})\,(\hat{\mathbb{1}}^{(1)} \otimes \hat{\mathbb{1}}^{(1)})\,\tfrac{1}{2}(\mathbb{1} - \hat{P}_{12}), \end{aligned} \tag{148}$$

which may be expressed with antisymmetric two-particle states $|q_1,q_2\rangle_a$ as

$$\begin{aligned} \hat{\mathbb{1}}^{(2)} = \int \frac{\mathrm{d}^3 r_1\, \mathrm{d}^3 p_1}{(2\pi)^3} \sum_{m_1} \int \frac{\mathrm{d}^3 r_2\, \mathrm{d}^3 p_2}{(2\pi)^3} \\ \times \sum_{m_2} \frac{|q_1,q_2\rangle_a\, {}_a\langle q_1,q_2|}{\langle q_1|q_1\rangle\langle q_2|q_2\rangle}, \end{aligned} \tag{149}$$

where

$$|q_1,q_2\rangle_a := \tfrac{1}{2}(|q_1\rangle\otimes|q_2\rangle - |q_2\rangle\otimes|q_1\rangle).$$

Following this line of reasoning, we can write the unit operator in the antisymmetric part of the N-particle Hilbert space as the projection of the N-particle unit operator onto the antisymmetric subspace. If $|Q\rangle$ is the unnormalized Slater determinant (70) of single-particle states $|q\rangle$,

$$|Q\rangle = \frac{1}{N!}\sum_P \mathrm{sgn}(P)(|q_{P(1)}\rangle\otimes\cdots\otimes|q_{P(N)}\rangle), \tag{150}$$

then the unit operator is

$$\hat{\mathbb{1}}^{(A)} = \int \mathrm{d}\mu(Q)\, \frac{|Q\rangle\langle Q|}{\langle Q|Q\rangle}, \tag{151}$$

with a measure

$$\mathrm{d}\mu(Q) = \langle Q|Q\rangle \prod_{k=1}^{N} \frac{1}{\langle q_k|q_k\rangle}\, \frac{\mathrm{d}^3 r_k\, \mathrm{d}^3 p_k}{(2\pi)^3} \sum_{m_k} \tag{152}$$

that accounts for antisymmetrization. In a sampling where the values of $\vec{r}_k$ and $\vec{p}_k$ are chosen according to Monte Carlo methods, this measure determines the

probability of finding the state $|Q\rangle$ belonging to the configuration $Q=\{\vec{r}_1,\vec{p}_1,m_1;\vec{r}_2,\vec{p}_2,m_2;\dots\}$ in Hilbert space. If, for example, two fermions with the same spin are close in $\vec{r}$ and $\vec{p}$ then this measure is small because the norm $\langle Q|Q\rangle=\det\{\langle q_k|q_l\rangle\}$ will be small. Equation (151) is very useful in calculating traces by means of Monte Carlo sampling (Ohnishi and Randrup, 1993).

Coherent states are Gaussian wave packets with fixed width, but the real and imaginary parts of the width, a_R and a_I, may also be integrated over appropriate ranges in order to get an improved coverage of the phase space when sampling:

$$\hat{\mathbb{1}}^{(1)}=\int\frac{\mathrm{d}^3r\,\mathrm{d}^3p}{(2\pi)^3}\sum_m\int_{\Omega_R}\frac{\mathrm{d}a_R}{\Omega_R}\int_{\Omega_I}\frac{\mathrm{d}a_I}{\Omega_I}\frac{|q\rangle\langle q|}{\langle q|q\rangle},\quad(153)$$

where Ω_R and Ω_I denote the intervals over which the width $a=a_R+ia_I$ is integrated,

$$\int_{\Omega_R}\mathrm{d}a_R=\Omega_R,\quad\int_{\Omega_I}\mathrm{d}a_I=\Omega_I.$$

Since the width a in the completeness relation, Eq. (145), is arbitrary, the additional integrations in Eq. (152) do not change the unit operator.

In the case of nuclear physics, one has two types of fermions, so that the measure for a system with N neutrons and Z protons is

$$\mathrm{d}\mu(Q)=\langle Q|Q\rangle\prod_{k=1}^{N}\frac{1}{\langle q_k|q_k\rangle}\frac{\mathrm{d}^3r_k\,\mathrm{d}^3p_k}{(2\pi)^3}\sum_{m_k}\times\prod_{l=N+1}^{A=N+Z}\frac{1}{\langle q_l|q_l\rangle}\frac{\mathrm{d}^3r_l\,\mathrm{d}^3p_l}{(2\pi)^3}\sum_{m_l}.\quad(154)$$

Once the resolution of unity is given in terms of model states, the partition function can be evaluated.

It is interesting to note that the norm $\langle Q|Q\rangle$ in the measure cancels with the norm denominator in Eq. (144). Provided the single-particle states are normalized, $\langle q_k|q_k\rangle=1$, and $\hat{H}$ does not depend on the spins, the partition function looks almost classical,

$$Z(T)=\frac{2^N}{(2\pi)^{3N}}\int\mathrm{d}^3r_1\,\mathrm{d}^3p_1\,\mathrm{d}^3r_2\,\mathrm{d}^3p_2\cdots\mathrm{d}^3r_N\,\mathrm{d}^3p_N\times\langle Q|\exp\{-\hat{H}/T\}|Q\rangle,\quad(155)$$

except that there is an operator in the exponent. Equation (155) is still the exact quantum expression. There is no contradiction between the fact that the Hamiltonian may have a discrete energy spectrum with gaps between the levels and the fact that the parameters $\vec{r}_k$ and $\vec{p}_k$ are integrated in a continuous fashion (Schnack, 1999). Only if the expectation value is moved up into the exponent do things go wrong. The Pauli exclusion principle is fully taken care of by the antisymmetric state $|Q\rangle$. If two particles with equal spin are at the same point in phase space, $|Q\rangle=0$ and hence $\langle Q|\exp\{-\hat{H}/T\}|Q\rangle=0$, so that forbidden states do not contribute to the partition function.

2. Example for many fermions

The above considerations can be illustrated by the example of N identical fermions in a common single-particle potential. Starting from the Hamilton operator

$$\hat{H}=\sum_{l=1}^{N}\hat{h}(l),\quad\hat{h}(l)=\frac{\hat{\vec{k}}^2(l)}{2m}+v(\hat{\vec{x}}(l)),\quad(156)$$

one can derive the mean energy of the N-fermion system from the partition function $Z(T)$, Eq. (143), as the derivative with respect to T

$$\langle\langle\hat{H}\rangle\rangle_{|T}=T^2\frac{\partial}{\partial T}\ln(Z(T))=\frac{\int\mathrm{d}\mu(Q)\mathcal{W}(T)\Sigma_{m,n}^{N}\mathcal{O}_{nm}(T)\left[T^2\frac{\partial}{\partial T}\langle q_m|\exp\{-\hat{h}/T\}|q_n\rangle\right]}{\int\mathrm{d}\mu(Q)\mathcal{W}(T)},\quad(157)$$

where the two abbreviations $\mathcal{W}(T)$ and $\mathcal{O}^{-1}(T)$ are introduced as

$$\mathcal{W}(T)\equiv\frac{\langle Q|\exp\{-\hat{H}/T\}|Q\rangle}{\langle Q|Q\rangle}=\frac{\det(\langle q_k|\exp\{-\hat{h}/T\}|q_l\rangle)}{\det(\langle q_k|q_l\rangle)}\quad(158)$$

and

$$(\mathcal{O}^{-1}(T))_{kl}=\langle q_k|\exp\{-\hat{h}/T\}|q_l\rangle.\quad(159)$$

For free motion, i.e., $v(\hat{\vec{x}})=0$, the matrix elements (159) are given by

$$\langle q_k|\exp\left\{-\frac{\hat{\vec{k}}^2}{2mT}\right\}|q_l\rangle=\left(\frac{2\pi a_k^*a_l}{a_k^*+a_l+\frac{1}{mT}}\right)^{3/2}\times\exp\left\{-\frac{(\vec{b}_k^*-\vec{b}_l)^2}{2\left(a_k^*+a_l+\frac{1}{mT}\right)}\right\}.\quad(160)$$

For the special case of the three-dimensional harmonic oscillator, i.e., $v(\hat{\vec{x}})=\frac{1}{2}m\omega^2\hat{\vec{x}}^2$, the matrix elements can easily be calculated if one sets all $a_k=a_0=1/(m\omega)$ (Schnack, 1996):

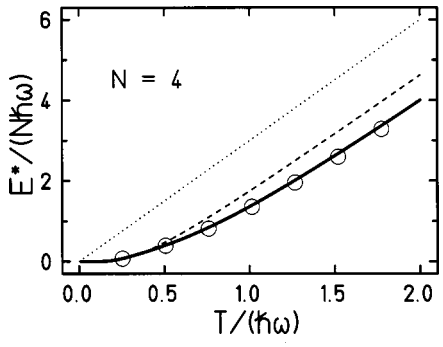

FIG. 7. Excitation energy as a function of temperature: ○, calculated with antisymmetrized Gaussian states; solid line, calculated with eigenfunctions of the harmonic oscillator; dotted line, the classical result $E^*/N=3T$; dashed line, the result of quantum Boltzmann statistics.

$$\langle q_k|\exp\left\{-\frac{\hat{h}_{\rm HO}}{T}\right\}|q_l\rangle=\left(\frac{\pi}{m\omega}\right)^{3/2}\exp\left\{-\frac{m\omega}{4}(\vec{b}_k^{\,*}-\vec{b}_l)^2-\frac{m\omega}{2}\vec{b}_k^{\,*}\vec{b}_l(1-e^{-\omega/T})-\frac{3\omega}{2T}\right\}. \tag{161}$$

For other potentials, the matrix elements (159) assume a more complicated form.

Figure 7 shows the result of a Metropolis integration (Metropolis *et al.*, 1953) over $\vec{r}_k$ and $\vec{p}_k$ of Eq. (157) for a system of four identical fermions with equal spins in a harmonic oscillator (open circles). The solid line displays the results when the traces are calculated by discrete sums over eigenstates of the many-body Hamilton operator $\hat{H}_{\rm HO}$ (Schmidt and Schnack, 1998). For comparison, the classical dependence is shown as a dotted line. The dashed line represents the result for the quantum Boltzmann case for distinguishable particles, where the trial state in Eq. (155) is a direct product of single-particle states. In both quantum cases the specific heat is vanishing at $T=0$ because of the finite energy gap between the ground state and the first excited state.

As expected from the general argument that traces are independent of the representation, provided one uses a complete set, the numerical Metropolis integration with a sampling of 10^6 points in the 24-dimensional phase space of the continuous parameters $\vec{r}_k,\vec{p}_k$, which specify the Slater determinants $|Q\rangle$, gives the same result as summing over eigenstates of the many-body Hamiltonian. The continuous integration is not in contradiction with Fermi statistics or the discrete spectrum of the Hamiltonian, and the classical-looking Eq. (155) is fully quantal.

3. Resumé

(1) The thermostatic properties of a model ought to be correct if the set of model states $|Q\rangle$ is complete, i.e., able to span the many-particle Hilbert space.
(2) In FMD and AMD, the antisymmetric many-body states of single-particle Gaussian wave packets form an overcomplete set and provide a full representation for the unit operator.

B. Thermodynamics

In molecular dynamics, the time evolution as given by the time-dependent variational principle, without a collision term or quantum branching, is deterministic. Given a state $|Q(t_0)\rangle$ at an initial time t_0, the system is described by the pure state $|Q(t)\rangle$ at all earlier and later times. Therefore, as in the exact solution of the Schrödinger equation, thermal properties have to be obtained by coarse graining or time averaging.

In this section time averaging is compared with the canonical statistical ensemble for a fermion system. If the system is ergodic, both are equivalent and equilibrium properties can be evaluated by molecular-dynamics simulations. For this, the ergodic ensemble is defined by the statistical operator $\hat{R}_{\rm erg}$ as

$$\hat{R}_{\rm erg}:=\lim_{t_2\to\infty}\frac{1}{(t_2-t_1)}\int_{t_1}^{t_2}{\rm d}t\,\frac{|Q(t)\rangle\langle Q(t)|}{\langle Q(t)|Q(t)\rangle}. \tag{162}$$

Hence the ergodic mean of an operator $\hat{B}$ is given by

$$\overline{\langle\hat{B}\rangle}_{|\langle\hat{H}\rangle}:={\rm Tr}(\hat{R}_{\rm erg}\hat{B})=\lim_{t_2\to\infty}\frac{1}{(t_2-t_1)}\int_{t_1}^{t_2}{\rm d}t\,\frac{\langle Q(t)|\hat{B}|Q(t)\rangle}{\langle Q(t)|Q(t)\rangle}. \tag{163}$$

If the ergodic assumption is fulfilled, the statistical operator $\hat{R}_{\rm erg}$ should depend only on $\langle\hat{H}\rangle$, which is actually a constant of motion. Therefore the notation with the condition "$\langle\hat{H}\rangle$" in Eq. (163) is used.

Expectation values are well defined with Eq. (163) so that one can easily calculate extensive quantities like the excitation energy. But it is not obvious how an intensive thermodynamic quantity such as temperature might be extracted from deterministic molecular dynamics with wave packets.

In classical mechanics with momentum-independent interactions the partition function

$$\begin{aligned}Z_{classical}(T)&=\int\prod_{k=1}^{N}\frac{{\rm d}^3r_k\,{\rm d}^3p_k}{(2\pi)^3}\times\exp\left\{-\frac{1}{T}\mathcal{H}_{classical}(\vec{r}_1,\vec{p}_1,\dots)\right\}\\&=\prod_{k=1}^{N}\int{\rm d}^3p_k\exp\left\{-\frac{1}{T}\frac{\vec{p}_k^{\,2}}{2m_k}\right\}\times\int\prod_{l=1}^{N}\frac{{\rm d}^3r_l}{(2\pi)^3}\exp\left\{-\frac{1}{T}\mathcal{V}(\vec{r}_1,\vec{r}_2,\dots)\right\}\end{aligned} \tag{164}$$

is a product of a term with the kinetic energy and a term containing the interactions. Therefore a fit of the momentum distribution with a Boltzmann distribution, or

the equipartition theorem, can be used to determine the temperature T. For example, in simple formulations of the Nosé-Hoover thermostat (Hoover, 1985; Kusnezov *et al.*, 1990; Nosé, 1991) the equipartition theorem serves as a basic ingredient.

In the quantum case, Eq. (144) has to be employed, which does not show this factorization. For an interacting finite system one cannot, in analogy to the Boltzmann case, fit a Fermi function to the momentum distribution to determine the temperature. An example is the ground state of a nucleus for which the momentum distribution has a smeared-out Fermi edge due to the finite size and the two-body interaction and not because of temperature.

1. Ergodic ensemble of fermions in a harmonic oscillator

In this section the ideal gas of fermions in a common one-dimensional harmonic-oscillator potential is used for demonstration. The Hamiltonian $\hat{H}_{\rm HO}$ is written in second quantization with the fermion creation operator $\hat{c}_n^+$ (which creates a fermion in the nth single-particle eigenstate of $\hat{h}_{\rm HO}$) as

$$\hat{H}_{\rm HO}=\sum_{l=1}^{N}\hat{h}_{\rm HO}(l)=\sum_{l=1}^{N}\left(\frac{\hat{\vec{k}}^2(l)}{2m}+\tfrac{1}{2}m\omega^2\hat{\vec{x}}^2(l)\right)$$

$$=\omega\sum_{n=0}^{\infty}(n+\tfrac{1}{2})\hat{c}_n^+\hat{c}_n\,, \tag{165}$$

and the trial state $|Q(t)\rangle$ describes four fermions with equal spins. To test the fermionic nature of the dynamical evolution, the ergodic ensemble averages of the occupation numbers, $\overline{\langle\hat{c}_n^+\hat{c}_n\rangle}_{|\langle\hat{H}\rangle}$ [see Eq. (163)] are evaluated and compared with $\langle\langle\hat{c}_n^+\hat{c}_n\rangle\rangle_{|T}$ of the canonical ensemble as discussed in the previous section.

The occupation numbers, which range from 0 to 1 for fermions, are chosen on purpose to make clear from the beginning that the equations of motion for the parameters $Q(t)=\{\vec{r}_1(t),\vec{p}_1(t),\ldots\}$, as given by Eq. (22), might be generalized Hamilton equations, but the observables always have to be calculated with the quantum state $|Q(t)\rangle$. If $\vec{r}_k(t)$ and $\vec{p}_k(t)$ were taken as the particle coordinates in a classical picture, the question of what was the mean occupation number of the nth eigenstate of the harmonic oscillator could not even be posed.

As pointed out already, in fermionic molecular dynamics the time evolution of Gaussian wave packets in a common oscillator is exact, and thus the occupation probabilities of the eigenstates of the Hamilton operator do not change over time. In order to equilibrate the system, a repulsive short-range two-body interaction is introduced. The strength of the interaction is chosen to be weak enough that the ideal-gas picture is still approximately valid.

In the initial state $|Q(t_0)\rangle$, which is far from equilibrium, three wave packets with a width of $a(t_0)=1/(m\omega)$ are put close to the origin at $x(t_0)=(-d,0,d)$ with $d=0.5/\sqrt{m\omega}$, while the fourth packet is pulled away from the center.

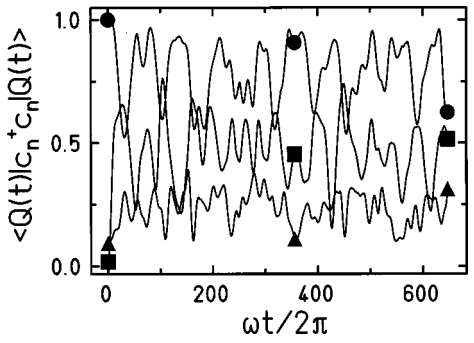

FIG. 8. Occupation probabilities vs time: ●, $n=0$; ♦, $n=3$; ▲, $n=6$.

Figure 8 gives an impression of the chaotic time dependence of $\langle Q(t)|\hat{c}_n^+\hat{c}_n|Q(t)\rangle$ for $n=0$, 3, and 6.

The result of time averaging is seen in Fig. 9 for four different initial displacements that correspond to four different excitation energies of the fermion system. To each case we assign a canonical ensemble that has the same mean energy, i.e., $E^*=\overline{\langle\hat{H}_{\rm HO}-E_0\rangle}_{|\langle\hat{H}\rangle}=\langle\langle\hat{H}_{\rm HO}-E_0\rangle\rangle_{|T}$. The solid lines in Fig. 9 show the corresponding distributions of occupation probabilities for these canonical ensembles. Their temperatures T are also given in the figure. The one-to-one correspondence between the occupation probabilities of the ergodic ensemble and those of the canonical ensemble, which has the same mean energy $\langle\hat{H}\rangle$ as the pure state, demonstrates that the system is ergodic and that the fermion molecular-dynamics trajectory covers the many-body phase space according to Fermi-Dirac statistics.

This result is not trivial because, first, the system is very small, consisting of only four particles, and second, the equations of motion are approximated by FMD.

2. Trial states with fixed-width

As already explained in Sec. V.A, both types of trial states—those with dynamic and those with fixed

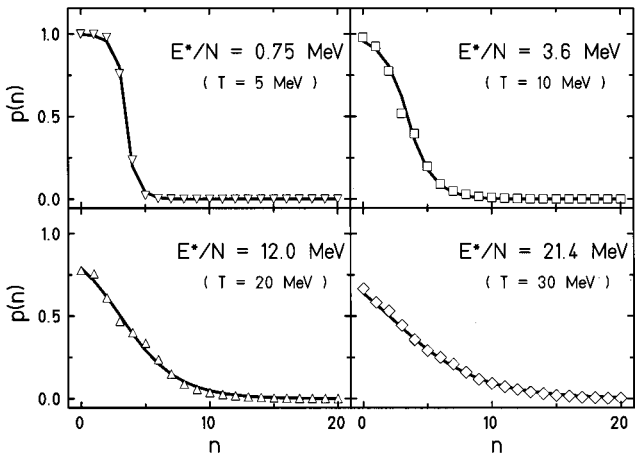

FIG. 9. Comparison of occupation probabilities: symbols, calculated in the ergodic ensemble $\overline{\langle\tilde{c}_n^+\tilde{c}_n\rangle}_{|\langle\hat{H}\rangle}$; solid line, calculated with the canonical ensemble $\langle\langle\tilde{c}_n^+\tilde{c}_n\rangle\rangle_{|T}$.

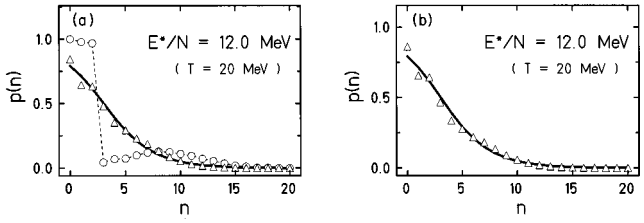

FIG. 10. Comparison of occupation probabilities: ○, △, calculated in the ergodic ensemble using trial states with fixed widths; solid line, calculated in the canonical ensemble. (a) without interaction: ○, $a_l=1/(m\omega)$; △, $a_l=1.2/(m\omega)$; (b) with interaction and $a_l=1.2/(m\omega)$.

widths—span the whole Hilbert space and thus their thermostatic properties are the same. Reducing the degrees of freedom by keeping all width parameters at a fixed value a_0, however, leads to a different dynamical behavior, as discussed in Sec. III.A. The equations of motion are no longer exact solutions for the case of free motion. In a common oscillator, the exact solution is obtained only if all $a_l=1/(m\omega)$ because da_l/dt is zero in that special case; see Sec. IV.A.3. If the width has a different value, spurious scattering occurs as in the case of free motion whenever two particles come too close in phase space.

Figure 10(a) displays the result of the time evolution for the very same system as in the previous section but without the randomizing two-body interaction. If the widths are chosen to be $a_l=1/(m\omega)$, the resulting exact time evolution is just a unitary transformation in the one-body space and the occupation probabilities are stationary (circles). But if the widths are taken as $a_l=1.2/(m\omega)$, the occupation probabilities change in time and the spurious scatterings equilibrate the system even without an interaction. Figure 10(b) shows the mean occupation probabilities when the interaction is switched on (triangles). Clearly, the nature of the randomizing force is not relevant; it may even be a spurious force that originates from too-restricted a trial state.

In antisymmetrized molecular dynamics (Ono *et al.*, 1992a, 1992b) trial states with time-independent widths are used, and as expected from the above simple example, the thermodynamic properties of the model comply with Fermi-Dirac statistics. It would be interesting to see how collision terms and branching influence the dynamical statistical properties of AMD. Since the Pauli blocking prescription is consistent with the AMD state, we expect a faster equilibration due to additional randomization.

3. Canonical and ergodic ensemble for distinguishable particles

To complete the discussion in this section, we replace the fermions by distinguishable particles, i.e., the antisymmetrized many-body state is replaced by a product state of Gaussian wave packets. In this case the relation between temperature T and excitation energy E^*/N is known and given by $E^*/N=\frac{1}{2}\omega[\coth(\omega/(2T))-1]$.

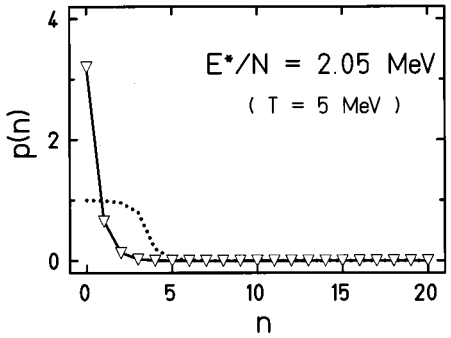

FIG. 11. Mean occupation numbers for a product state (Boltzmann statistics): △, ergodic ensemble; solid line, canonical ensemble, both for an excitation energy of $E^*/N=2.05$ MeV, which corresponds to a temperature $T=5$ MeV in the canonical ensemble; dotted line, the result for Fermi-Dirac statistics at the same temperature.

The ergodic ensemble is again investigated at different energies and compared with the corresponding canonical ensembles with the same mean energies (Schnack and Feldmeier, 1996; Feldmeier and Schnack, 1997). For this case, also, the time evolution of the system exhibits ergodic behavior at all excitation energies. As an example, Fig. 11 shows the case of $E^*/N=2.05$ MeV (which corresponds to $T=5$ MeV) after a time averaging of about 2000 periods. The ergodic ensemble (triangles) and the Boltzmann canonical ensemble (solid line) are the same within the size of the symbols. This means that the ergodic ensemble is again equivalent to the quantum canonical ensemble and not to the classical one, because one is still in the quantal regime for $E^*/N=2.05$ MeV and $T=5$ MeV according to the relation given above. The classical relation $E^*/N=T$ for a one-dimensional oscillator holds only for $E^*/N\gg\omega$ (here $\omega=8$ MeV).

However, since distinguishable particles are not affected by the Pauli exclusion principle, the occupation numbers for the many-body ground state look quite different from those of the Fermi-Dirac distribution at the same temperature (dotted line in Fig. 11).

4. Resumé

When discussing statistical properties of molecular dynamics with Gaussian wave packets (coherent states), one should always keep in mind that any observable or statistical weight has to be calculated with the trial state according to quantum mechanics. One should not fall into a completely classical approach, misled by the "classical" appearance of equations of motion or phase-space integrals, which is due to the representation of the coherent states in terms of $\vec{r}_k$ and $\vec{p}_k$.

Statistical properties of molecular dynamics for fermions can be deduced from simulations of equilibrium situations, but because of quantum effects, a measure for intensive quantities like temperature is not readily available.

C. Thermal properties of interacting systems by time averaging

In the previous section only noninteracting or weakly interacting systems were considered, for which partition functions can often be calculated because the Hamilton operator is a one-body operator. If the interaction between the particles is strong enough, for example, if it is attractive enough to form self-bound many-body systems, the ideal-gas picture is no longer valid and solid and liquid phases appear in addition to the vapor phase. Here the partition function $Z(T)$ can no longer be evaluated analytically because this would amount to solving the full interacting many-body problem $\hat{H}|\Psi_n\rangle = E_n|\Psi_n\rangle$ in the desired range of energies.

Take, for example, a fermion system in a large spherical container with repulsive walls. At zero temperature, the lowest eigenstate $|\Psi_{n=1}\rangle$ describes a self-bound system, or liquid drop, in its internal ground state located at the center of the container. With increasing energies, not only do internal excitations and c.m. motion of this drop occur, but there is also the possibility of having two or more bound objects which are separated from each other and surrounded by vapor. These drops can be in different states of excitation with various c.m. energies and vapor energies, all adding up to the total eigenenergy E_n. This means that the quantum number n enumerates not only the excited eigenstates but also the c.m. degrees of freedom, the partition into different drops, and the fermion vapor state. The number of eigenstates in an energy interval increases rapidly with excitation energy.

In principle, one can deduce all thermodynamic properties from the level density, but it is obvious that for those complex and highly correlated states $|\Psi_n\rangle$ it is impossible to solve the eigenvalue problem either analytically or numerically. Therefore one tries to simulate correlated many-body systems by means of molecular dynamics (which describes the time evolution in an approximate way) and replace the ensemble average with a time average.

1. Fermionic molecular dynamics—the nuclear caloric curve

As discussed in Sec. V.B, even a small system with only a few particles in a harmonic-oscillator potential is ergodic. So one can use one such a system, for which the relation between excitation energy and temperature is known, as a thermometer to determine the temperature of another system. This idea has been used in FMD simulations of phase transitions in nuclei where the ideal Fermi-gas picture does not apply because the nucleons are interacting through strong two-body forces. The coupling to a thermometer is necessary because the temperature cannot be determined from the momentum distribution (Schnack and Feldmeier, 1997). In an interacting small fermion system, the Fermi edge is broadened not only because of temperature but also because of the finite size of the system and two-body correlations.

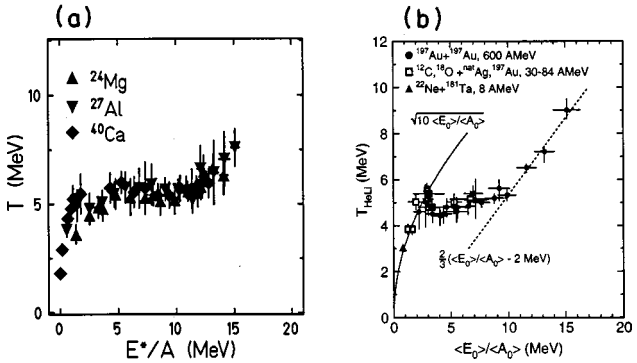

FIG. 12. Caloric curves: (a) of ^{24}Mg, ^{27}Al, and ^{40}Ca at $\hbar\omega = 1$ MeV, from Schnack and Feldmeier, 1997; (b) as determined by the ALADIN group from the decay of spectator nuclei, from Pochodzalla *et al.*, 1995.

A thermostat (large heat bath coupled to the system) is not advisable because phase transitions in small systems are recognized best in a microcanonical situation where the energy distribution is within a narrow energy range and variations of the level density $\rho(E)$, which indicate a phase transition, are not blurred by the Boltzmann factor $e^{-E/T}$ of the canonical ensemble.

The thermometer consists of a quantum system of distinguishable particles that move in a common harmonic-oscillator potential and interact with the nucleons. The nucleus itself is confined by a wide harmonic-oscillator potential that serves as a containment. This is an important part of the setup because it keeps the evaporated nucleons (vapor) in the vicinity of the remaining liquid drop so that equilibration with the surrounding vapor can take place. The coupling between nucleons and thermometer particles is chosen to be weak, repulsive, and of short range. It has to be as weak as possible in order to avoid influencing the nuclear system too much. On the other hand, it has to be strong enough to allow for reasonable equilibration times.

The determination of the relation between excitation energy E^* and temperature T (caloric curve) is done by time-averaging the energy of both the nucleonic system and the thermometer over a long period according to Eq. (163). The time-averaged energy of the thermometer E_{th} determines the temperature T through the known relation $E_{th}/N_{th} = \frac{3}{2}\omega_{th}\coth(\omega_{th}/(2T))$ for an ideal gas of distinguishable particles in a common harmonic-oscillator potential with frequency ω_{th} (quantum Boltzmann statistics).

The resulting caloric curves for the nuclei ^{24}Mg, ^{27}Al, and ^{40}Ca are displayed in Fig. 12(a). All caloric curves clearly exhibit three different parts. Beginning at small excitation energies, the temperature rises steeply with increasing energy, as expected for a Fermi gas in the shell model. There the nucleons remain bound in the excited nucleus, which behaves like a drop of liquid. At an excitation energy of 3 MeV per nucleon, the curve flattens and stays almost constant up to about 11 MeV. This plateau at $T \approx 5-6$ MeV marks the coexistence phase where, at low excitation energy, one big drop is

surrounded with low-density vapor. With increasing energy, the drop dissolves more and more into vapor until all nucleons are unbound and the system has reached the vapor phase. The latent heat is hence about 8 MeV at a pressure that is estimated to be close to zero.

The caloric curve shown in Fig. 12(a) is strikingly similar to the caloric curve determined experimentally from the fragmentation of colliding nuclei by the ALADIN group (Pochodzalla *et al.*, 1995; Pochodzalla, 1997). Their results are displayed in Fig. 12(b). The position and the extension of the plateau agree quite well with the FMD calculation. Nevertheless, there are important differences between the experimental setup and the one used in the simulations. For further details, see Pochodzalla (1997) and Schnack and Feldmeier (1997).

2. Phase transitions of hydrogen plasma

Hydrogen plasma under extreme conditions—high temperature or pressure—is of great current interest, since it reveals new structural, dynamical and electronic properties like orientational ordering, pressure-induced metallization and changes in the vibronic spectra (Hemley and Mao, 1992; Klakow *et al.*, 1994a, 1994b; Knaup *et al.*, 1999).

One model employed in this context is called wave-packet molecular dynamics. It uses Gaussian packets with time-dependent widths and a Pauli potential derived from the antisymmetrization of pairs of nucleons; see Sec. IV.C and Klakow *et al.* (1994a, 1994b). Here 256 protons and 256 electrons are distributed in a cubic box with periodic continuation in all directions. Since the protons are classical, their temperature is simply given by their kinetic energy via the equipartition theorem.

The equations of motion are followed over 6×10^{-14} s. One observable that is sampled over this time period is the proton-pair distribution function $g_{pp}(r)$, which is related to the probability of finding two particles at the distance r. The proton-pair distribution reveals details about the binding and short-range correlations in the system. In Fig. 13, the pair distribution function $g_{pp}(r)$ is plotted for two temperatures. The peak at $r=1.3$ a.u. signals that the protons are bound in H_2 molecules. The authors find that due to medium effects, this bond length is shifted to a smaller value compared to the free one, which is $r=1.47$ a.u. in their model. At $T=300$ K, pronounced peaks can be seen around $r=4$ a.u. which indicate a solid structure of the H_2 molecules. The fact that these peaks are smoother at the higher temperature is interpreted as a signal that the system is now in the liquid phase.

The authors also find that wave-packet molecular dynamics is very efficient for the discussed problem and faster than the Car-Parrinello method (Car and Parrinello, 1985) while providing comparable results (Klakow *et al.*, 1994a, 1994b).

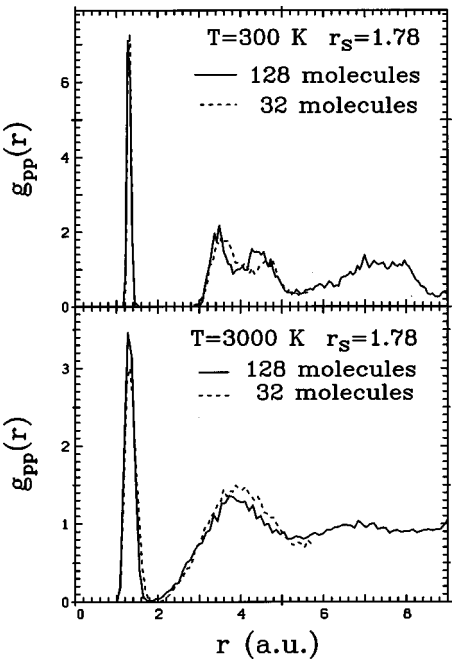

FIG. 13. The proton pair distribution function $g_{pp}(r)$: top, at $T=300$ K; bottom, at $T=3000$ K. Solid line shows the simulation with 128 molecules, the dashed line with 32 molecules. Figure provided by P.-G. Reinhardt.

ACKNOWLEDGMENTS

For supplying us with references or figures we would like to thank S. Bass, M. Belkacem, Ph. Chomaz, P. Danielewicz, W. Ebeling, O. Knospe, Tomoyuki Maruyama, A. Ono, J. Randrup, P.-G. Reinhard, U. Saalmann, R. Schmidt, and H. Stöcker. We also thank R. Roth for carefully reading the manuscript.

REFERENCES

Aichelin, J., 1991, "Quantum molecular dynamics—a dynamical microscopic N-body approach to investigate fragment formation and the nuclear equation of state in heavy-ion collisions," Phys. Rep. **202**, 233.

Aichelin, J., and G. Bertsch, 1985, "Numerical simulation of medium-energy heavy-ion reactions," Phys. Rev. C **53**, 1730.

Aichelin, J., A. Rosenhauer, G. Peilert, H. Stöcker, and W. Greiner, 1987, "Importance of momentum-dependent interactions for the extraction of the nuclear equation of state from high-energy heavy-ion collisions," Phys. Rev. Lett. **58**, 1926.

Aichelin, J., and H. Stöcker, 1986, "Quantum molecular dynamics—a novel approach to N-body correlations in heavy-ion collisions," Phys. Lett. B **176**, 14.

Arnol'd, V.I., 1989, *Mathematical Methods of Classical Mechanics* (Springer, Berlin).

Balian, R., and M. Veneroni, 1988, "Static and dynamic variational principles for expectation values of observables," Ann. Phys. (N.Y.) **187**, 29.

Balian, R., and M. Veneroni, 1992, "Correlations and fluctuations in static and dynamic mean-field approaches," Ann. Phys. (N.Y.) **216**, 351.

Bass, S.A., *et al.*, 1998, "Microscopic models for ultrarelativistic heavy-ion collisions," Prog. Part. Nucl. Phys. **41**, 225.

Bauhoff, W., E. Caurier, B. Grammaticos, and M. Płoszajczak, 1985, "Description of light-ion collisions in the time-dependent cluster model," Phys. Rev. C **32**, 1915.

Belkacem, M., *et al.*, 1998, "Equation of state, spectra and composition of hot and dense infinite hadronic matter in a microscopic transport model," Phys. Rev. C **58**, 1727.

Bertsch, G.F., and S. Das Gupta, 1988, "A guide to microscopic models for intermediate-energy heavy-ion collisions," Phys. Rep. **160**, 189.

Blaise, P., P. Durand, and O. Henri-Rousseau, 1994, "Irreversible evolution towards equilibrium of coupled quantum harmonic oscillators. A coarse-grained approach," Physica A **209**, 51.

Boal, D.H., and J.N. Glosli, 1988, "Quasiparticle model for nuclear dynamics studies: Ground-state properties," Phys. Rev. C **38**, 1870.

Bodmer, A.R., and C.N. Panos, 1977, "Classical microscopic calculations of high-energy collisions of heavy ions," Phys. Rev. C **15**, 1342.

Bodmer, A.R., C.N. Panos, and A.D. MacKellar, 1980, "Classical-equations-of-motion calculations of high-energy heavy-ion collisions," Phys. Rev. C **22**, 1025.

Bondorf, J.P., D. Idier, and I.N. Mishustin, 1995, "Self-organization in expanding nuclear matter," Phys. Lett. B **359**, 261.

Broeckhove, J., L. Lathouwers, E. Kesteloot, and P. van Leuven, 1988, "On the equivalence of the time-dependent variational principles," Chem. Phys. Lett. **149**, 547.

Broeckhove, J., L. Lathouwers, and P. van Leuven, 1989, "Time-dependent variational principles and conservation laws in wave-packet dynamics," J. Phys. A **22**, 4395.

Car, R., and M. Parrinello, 1985, "Unified approach for molecular dynamics and density functional theory," Phys. Rev. Lett. **55**, 2471.

Caurier, E., B. Grammaticos, and T. Sami, 1982, "The time-dependent cluster model," Phys. Lett. **109B**, 150.

Chiba, S., O. Iwamoto, T. Fukahori, K. Niita, T. Maruyama, T. Maruyama, and A. Iwamoto, 1996, "Analysis of proton-induced fragment production cross sections by the quantum molecular dynamics plus statistical decay model," Phys. Rev. C **54**, 285.

Chomaz, Ph., M. Colonna, and A. Guarnera, 1996, "Spinodal deomposition of atomic nuclei," in *Advances in Nuclear Dynamics 2*, edited by B. Arruada and G. Westfall (Plenum, New York).

Colonna, M., and Ph. Chomaz, 1998, "Spinodal decomposition in nuclear molecular dynamics," Phys. Lett. B **436**, 1.

Davies, K.T.R., K.R.S. Devi, S.E. Koonin, and M.R. Strayer, 1985, "TDHF calculations of heavy-ion collisions," in *Treatise of Heavy-Ion Science, Vol. 3*, edited by D.A. Bromley (Plenum, New York), p. 3.

Dorso, C., S. Duarte, and J. Randrup, 1987, "Classical simulation of the Fermi gas," Phys. Lett. B **188**, 287.

Dorso, C., and J. Randrup, 1987, "Classical simulation of nuclear systems," Phys. Lett. B **215**, 611.

Dorso, C., and J. Randrup, 1989, "Quasiclassical simulation of nuclear dynamics. Phase evolution of disassembling nuclei," Phys. Lett. B **232**, 29.

Drożdż, S., J. Okołowicz, and M. Płoszajczak, 1982, "The time-dependent cluster theory—application to the α-α collision," Phys. Lett. **109B**, 145.

Drożdż, S., M. Płoszajczak, and E. Caurier, 1986, "Variational approach to the Schrödinger dynamics in the Klauder's continuous representations," Ann. Phys. (N.Y.) **171**, 108.

Ebeling, W., A. Förster, and V. Yu. Podlipchuk, 1996, "Quantum wave-packets simulation of ionization processes in dense plasmas," Phys. Lett. A **218**, 297.

Ebeling, W., and B. Militzer, 1997, "Quantum molecular dynamics of partially ionized plasmas," Phys. Lett. A **226**, 298.

Ebeling, W., and F. Schautz, 1997, "Many-particle simulations of the quantum electron gas using momentum-dependent potentials," Phys. Rev. E **56**, 3498.

Feldmeier, H., 1990, "Fermionic molecular dynamics," Nucl. Phys. A **515**, 147.

Feldmeier, H., K. Bieler, and J. Schnack, 1995, "Fermionic molecular dynamics for ground states and collisions of nuclei," Nucl. Phys. A **586**, 493.

Feldmeier, H., T. Neff, R. Roth, and J. Schnack, 1998, "A unitary correlation operator method," Nucl. Phys. A **632**, 61.

Feldmeier, H., and J. Schnack, 1997, "Fermionic molecular dynamics," Prog. Part. Nucl. Phys. **39**, 393.

Frenkel, J., 1934, *Wave Mechanics; Advanced General Theory* (Clarendon, Oxford), p. 235.

Gaitanos, T., C. Fuchs, and H.H. Wolter, 1999, "Heavy-ion collisions with nonequilibrium Dirac-Brueckner mean fields," Nucl. Phys. A **650**, 97.

Gerjuoy, E., A.R.P. Rau, and Larry Spruch, 1983, "A unified formulation of the construction of variational principles," Rev. Mod. Phys. **55**, 725.

Goeke, K., and P.-G. Reinhard, Eds., 1982, *Time-dependent Hartree-Fock and Beyond: Proceedings of the International Symposium Held in Bod Honnef, Germany*, Lecture Notes in Physics No. 171 (Springer, Berlin).

Griffin, J.J., P.C. Lichtner, and M. Dworzecka, 1980, "Time-dependent S-matrix Hartree-Fock theory of complex reactions," Phys. Rev. C **21**, 1351.

Hartnack, C., R.K. Puri, J. Aichelin, J. Konopka, S.A. Bass, H. Stöcker, and W. Greiner, 1998, "Modeling the many-body dynamics of heavy-ion collisions: present status and future perspective," Eur. Phys. J. A **1**, 151.

Hartnack, C., L. Zhuxia, L. Neise, G. Peilert, A. Rosenhauer, H. Sorge, J. Aichelin, H. Stöcker, and W. Greiner, 1989, "Quantum molecular dynamics: a microscopic model from UNILAC to CERN energies," Nucl. Phys. A **495**, 303.

Heller, E.J., 1975, "Time-dependent approach to semiclassical dynamics," J. Chem. Phys. **62**, 1544.

Hemley, R.J., and H.K. Mao, 1992, "Anomalous low-frequency excitations in diamond-cell studies of hydrogen at megabar pressures," Phys. Lett. A **163**, 429.

Hoover, W.G., 1985, "Canonical dynamics: equilibrium phase-space distributions," Phys. Rev. A **31**, 1695.

Hoover, W.G., 1986, *Molecular Dynamics*, Lecture Notes in Physics No. 258 (Springer, Berlin).

Kanada-En'yo, Y., H. Horiuchi, and A. Ono, 1995, "Structure of Li and Be isotopes studied with antisymmetrized molecular dynamics," Phys. Rev. C **52**, 628.

Katz, A., 1965, *Classical Mechanics, Quantum Mechanics, Field Theory* (Academic, New York).

Kerman, A.K., and S.E. Koonin, 1976, "Hamiltonian formulation of time-dependent variational principles for the many-body system," Ann. Phys. (N.Y.) **100**, 332.

Khoa, D.T., N. Ohtsuka, M.A. Matin, A. Faessler, S.W. Huang, E. Lehmann, and R.K. Puri, 1992, "In-medium ef-

fects in the description of heavy-ion collisions with realistic NN interactions,'' Nucl. Phys. A **548**, 102.
Kiderlen, D., and P. Danielewicz, 1996, ''Fragments in Gaussian wave-packet dynamics with and without correlations,'' Nucl. Phys. A **620**, 346.
Klakow, D., C. Toepffer, and P.-G. Reinhard, 1994a, ''Hydrogen under extreme conditions,'' Phys. Lett. A **192**, 55.
Klakow, D., C. Toepffer, and P.-G. Reinhard, 1994b, ''Semiclassical molecular dynamics for strongly coupled Coulomb systems,'' J. Chem. Phys. **101**, 1.
Klauder, J.R., and B.-S. Skagerstam, 1985, *Coherent States* (World Scientific, Singapore).
Knaup, M., P.-G. Reinhard, and Ch. Toepffer, 1999, ''Wave-packet molecular dynamics simulations of hydrogen near the transition to a metallic fluid,'' Contrib. Plasma Phys. **39**, 57.
Knoll, J., and B. Strack, 1984, ''The dynamics of the nuclear disassembly in a field-theoretical model at finite entropies,'' Phys. Lett. **149B**, 45.
Knoll, J., and J. Wu, 1988, ''Expansion dynamics and multifragmentation of a saturating system of fermions,'' Nucl. Phys. A **481**, 173.
Konopka, J., H. Stöcker, and W. Greiner, 1995, ''On the impossibility of temperature extraction from heavy-ion-induced particle spectra,'' Nucl. Phys. A **583**, 357c.
Kramer, P., and M. Saraceno, 1981, *Geometry of the Time-Dependent Variational Principle in Quantum Mechanics*, Lecture Notes in Physics No. 140 (Springer, Berlin).
Kusnezov, D., A. Bulgac, and W. Bauer, 1990, ''Canonical ensembles from chaos,'' Ann. Phys. (N.Y.) **204**, 155.
Kusnezov, D., 1993, ''Quantum ergodic wave functions from a thermal nonlinear Schrödinger equation,'' Phys. Lett. A **184**, 50.
Lacroix, D., Ph. Chomaz, and S. Ayik, 1998, ''Quantal extension of mean-field dynamics,'' in Proceedings of the 36th International Winter Meeting on Nuclear Physics, Bormio, Italy, edited by I. Iori (Università Degli Studi di Milano, Milan), p. 485.
Lacroix, D., Ph. Chomaz,, and S. Ayik, 1999, ''On the simulation of extended TDHF theory,'' Nucl. Phys. A **651**, 369.
Latora, V., M. Belkacem,, and A. Bonasera, 1994, ''Dynamics of instabilities and intermittency,'' Phys. Rev. Lett. **73**, 1765.
Lehmann, E., R.K. Puri, A. Faessler, G. Batko, and S.W. Huang, 1995, ''Consequences of a covariant description of heavy-ion reactions at intermediate energies,'' Phys. Rev. C **51**, 2113.
Maruyama, Toshiki, K. Niita, and A. Iwamoto, 1996, ''Extension of quantum molecular dynamics and its application to heavy-ion collisions,'' Phys. Rev. C **53**, 297.
Maruyama, Toshiki, A. Ohnishi, and H. Horiuchi, 1992, ''Evolution of reaction mechanisms in the light heavy-ion system,'' Phys. Rev. C **45**, 2355.
Maruyama, Toshiki, A. Ono, A. Ohnishi, and H. Horiuchi, 1992, ''Fragment mass distribution in intermediate-energy heavy-ion collisions and the reaction time scale,'' Prog. Theor. Phys. **87**, 1367.
Metropolis, M., A.W. Metropolis, M.N. Rosenbluth, A.H. Teller, and E. Teller, 1953, ''Equation-of-state calculations by fast computing machines,'' J. Chem. Phys. **21**, 1087.
Neff, T., H. Feldmeier, R. Roth, and J. Schnack, 1999, ''Realistic interactions and configuration mixing in fermionic molecular dynamics,'' in *Hirschegg '99 Multifragmentation; Proceedings of the International Workshop XXXVII on Gross Properties of Nuclei and Nuclear Excitations in Hirschegg, Austria, January 17–23, 1999*, edited by H. Feldmeier, J. Knoll, W. Nörenburg, and J. Wambach (Gesellschaft für Schwerionenforschung, Darmstadt), p. 283.
Neuman, J.J., and G. Fai, 1994, ''Classical Lagrangian model of the Pauli principle,'' Phys. Lett. B **329**, 419.
Niita, K., S. Chiba, T. Maruyama, T. Maruyama, H. Takada, T. Fukahori, Y. Nakahara, and A. Iwamoto, 1995, ''Analysis of the $(N\times N')$ reactions by quantum molecular dynamics plus statistical model,'' Phys. Rev. C **52**, 2620.
Nosé, S., 1984, ''A unified formulation of the constant-temperature molecular dynamics methods,'' J. Chem. Phys. **81**, 511.
Nosé, S., 1991, ''Constant-temperature molecular dynamics methods,'' Prog. Theor. Phys. Suppl. **103**, 1.
Ohnishi, A., and J. Randrup, 1993, ''Statistical properties of antisymmetrized molecular dynamics,'' Nucl. Phys. A **565**, 474.
Ohnishi, A., and J. Randrup, 1995, ''Incorporation of quantum statistical features in molecular dynamics,'' Phys. Rev. Lett. **75**, 596.
Ohnishi, A., and J. Randrup, 1997a, ''Inclusion of quantum fluctuations in wave-packet dynamics,'' Ann. Phys. (N.Y.) **253**, 279.
Ohnishi, A., and J. Randrup, 1997b, ''Quantum fluctuations affect the critical properties of noble gases,'' Phys. Rev. A **55**, R3315.
Ono, A., 1998, ''Antisymmetrized molecular dynamics with quantum-branching processes for collisions of heavy nuclei,'' Phys. Rev. C **59**, 853.
Ono, A., and H. Horiuchi, 1996a, ''Statistical properties of AMD for non-nucleon-emission and nucleon-emission processes,'' Phys. Rev. C **53**, 2341.
Ono, A., and H. Horiuchi, 1996b, ''Antisymmetrized molecular dynamics of wave packets with stochastic incorporation of Vlasov equation,'' Phys. Rev. C **53**, 2958.
Ono, A., H. Horiuchi, Toshiki Maruyama, and A. Ohnishi, 1992a, ''Fragment formation studied with antisymmetrized version of molecular dynamics with two-nucleon collisions,'' Phys. Rev. Lett. **68**, 2898.
Ono, A., H. Horiuchi, Toshiki Maruyama, and A. Ohnishi, 1992b, ''Antisymmetrized version of molecular dynamics with two-nucleon collisions and its application to heavy-ion reactions,'' Prog. Theor. Phys. **87**, 1185.
Ono, A., H. Horiuchi, Toshiki Maruyama, and A. Ohnishi, 1993, ''Momentum distribution of fragments in heavy-ion reactions: dependence on the stochastic collision process,'' Phys. Rev. C **47**, 2652.
Peilert, G., J. Konopka, M. Blann, M.G. Mustafa, H. Stöcker, and W. Greiner, 1992, ''Dynamical treatment of Fermi motion in a microscopic description of heavy-ion collisions,'' Phys. Rev. C **46**, 1457.
Peilert, G., J. Randrup, H. Stöcker, and W. Greiner, 1991, ''Clustering in nuclear matter at subsaturation densities,'' Phys. Lett. B **260**, 271.
Pochodzalla, J., 1997, ''The search for the liquid-gas phase transition in nuclei,'' Prog. Part. Nucl. Phys. **39**, 443.
Pochodzalla, J., *et al.*, 1995, ''Probing the nuclear liquid-gas phase transition,'' Phys. Rev. Lett. **75**, 1040.
Pühlhofer, F., 1977, ''On the interpretation of evaporation residue mass distributions in heavy-ion induced fusion reactions,'' Nucl. Phys. A **280**, 267.

Reinhard, P.-G., and E. Suraud, 1992, ''Stochastic TDHF and the Boltzmann-Langevin equation,'' Ann. Phys. (N.Y.) **216**, 98.

Saraceno, M., P. Kramer, and F. Fernandez, 1983, ''Time-dependent variational description of $\alpha\alpha$ scattering,'' Nucl. Phys. A **405**, 88.

Schmidt, H.-J., and J. Schnack, 1998, ''Investigations on finite ideal quantum gases,'' Physica A **260**, 479.

Schnack, J., 1996, ''Kurzreichweitige Korrelationen in der Fermionischen Molekulardynamik,'' Ph.D. thesis (Technical University of Darmstadt).

Schnack, J., 1998, ''Molecular dynamics investigations on a quantum system in a thermostat,'' Physica A **259**, 49.

Schnack, J., 1999, ''Thermodynamics of the harmonic oscillator using coherent states,'' Europhys. Lett. **45**, 647.

Schnack, J., and H. Feldmeier, 1996, ''Statistical properties of fermionic molecular dynamics,'' Nucl. Phys. A **601**, 181.

Schnack, J., and H. Feldmeier, 1997, ''The nuclear liquid-gas phase transition within fermionic molecular dynamics,'' Phys. Lett. B **409**, 6.

Sorge, H., 1995, ''Flavor production in Pb (160AGeV) on Pb collisions: effect of color ropes and hadronic rescattering,'' Phys. Rev. C **52**, 3291.

Sorge, H., H. Stöcker, and W. Greiner, 1989, ''Poincaré invariant Hamiltonian dynamics: modeling multihadronic interactions in a phase space approach,'' Ann. Phys. (N.Y.) **192**, 266.

Stöcker, H., and W. Greiner, 1986, ''High-energy heavy-ion collisions: probing the equation of state of highly excited hadronic matter,'' Phys. Rep. **137**, 277.

Suarez-Barnes, I.M., M. Nauenberg, M. Nockleby, and S. Tomsovic, 1993, ''Semiclassical theory of quantum propagation: the Coulomb potential,'' Phys. Rev. Lett. **71**, 1961.

Topaler, M.S., M.D. Hack, T.C. Allison, Yi-Ping Liu, S.L. Mielke, D.W. Schwenke, and D.G. Truhlar, 1997, ''Validation of trajectory surface hopping methods against accurate quantum mechanical dynamics and semiclassical analysis of electronic-to-vibrational energy transfer,'' J. Chem. Phys. **106**, 8699.

Tsue, Y., and Y. Fujiwara, 1991, ''Time-dependent variational approach in terms of squeezed coherent states,'' Prog. Theor. Phys. **86**, 443.

Tully, J.C., 1990, ''Molecular dynamics with electronic transitions,'' J. Chem. Phys. **93**, 1061.

Wilets, L., and J.S. Cohen, 1998, ''Fermion molecular dynamics in atomic, molecular, and optical physics,'' Contemp. Phys. **39**, 163.

Wilets, L., E.M. Henley, M. Kraft, and A.D. MacKellar, 1977, ''Classical many-body model for heavy-ion collisions incorporating the Pauli principle,'' Nucl. Phys. A **282**, 341.

Wilets, L., Y. Yariv, and R. Chestnut, 1978, ''Classical many-body model for heavy-ion collisions (II),'' Nucl. Phys. A **301**, 359.

Wolf, Gy., G. Batko, W. Cassing, U. Mosel, K. Niita, and M. Schäfer, 1990, ''Dilepton production in heavy-ion collisions,'' Nucl. Phys. A **517**, 615.